Control and estimation methods for microbial communities

Alex dos Reis de Souza

Doctoral Thesis

École Doctorale Sciences pour l'Ingénieur

Control and Estimation Methods for Microbial Communities

Author:

Alex dos Reis de Souza

Committee members:

Denis Efimov	Research Director, Inria Lille Nord – Europe	Advisor
Jean-Luc Gouzé	Research Director, Inria Sophia Antipolis	Advisor
Andrey Polyakov	Research Scientist, Inria Lille Nord – Europe	Co-advisor
Denis Dochain	Professor, Univ. Catholique de Louvain	Reviewer
Mario di Bernardo	Professor, Univ. of Naples Federico II	Reviewer
Catherine Bonnet	Research Director, Inria Paris Saclay	President
Eugenio Cinquemani	Research Scientist, Inria Grenoble Rhône – Alpes	Examiner

Presented at September 24th 2021 in view of obtaining the grade of

DOCTOR in Automatic Control and Informatics

Université de Lille

Inria

Thèse

École Doctorale Sciences pour l'Ingénieur

Méthodes de contrôle et d'estimation appliquées aux communautés microbiennes

Auteur:

Alex dos Reis de Souza

Jury:

Denis Efimov	Research Director, Inria Lille Nord – Europe	Directeur de thèse
Jean-Luc Gouzé	Research Director, Inria Sophia Antipolis	Directeur de thèse
Andrey Polyakov	Research Scientist, Inria Lille Nord – Europe	Co-encadrant
Denis Dochain	Professor, Univ. Catholique de Louvain	Rapporteur
Mario di Bernardo	Professor, Univ. of Naples Federico II	Rapporteur
Catherine Bonnet	Research Director, Inria Paris Saclay	Présidente
Eugenio Cinquemani	Research Scientist, Inria Grenoble Rhône – Alpes	Examinateur

Thèse presentée le 24 Septembre 2021 en vue d'obtenir la grade de
DOCTEUR en Automatique et Informatique

To my parents, Reis and Marlene,
for their unconditional love and lifelong support.

"Endeavour always leads so far,
beyond the scene,
endeavour always sows love,
the struggle ends up here..."
André Matos
(in memoriam)

Résumé

Cette thèse est divisée en deux parties principales. Premièrement, l'objectif est d'étudier méthodes appropriées au contrôle et l'estimation des bio-procédés complexes. Deuxièmement, le problème du contrôle des systèmes incertains avec contraintes (sur les états et sur la commande) est résolu en fusionnant des estimateurs à intervalles avec la commande prédictive (MPC).

Pour la première partie, les bio-procédés concernés décrivent la croissance de populations microbiennes en culture continue. Deux scénarios différents sont envisagés : la compétition entre deux espèces pour un seul nutrient, et le cas d'un consortium microbien producteur-nettoyeur, où deux souches de microbes effectuent des tâches en mutualisme.

Ces systèmes biologiques sont très complexes en raison de leurs non-linéarités, de leur nature contrainte (en raison de leur signification physique, les états sont toujours non-négatifs et caractérisent ces systèmes comme positifs) et sur la commande (les actionneurs sont physiquement limités à des valeurs non négatives), et en raison de l'incertitude inhérente aux processus biologiques.

Tout d'abord, profitant de leurs similitudes structurelles, l'observabilité de tels systèmes est étudiée, suivie par la conception d'estimateurs d'état appropriés utilisant des mesures réalistes. Ensuite, les architectures de contrôle proposées visent à garantir la coexistence de deux espèces (ou souches) et deux scénarios distincts sont considérés : dans le premier, une architecture de contrôle robuste est conçue pour le modèle de compétition, en utilisant un ensemble de différentes lois de commande discontinues et qui prennent explicitement en compte les incertitudes. Puis, dans un second temps, la conception des lois de commande pour le consortium microbien producteur-nettoyeur est présentée en considérant le cas nominal.

Pour la deuxième partie de la thèse, l'idée principale est d'aborder le problème de la commande robuste pour les systèmes contraints en incorporant des estimateurs à intervalles (un observateur et un prédicteur) dans l'algorithme classique du MPC. Ces estimateurs, sous certaines conditions de non-négativité des erreurs d'estimation, fournissent des enveloppes qui contiennent toutes les trajectoires possibles du système incertain. En couplant cette caractéristique avec un problème d'optimisation, les algorithmes proposés offrent faisabilité récursive, ainsi que la satisfaction robuste des contraintes, à une faible complexité de calcul et avec une mise en œuvre très simple.

Deux classes générales de systèmes sont concernées dans ce cadre : les systèmes linéaires invariants dans le temps et les systèmes linéaires à paramètres variables. Pour chaque cas, les conditions de conception pour les estimateurs d'intervalle, ainsi que pour leur commande à retour d'état, sont données sous la forme d'inégalités matricielles linéaires (résolues hors ligne).

Abstract

This thesis is divided in two main parts. First, the objective is to investigate control and estimation methods applied to complex bioprocesses. Second, the problem of controlling constrained uncertain systems is tackled by merging interval estimators with Model Predictive Control.

For the first part, the concerned bioprocesses describe the growth of microbial populations in continuous culture. Two different scenarios are considered: the competition between two species for a single limiting substrate, and the case of a microbial consortium composed of a producer and a cleaner strain.

These biological systems are highly complex due to their nonlinearities, their constrained nature in both states (due to their physical meaning, which characterizes such systems as *positive*) and control inputs (the actuators are physically restrained to non-negative values), and due to the inherent uncertainty of biological processes.

First, profiting of their structural similarities, the observability of such systems is studied, proceeded by the design of proper state estimators using realistic measurements. Then, the control solutions aim at guaranteeing coexistence of all species and is then divided in two scenarios: in the first one, a robust control architecture is designed for the competition model, using a set of different discontinuous control laws that take the uncertainties explicitly into account. Then, in a second moment, the design of control laws for the microbial consortium is presented considering the nominal case.

For the second part of the thesis, the main idea is to tackle the robust constrained control problem by incorporating interval estimators (an observer and a predictor) into the classical MPC algorithm. These estimators, under some conditions on non-negativity of the estimation errors, provide envelopes that contain all possible trajectories of the uncertain system. Casting this feature into an optimization problem, the proposed algorithms offer robust constraint satisfaction and recursive feasibility at a low computational complexity and ease of implementation.

Two general classes of systems are concerned in the framework: Linear Time Invariant and Linear Parameter Varying systems. For each case, the conditions of design for the interval estimators, as well as for their feedback control, are given in the form of (offline) Linear Matrix Inequalities.

Acknowledgments

First and foremost, I wholeheartedly thank the Lord for guiding me every single day of this journey. Under Your light, I have never felt truly alone along this journey.

I'd like to express my eternal gratitude to my parents, Sebastião and Marilene, who have always made everything possible so I could become what I am today. You are the reason for all my efforts and your love always fueled my will of becoming a good and better man.

I extend this gratitude to my supervisors Dr. Denis Efimov, Dr. Jean-Luc Gouzé and Dr. Andrey Polyakov, for entrusting me to this position and for providing me with the best advice. Thank you for your kindness and for sharing your extensive knowledge with me (and so patiently!). In special to Denis, who I have been working the closest during my PhD: I'll always be indebted for everything you have taught me, both professionally and personally. I wish, independently of the road I choose for my future, to be a good professional and thoughtful man as you are.

To the members of the thesis committee: the reviewers Dr. Denis Dochain and Dr. Mario di Bernardo, as well as for the examiners Dr. Catherine Bonnet and Dr. Eugenio Cinquemani, my sincere thanks for accepting to evaluate my working and to participate in this precious moment of my career.

For my fellow mates of the Valse team: Anatolli K., Artem N., Cyrille C., Fiodar H., Haik S., Nicolas E., Nelson F., Francisco L., Quentin V., Syiuan W., Tonametl S., Wenjie M., Yu Z., Yue W. and Youness B., thank you for making my stay in Lille such a great time.

I express my warmest thanks to my professor and friend Dr. Leonardo Sanches, who taught me what it is like to be a passionate professor and who supported and encouraged me for so many years, to my friend Dr. Mario Cassaro for being a true mentor, and to Dr. Rosane Ushirobira, for all support and all life lessons that definitely allowed me to grow as a person.

This letter would be incomplete without mentioning my best friends who, even far away, were always there for me with a good talk and fondness: Alexandre S., Arthur D., Renata B., Renata C., Jeancarlo O., Leonardo L., and Natalia U.

At last, but not at least, I thank my beautiful Daniella, whose companionship has made my life much warmer and full of meaning.

Summary

List of Figures

List of Tables

Notation

Sets, matrices and vectors

- The sets of real and integer numbers are defined by $\mathbb{R}$ and $\mathbb{Z}$, respectively, $\mathbb{R}_+ = \{s \in \mathbb{R} : s \geq 0\}$ and $\mathbb{Z}_+ = \mathbb{Z} \cap \mathbb{R}_+$.

- The absolute value of an element is denoted $|\cdot|$, while the Euclidean norm is denoted $\|\cdot\|$.

- The vector $V = \mathrm{vec}(v_1, \ldots, v_n) \in \mathbb{R}^\nu$ represents the concatenation of vectors $v_1, \ldots, v_n$ and $\nu = \sum_{i=1}^n \nu_i$, where ν_i is the dimension of each vector v_i. The matrix $M = \mathrm{diag}(m_1, \ldots, m_n)$ is a diagonal matrix whose elements are $M_{ii} = m_i$, where m_i are vectors or matrices of appropriate dimension. The transpose of the matrix M is denoted $M^\top$. For a symmetric matrix M, the symmetric entry (*i.e.*, $M_{i,j} = M_{j,i}$, for $i \neq j$) is denoted by $\star$. The determinant of a matrix M is denoted $\det(M)$.

- A matrix M is said to be non-negative if all of its elements are non-negative. A matrix M is said to be Schur stable if all of its eigenvalues have absolute value less than one. The identity matrix is denoted by $\mathcal{I}_n \in \mathbb{R}^{n \times n}$.

- Let $x_1, x_2 \in \mathbb{R}^n$ be two vectors and $A_1, A_2 \in \mathbb{R}^{n \times n}$ be two matrices, then the relations $x_1 \leq x_2$ and $A_1 \leq A_2$ are to be understood component-wise. For a matrix A we define $A^+ = \max\{0, A\}$, $A^- = A^+ - A$ (also understood in a component-wise sense, similarly for vectors), and also denote the matrix of absolute values of all elements by $|A| = A^+ + A^-$. For a symmetric matrix $A \in \mathbb{R}^{n \times n}$ the relation $A \prec 0$ (resp. $A \succeq 0$) means that $A \in \mathbb{R}^{n \times n}$ is negative (resp. positive semi-) definite. If A is diagonal, then $A > 0$ is equivalent to $A \succ 0$.

Continuous-time systems

- A continuous function $\alpha : \mathbb{R}_+ \to \mathbb{R}_+$ belongs to the class $\mathcal{K}$ if $\alpha(0) = 0$ and the function is strictly increasing. A function $\beta : \mathbb{R}_+ \times \mathbb{R}_+ \to \mathbb{R}_+$ belongs to the class $\mathcal{KL}$ if $\beta(\cdot, t) \in \mathcal{K}$ for each fixed $t \in \mathbb{R}_+$ and $\beta(s, \cdot)$ is decreasing and $\lim_{t \to +\infty} \beta(s, t) = 0$ for each fixed $s \in \mathbb{R}_+$. A function $\beta : \mathbb{R}_+ \times \mathbb{R}_+ \to \mathbb{R}_+$ belongs to the class $\mathcal{GKL}$ if $\beta(s, 0) \in \mathcal{K}$, $\beta(s, \cdot)$ is decreasing and for each $s \in \mathbb{R}_+$ there is $T_s \in \mathbb{R}_+$ such that $\beta(s, t) = 0$ for all $t \geq T_s$;

- For a Lebesgue measurable and essentially bounded function $x : \mathbb{R} \to \mathbb{R}^n$, denote $|x|_\infty = \operatorname{ess\,sup}_{t \in \mathbb{R}} \|x(t)\|$, and define $\mathcal{L}_\infty(\mathbb{R}, \mathbb{R}^n)$ as the set of all such functions with finite norms $|\cdot|_\infty$;

Discrete-time systems

- For a function $x : \mathbb{Z}_+ \to \mathbb{R}^n$, the convention $x_k = x(k)$ is adopted and denote $|x|_\infty = \sup_{k\in\mathbb{Z}_+} \|x_k\|$. Furthermore, we define as ℓ_∞^n the set of all sequences such that $|x|_\infty < \infty$;
- The convention $x_{k,i}$ is adopted to denote the i-*th* prediction step of the variable x, cast at each decision instant k.

Part 1:

Introduction and overview

Chapter 1

General Introduction

1.1 Background and motivation

Biotechnology has applications in several societal domains, such as medicine, agriculture, environmental sciences and industry. Indeed, many *bioprocesses* – processes in which a living organism (such as bacteria, yeast and microalgae), or their components, participate in the reactions – have been used by humans to obtain special products: ranging from brewing and fermentation to the development of new medicines.

Eventually, the interest in having biological systems with different capabilities or that do not occur in nature gave rise to synthetic biology [Fu and Panke, 2009]. This multidisciplinary and rather new field applies engineering approaches to design (or re-design existing) biological systems [Schmidt, 2012] and leverage new advanced technologies.

A recent trend in modern biotechnology is the concept of *microbial consortia* (or co-cultures), *i.e.*, the association of different species in a community (or the same species, but different strains[1]) [Rosero-Chasoy et al., 2021]. The objective of such an association is that it might allow more complex tasks to accomplished, or even have a better performance than possible by a single organism [Said and Or, 2017]. Indeed, many applications employing microbial consortia, such as bioprocessing [Peng et al., 2016], biorefinery and the production of high-valuable compounds [Rosero-Chasoy et al., 2021], biosynthesis and biodegradation [Che and Men, 2019], have shown to be promising in industrial, medical, and environmental sciences.

In this light, synthetic biology and systems biology offer interesting tools regarding bio-engineered synthetic microbial communities. For instance, it is possible to establish communication between organisms, "program" reactions to exogenous molecules or stimuli (such as light) to induce specific behaviours or establish syntrophic interactions in a network of microorganisms [McCarty and Ledesma-Amaro, 2019].

Over the last years, many researchers have devoted their attention to potential applications of control theory in synthetic biology [Hsiao et al., 2018]. Indeed, control theory offers several mature tools to deal with modelling, analysis, identification, control and observer design for general dynamical systems. However, several challenges arise when it comes to biological

[1] A strain is a genetic variant or subtype of a microorganism.

processes:

1. Uncertainty: biological processes are inherently uncertain thanks to variations due to internal and external factors. Also, the models available for control and estimation often fail to provide an accurate description of the real process, since many complex functions are still not elucidated by biologists.

2. Monitoring: online measurements of some key variables are often not available, due to the lack of sensors. Depending on the type of measurement, this information might be subject to several sources of noise and also suffer from slow sampling (which might take several minutes, depending on the type of sensor).

3. Control: designing a controller for such systems is not a simple task thanks to its inherent complexity, uncertainty and non-linear nature.

4. Constraints: thanks to their physical meaning, these systems are highly constrained. For instance, both state and input take only non-negative values.

5. Unusual supervision problems: frequently, the plant model in some operational mode becomes uncontrollable/unobservable (or close to it), which prevents a direct application of many existing approaches, since these properties often serve as obligatory prerequisites in theoretical studies.

There are two different ways of addressing control design for biological processes [Hsiao et al., 2018]: *in vivo*, which implements the control directly at a cell level (*i.e.*, each cell has a copy of the controller), by using a set of chemical species and reactions, or *in silico*, which implements it at a population level by using a computer on the loop (see the illustration in Figure 1.1). While the first scenario highly constrains the control design, the second one flaws by offering control only up to a community-averaged sense.

Concerning the second approach, it has been shown that it is possible to control communities by using an external stimulus. For instance, the coexistence of co-cultures has been shown to be possible in an early work [Davison and Stephanopoulos, 1986] by oscillating pH levels and, similarly, in [Krieger et al., 2020] by cycling temperature levels. Microfluidics has also been used for control purposes [Postiglione et al., 2018]. Also, the use of *optogenetics* is popular, *i.e.*, bio-engineering strains so it expresses certain genes when stimulated by light [Toettcher et al., 2011], [Milias-Argeitis et al., 2016], [Scott et al., 2019].

However, despite the huge variety of existing control and estimation algorithms designed for biological processes, there is a persistent need for their development and adaptation to new tasks and tools in the domain.

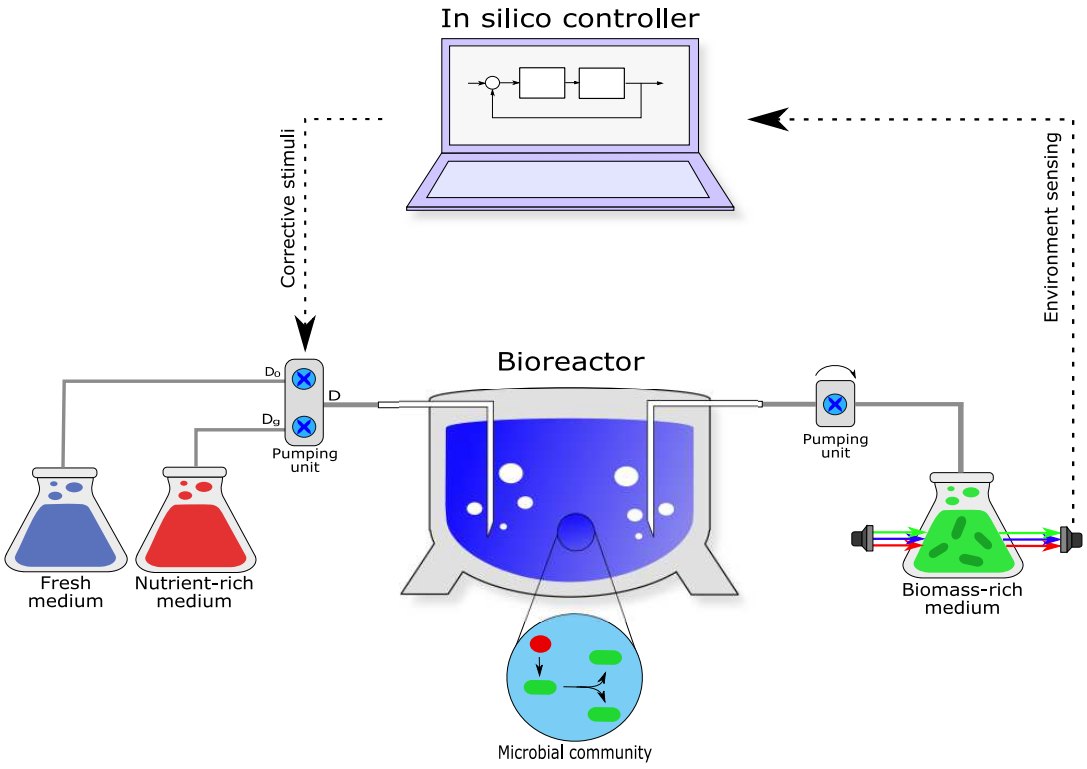

Figure 1.1: Schematic of a computed-based control of biological process

1.1.1 The *défi COSY*

This thesis was hosted in the framework of the Inria project lab *real-time COntrol of SYnthetic communities* (COSY)[2]. The objective of this project was to promote the collaboration between different research teams and to foment interdisciplinary approaches to address synthetic microbial communities and their possible applications in biotechnology.

The central interest of this project was the development of a microbial consortium and its related mathematical model, as well as its subsequent analysis, and design of control and estimation algorithms. This model, presented in [Mauri et al., 2020], describes the interaction of two different strains a bacteria *E. coli*, where one of them is called the *producer* (since it produces some compound of interest, *e.g.*, a heterologous protein), and a second one called the *cleaner*. This association is motivated by the fact that, while growing, the producer excretes a toxifying by-product (acetate) that inhibits its growth. The cleaner, having more affinity with the acetate, "cleans" the environment by consuming it and therefore alleviates inhibitory effects on the producer. The interest here is to observe if this association could lead to enhanced production of the compound of interest.

The design of control and estimation algorithms for this consortium based on that model is the primary objective of the present thesis.

[2]https://project.inria.fr/iplcosy/

1.2 Robust output feedback MPC

The control of constrained systems is known to be a hard (or even impossible) task to be tackled using classical feedback tools, such as the ones based on Lyapunov methods [Mayne et al., 2000]. However, in practice, there exist several limitations on control (such as physical limitations on actuators) or states (such as safety margins or natural constraints, such as non-negativity), which can be usually met in the regulation of bioprocesses, as discussed in the previous subsection, for instance. In this light, Model Predictive Control (MPC) has been an active research topic over the last three decades since it offers a way to handle constrained, possibly non-linear and multivariate optimal control problems.

The MPC algorithm is intuitive: at each decision instant, the states are measured and the future behaviour of the system is predicted using a dynamical model. Using this prediction, an optimization problem is solved and the optimal input sequence that solves the control problem is obtained. Finally, the first control move of this sequence is applied to the system, and the procedure is iteratively repeated. However, although simple, two challenges arise with the implementation of this algorithm:

1. The model used for prediction is often uncertain due to unmodelled dynamics, parametric uncertainties, disturbances, and unaccounted delays. These sources of errors lead to discrepancies between the predicted and real behaviour of the system. These discrepancies might lead to the transgression of constraints and even to instability;

2. To achieve constraint satisfaction, MPC requires full state feedback – which is often unavailable. This fact leads to the need for estimation techniques which, consequently, increases the level of uncertainty due to inherent estimation errors;

An MPC scheme is said to be *robust* if it achieves the control task while robustly respecting all constraints for a given range of all these uncertainties. Furthermore, item *(2)* characterizes the *robust output-feedback MPC* (OF-MPC) problem and is the subject studied in this thesis.

Before formulating the thesis' problematics with more details, let us briefly survey the existing results and approaches for monitoring/control of bioprocesses and MPC design. Such a preliminary discussion will help us with the positioning of the thesis, indicating some of the remaining gaps that have to be filled.

1.3 State of the art

Control and observation of microbial communities

If only a single species is considered, the existing literature disposes of a myriad of results concerning control and observation. Indeed, the bioreactor model has been extensively used as a benchmark due to its high nonlinearities, yielding results on time-optimal [D'ans et al., 1971] [Bayen et al., 2017], sliding-mode [Kravaris and Savoglidis, 2012], robust [Robledo, 2006], nonlinear feedback [Karafyllis and Jiang, 2012] and adaptive control [Mailleret et al., 2004]. In [Mazenc et al., 2017], the authors propose a nonlinear controller taking into account sampled and delayed measurements, as well as robustness against model uncertainty. The estimation problem (also called the *monitoring* problem, in which the objective is to design *soft sensors*) also disposes of a rich literature, such as presented in [Bastin and Dochain, 1990] and reviewed in [Dochain, 2003] [Mohd Ali et al., 2015].

On the other hand, if microbial consortia are considered, the results are more scarce. For instance, *in vivo* controllers have been proposed by [Fiore et al., 2017] and [Kerner et al., 2012]. The use of *in silico* control (as well as experiments using such controllers) are yet rare [Schlembach et al., 2021]. In [Hoo and Kantor, 1986] the authors propose a control law of a community of yeasts (competing and externally inhibited) by means of global linearization. In [Treloar et al., 2020], a reinforcement learning technique has been used.

In this sense, the control and the estimation problems applied to the microbial consortia are less studied in the literature. Furthermore, the robust versions of these problems are still relatively open, especially in the context presented by the project COSY.

Robust output feedback MPC

The second part of this thesis is devoted to the robust output feedback (ROF) MPC problem, *i.e.*, using a predictive controller to control a system that is subject to constraints (on control input and states) and does not dispose of full state measurement. The cases of linear time-invariant (LTI) and linear parameter-varying (LPV) systems are addressed.

For LTI systems, the ROF-MPC problem is very mature. Early results ranges from min-max optimization (*i.e.*, the minimization of a cost function while considering worst-case of the disturbances) [Bemporad et al., 2003, Raimondo et al., 2009], to the repeated solution of LMIs [Kothare et al., 1996, Rodrigues and Odloak, 2000]. Set-membership techniques, such as moving-horizon estimation (MHE) [Bemporad and Garulli, 2000], [Brunner et al., 2018], [Chisci and Zappa, 2002], have also been applied. These techniques use the available measurements to compute sets of admissible states (based on the available dynamics, bounds on the disturbances and initial uncertainty) and use them to guarantee constraint satisfaction.

Finally, Tube-based approaches [Mayne et al., 2006] [Mayne et al., 2009] [Langson et al., 2004] have also grown popular thanks to their reduced computational complexity: by predicting the trajectory of the nominal system, the controller is designed to enforce any deviation of the perturbed one to remain inside a tube.

For the LPV case, the problem becomes more complex since the scheduling parameter is unknown in future steps, making it harder to obtain reliable predictions. Nevertheless, several dynamic output feedback controllers have been proposed over the last years [Ding, 2010] [Ding et al., 2013]. In a different approach, [Yang et al., 2016] proposes an observer-based technique relying on input-to-state stability and robust positively invariant sets of the estimation error. In [Ping et al., 2020], the authors develop an approach that optimizes, simultaneously, both controller and observer. A tube-based method is presented by [Yang et al., 2019]. Parameter-dependent Lyapunov functions have also been used [Lee and Park, 2007]. Min-max optimization has been utilized in [Huang et al., 2014] and [Kim et al., 2006], although no state constraints are imposed. Most of these works recursively update the *estimation error sets* and thus require the common assumption that the scheduling parameter is measured, (there are exceptions, *e.g.*, [Ding et al., 2018], [Ding and Pan, 2016], but with a constrained prediction horizon).

In the literature mentioned above, sets bounding the uncertain states or the estimation error are used. However, these techniques face some drawbacks such as numerical complexity and an intricate implementation, which can be relaxed by the use of interval tools [Gouzé et al., 2000]. Especially concerning the LPV case, many of these techniques fix the prediction horizon to a one-step-ahead fashion (which can potentially shrink the feasible region of the optimization problem) and assume that the scheduling parameter is available, which is not always true in practice.

1.4 Thesis outline

In the light of the discussion above, the following problems were selected to be tackled in this thesis:

1. Estimate, in real-time, the concentration of the species in the consortium by using realistic measurements. These state estimators are then applied to the COSY problem;

2. Develop a control algorithm for the co-population, aiming at a certain task. This control should take into account possible uncertainties and robustly achieve the control problem;

3. By developing the interval observers and predictors, propose new robust output feedback MPC algorithms that are less computationally expensive, less conservative and easier

to implement.

Therefore, this thesis is divided into four parts: the general introduction, the results concerning control and observation of microbial communities, the development of new robust output feedback MPC algorithms using interval estimators and, finally, general conclusions and outlooks.

Part 2 is divided in two chapters: Chapter 2 addresses the problem of observation of microbial communities, considering a continuous bioreactor with a community of different microbes competing for a single limiting substrate and also the specific problem statement of the COSY model. Chapter 3 addresses the problem of robust stabilization of competing species at given concentration levels using a hybrid control architecture consisting of different discontinuous control laws. The control problem considering the COSY model is also presented.

Part 3 is composed of a single chapter, which discusses the developments on the OF-MPC problem for both LTI and LPV systems. In this chapter, new interval estimators (observers and predictors), as well as their corresponding feedback control laws, are proposed. The MPC algorithms incorporate these estimators and stability is proven using classic arguments. It is shown that robust constraint satisfaction is assured and the complexity of the resulting algorithm is low. Numerical examples illustrate these novel algorithms.

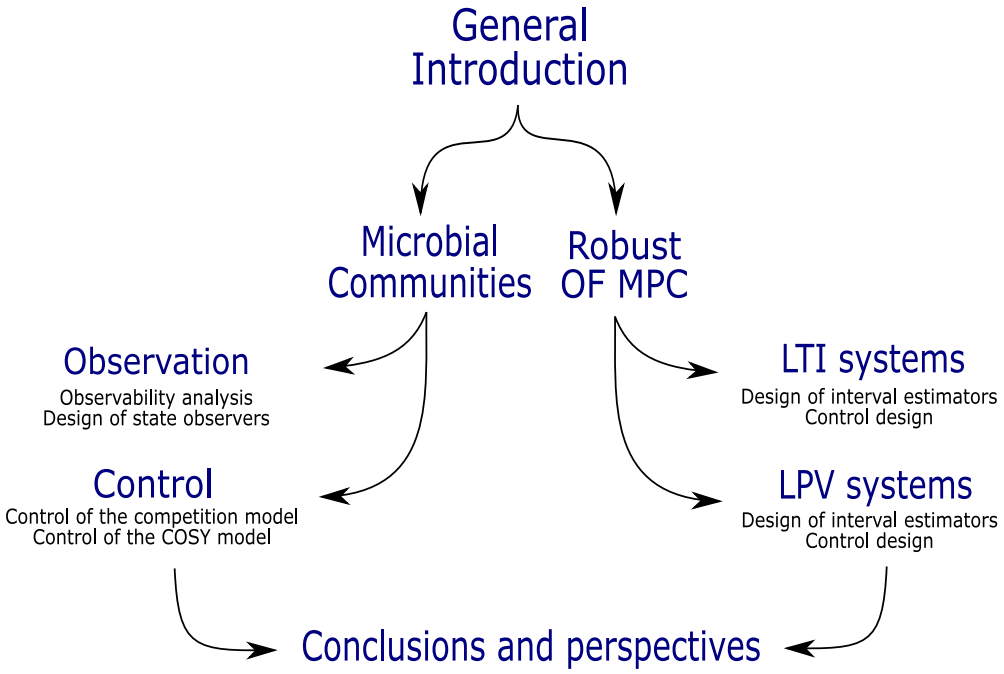

Figure 1.2: Overview of the thesis organization

1.5 Publication list

1.5.1 Peer-reviewed international journals

1. A. Reis de Souza, D. Efimov, A. Polyakov and J-L. Gouzé. *Robust stabilization of competing species in the chemostat.* Journal of Process Control 87, pages 138-146, 2019).

2. A. Reis de Souza, D. Efimov, A. Polyakov and J-L. Gouzé. *Robust adaptive estimation in the competitive chemostat.* Computers & Chemical Engineering 142, page 107030, 2020.[3]

3. A. Reis de Souza, D. Efimov, T. Raïssi and X. Ping. *Robust output feedback model predictive control for constrained linear systems via interval observers.* Submitted to Automatica (2021).

4. A. Reis de Souza, D. Efimov and T. Raïssi. *Robust output feedback MPC for LPV systems using interval observers.* Accepted on the IEEE Transactions on Automatic Control (2021).

5. A. Reis de Souza, D. Efimov and T. Raïssi. *Robust output feedback MPC for time-delayed systems using interval observers.* Submitted to International Journal of Robust and Nonlinear Control (2021).[3]

6. A. Reis de Souza, D. Efimov, A. Polyakov, J-L. Gouzé and E. Cinquemani.*State observation in microbial consortia: a case study on a synthetic producer-cleaner consortium.* Submitted to International Journal of Robust and Nonlinear Control (2021).

1.5.2 Peer-reviewed international conferences

1. A. Reis de Souza, D. Efimov, A. Polyakov and J-L. Gouzé. *Robust control of a competitive Environment in the chemostat using discontinuous control laws.* Proceedings of the 58th IEEE Conference on Decision and Control, pp. 13-018, 2019.

2. A. Reis de Souza, D. Efimov, A. Polyakov and J-L. Gouzé. *On Adaptive Estimation of Bacterial Growth in the Competitive Chemostat.* Proceedings of the 11th IFAC Symposium on Nonlinear Control Systems,pp. 262-267, 2019.[3]

[3]These works are not reported in this manuscript.

3. A. Reis de Souza, D. Efimov, A. Polyakov and J-L. Gouzé. *Observer-Based Robust Control of a Continuous Bioreactor with Heterogeneous Community.* Proceedings of the 21st IFAC World Congress, 2020.[4]

4. A. Reis de Souza, D. Efimov, T. Raïssi and X. Ping. *Robust Output Feedback MPC: An Interval-Observer Approach.* Proceedings of the 59th IEEE Conference on Decision and Control, pp. 2529-2534, 2020.

[4]These works are not reported in this manuscript.

Part 2:

Control and Observation of Microbial Communities

Chapter 2

Introduction to the overall framework

2.1 Introduction

In this chapter, the models used for the observer and control design, as well as their features, are introduced. Two models are considered: *(i)* the *competition* model, which describes the competition of two different species for a single limiting substrate, and *(ii)* the model developed by the COSY project, which describes the syntrophic relationship of two different strains. The main difference between these models is that, while in the former there is only one nutrient and there is competition, in the latter two nutrients are considered but the species do not compete directly for survival.

2.1.1 The competition model

The competition model is described by the following nonlinear differential equations [Smith and Waltman, 1995]:

$$\begin{aligned}
\frac{dS(t)}{dt} &= D(t)(S_{in}(t) - S(t)) - \mu_1(S(t))x_1(t) - \mu_2(S(t))x_2(t) \\
\frac{dx_1(t)}{dt} &= (k_1\mu_1(S(t)) - D(t))x_1(t), \\
\frac{dx_2(t)}{dt} &= (k_2\mu_2(S(t)) - D(t))x_2(t),
\end{aligned} \tag{2.1}$$

where the states S and x_i are, respectively, the concentrations of nutrient and the concentration of the i-th species. D is the dilution rate, which describes the rate of inflow and outflow of media of the bioreactor. S_{in} is the concentration of nutrient diluted in the inflow of medium. The functions $\mu_i(S)$ are the reaction rates (also called *specific growth rates*) and describe the kinetics of nutrient uptake by each species. Finally, k_i are yield coefficients, describing the portion of nutrient uptake that is used for growth by each strain.

This model (and also the one described in the next subsection) is a *mass balance model*. From (2.1), one can see that the concentration of nutrient is increased by the inflow $D(t)S_{in}(t)$ and decreased by the consumption of the species (*i.e.*, $\mu_i(S)x_i(t)$). The concentrations of the species are positively influenced by this consumption. Finally, since a bioreactor usually operates with a constant volume, the outflow is equal to the inflow, meaning that all concentrations

are negatively affected by the dilution rate $D(t)$.

The main source of uncertainty in (2.1) comes from the description of nutrient uptake. Indeed, the functions μ_i might depend on a series of factors (such as substrate and population concentration, pH, temperature, inhibitors) [Bastin and Dochain, 1986], not always evident in experimentation. Furthermore, it is also hard to quantify how much of this uptake is indeed used for growth, leading the parameters k_i to be also an approximation.

The functions $\mu_i(S)$ may have many different forms. The most common one, known as *Monod's law* (or Michaelis-Menten kinetics), describes the growth of a species by consuming a single nutrient, being described by the following equation:

$$\mu(S) = \mu_{\max} \frac{S}{K_m + S}, \tag{2.2}$$

where $\mu_{\max} > 0$ and $K_m > 0$ are the maximum reaction rate and the half-saturation constant.

Inhibitory effects (*i.e.*, the decrease of the growth rate caused by high concentration of a nutrient) are usually modelled by the *Haldane equation*:

$$\mu(S) = \mu_{\max} \frac{S}{K_m + S + \frac{S^2}{K_i}}. \tag{2.3}$$

where $K_i > 0$ is the inhibition constant. Figure 2.1 illustrate functions (2.2) and (2.3). A

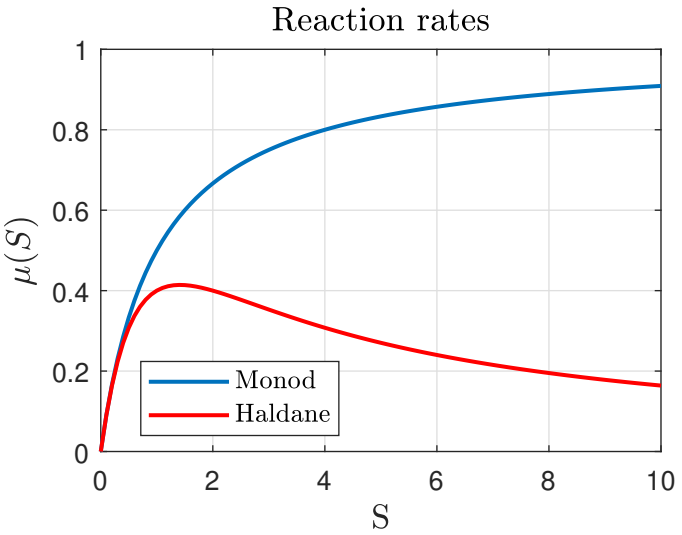

Figure 2.1: Illustration of the reactions rates ($\mu_{\max} = 1$,$K_m = 1$ and $K_i = 2$).

very important concept concerning competition models is the *competitive exclusion principle*: the competition between two or more species for a single limiting substrate will result in the survival of, at most, one species.

This principle has been proven mathematically in [Hsu et al., 1977] for monotone response function, and in [Wolkowicz and Lu, 1992] for general functions.

2.1.2 The COSY model

The COSY model, presented by [Mauri et al., 2020], describes the dynamics of a producer strain that grows and produces a special compound by consuming *glucose* and, by doing so, excretes *acetate* (which is toxifying, in the sense that it inhibits its growth). The syntrophic relationship is established by adding a second cleaning strain, that has more affinity in consuming acetate and therefore "detoxifies" the environment and alleviates inhibitory effects on the producer growth (see the pathways illustrated in Figure 2.3 below). The producer and the cleaner strains are henceforth denoted B_p and B_c, respectively. The glucose and acetate are denoted by G and A, respectively, and the nutrient state vector is denoted $\text{vec}(G, A)$. The equations of the model have the following form:

$$\begin{aligned}
\dot{G} &= D_g G_{in} - DG - r_1(G,A)B_p - r_2(G,A)B_c \\
\dot{A} &= D_a A_{in} - DA - r_3(G,A)B_p - r_4(G,A)B_c \\
\dot{B}_p &= (1-k_h)\mu_p(G,A)B_p - (k+D)B_p \\
\dot{B}_c &= \mu_c(G,A)B_c - (k+D)B_c
\end{aligned} \tag{2.4}$$

In this model, G_{in} and A_{in} are the concentration of each nutrient at the bioreactor inflow. Also, D_g and D_a are the dilution rates of glucose and acetate, respectively, while k is a positive scalar representing degradation (or *death rate*).

In (2.4), the functions μ_p and μ_c are given by

$$\begin{aligned}
\mu_p(G,A) &= Y_g r_1(G,A) + Y_a r_3(G,A), \\
\mu_c(G,A) &= Y_g r_2(G,A) + Y_a r_4(G,A),
\end{aligned} \tag{2.5}$$

where Y_g and the Y_a being the yield coefficients, denoting how much of each nutrient uptake is used for growth. Functions r_i, $i \in \{1, \ldots, 4\}$, similarly as for the competitive model, are the kinetic rates and denote the rates of exchange between the environment and the microbial cells and defined as

$$\begin{aligned}
r_1(G,A) &= k_g^p \frac{G}{G+K_g}\frac{\Theta_a}{A+\Theta_a}, \\
r_2(G,A) &= k_g^c \frac{G}{G+K_g}\frac{\Theta_a}{A+\Theta_a}, \\
r_3(G,A) &= k_a \frac{A}{A+K_a}\frac{\Theta_g}{r_1(G,A)+\Theta_g} - k_{over}\max(0, r_1(G,A)-l), \\
r_4(G,A) &= k_a \frac{A}{A+K_a}\frac{\Theta_g}{r_2(G,A)+\Theta_g} + k_{ac}\frac{A}{A+K_{ac}} - k_{over}\max(0, r_2(G,A)-l)),
\end{aligned} \tag{2.6}$$

and determine the nutrient uptake and acetate over-expression. The constant, positive, scalar parameters k_g^*, k_a, k_{ac}, k_{over} are yield coefficients, while K_a, K_g, K_{ac}, Θ_g, Θ_a are half saturation

constants. The constant scalar l represents a threshold in which acetate starts to be secreted.

It is worth noticing that the term $r_1(G, A)$ indicates that the producer grows by consuming glucose (the first term), while it is inhibited by the concentration of acetate (the second term). An illustration of this effect is depicted in Figure 2.2. Also, from $r_3(G, A)$ and $r_4(G, A)$, it is readily seen that some terms enter positively in the equation for A in (2.4), showing that acetate might be increased by excretion of the microbes.

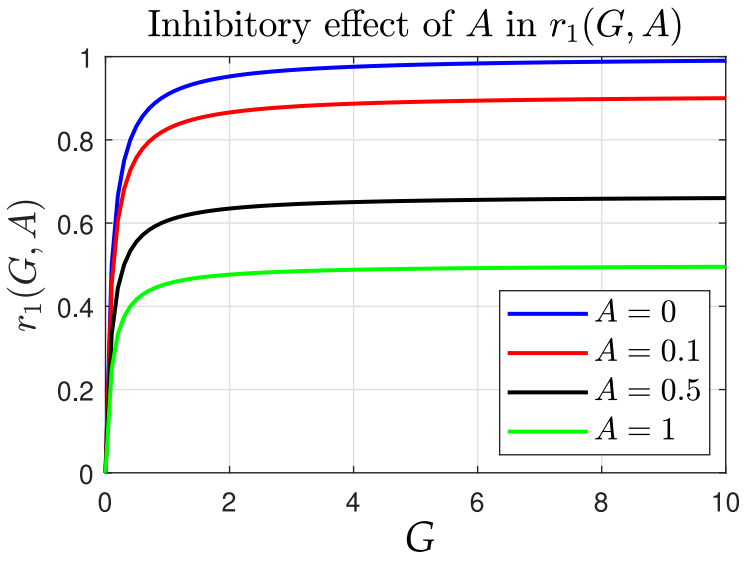

Figure 2.2: Inhibitory effect of A in the growth of the producer strain (parameters: $\mu_{max} = 1$, $K_g = 0.1$, $\Theta_a = 1$).

Along with (2.4), additional dynamics can be considered to express production by the producer:

$$\dot{H}(t) = k_h \mu_p(G(t), A(t)) B_p(t) - DH(t), \tag{2.7}$$

$$\dot{F}(t) = mH(t) - D(t)F(t). \tag{2.8}$$

where H is the product (*e.g.*, a heterologous protein) and F is a by-product (for instance, a fluorescent reporter resulting of the maturation of H) and k_h, m are proportionality constants. Figure 2.3 illustrates the pathways of the complete model.

Remark 2.1. *The dynamics* (2.7) *basically means that the uptake of substrate G is used for another purposes other than growth. Therefore, similar additional dynamics can be also considered for the competition model* (2.1).

Interesting features of the model (2.4) have been pointed out in [Mauri et al., 2020]. The coexistence of producer and cleaner strains depends on the growth parameters (such as the product yield k_h), as well as on the operating conditions (*i.e.*, the dilution rate D and nutrient inflow concentration G_{in}).

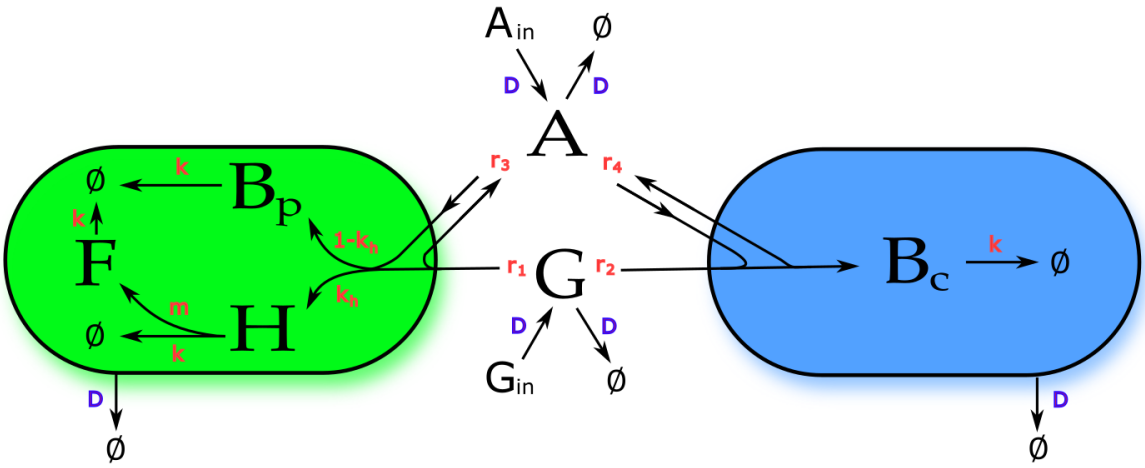

Figure 2.3: Pathways of the COSY model. The arrows indicate transfers, whose rates are depicted in red and purple. The transfers shown in red describe biological mechanisms (such as uptake, overflow, degradation, etc.), while the ones shown in purple are physical transfers (such as dilution rates). The symbol $\emptyset$ means that the refereed concentration is depleted out from the bioreactor (either by degradation or by dilution).

The cleaner strain grows, primarily, by consuming acetate. Although model (2.4) foresees an input of this nutrient (through the term $D_a A_{in}$), its concentration in the bioreactor is mainly due to secretion by the producer strain, which might only occur if $r_1(G, A) > l$ or $r_2(G, A) > l$. Therefore, the persistence of the cleaner strain in the bioreactor is guaranteed only if the producer grows sufficiently fast. Furthermore, since this growth is affected by k_h, this coefficient also needs to be taken into account when coexistence is analyzed.

Figure 2.4 illustrates the simulation of (2.4) in two scenarios: one with $D = 0.2$ $[h^{-1}]$ and with $D = 0.3$ $[h^{-1}]$, both considering $G_{in} = 20$ $[gL^{-1}]$ and $A_{in} = 0$. In the left plot, the trajectories of B_p and B_c are shown and it is clear that, with a lower dilution rate, the cleaner is washed out (*i.e.*, $B_c \to 0$). This is due to the insufficient acetate excretion by the producer species: the glucose inflow is not enough to ensure acetate overflow (*i.e.*, if $r_1(G, A) > l$). This acetate production (as illustrated by the solid line in the right plot) allows the dynamics of B_c to converge to a positive steady-state.

In the same scenarios, Figure 2.5 illustrates the trajectories of the product H. As it can be seen, although B_p reached a higher concentration with $D = 0.2$ $[h^{-1}]$, the scenario in which coexistence happens has yielded a higher production of H.

Following [Mauri et al., 2020], Figure 2.6 illustrates the relation between the inputs G_{in} and D in the steady-state values of each species. As it can be seen, there is a narrow region of D that permits coexistence. Obviously, for too high values of D, no species can survive and the biomass is washed-out of the bioreactor.

Clearly, the investigation above is carried out in an open-loop setup. Therefore, inspired

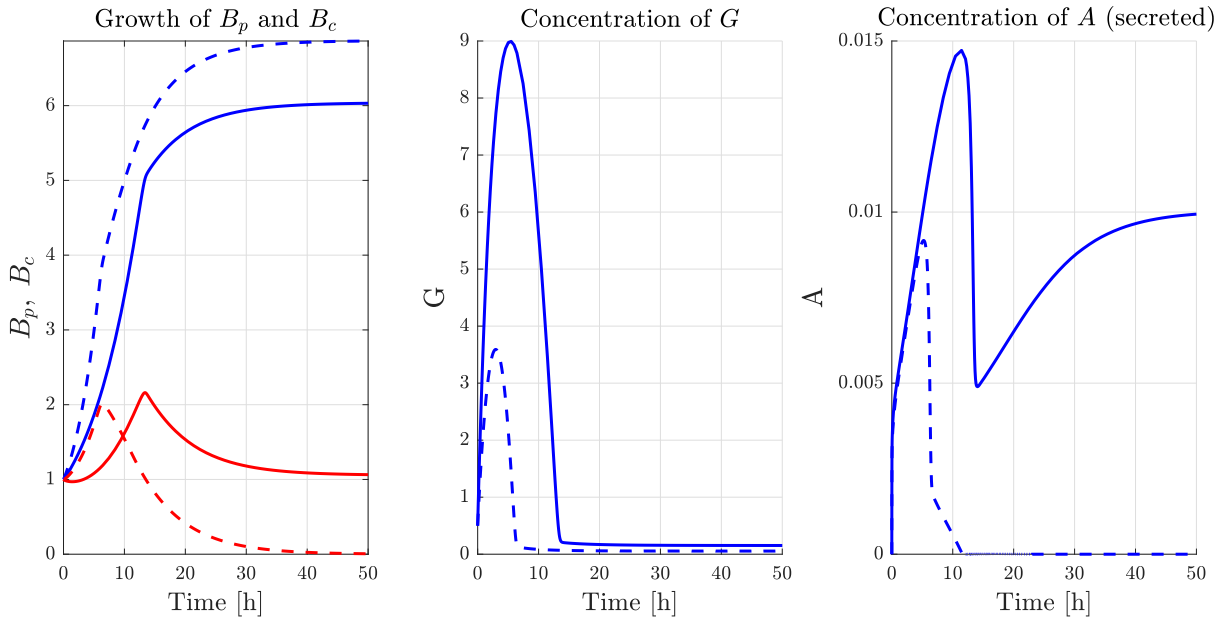

Figure 2.4: Simulation of (2.4) for $D = 0.2$ $[h^{-1}]$ (dashed lines) and $D = 0.3$ $[h^{-1}]$ (solid lines). Left plot: trajectories of B_p (in blue) and B_c (in red). Center plot: trajectories of G. Right plot: trajectories of A.

by these facts, it is of interest to study the use of closed-loop control algorithms to control this consortium. In addition, the objective is to evaluate the conditions in which the consortium will outperform the producer-only scenario. The control algorithm development also aims to enhance the operation of the consortium in terms of performance and robustness.

In the two next chapters, the estimation and the control algorithms are discussed. First, the conditions of observability and the subsequent state observers are proposed (these results can be applied to both systems). Then, the control algorithms are discussed: first a robust approach for the competition model, then the (nominal) control of the COSY model. For the latter, a nominal scenario (*i.e.*, all parameters and variables are perfectly known) is considered.

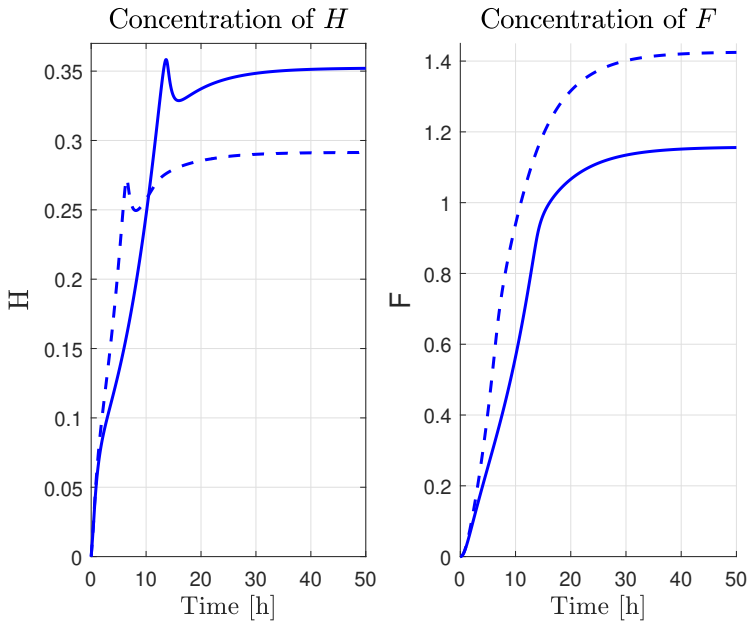

Figure 2.5: Trajectories of the concentrations of the product H (left) and its fluorescent reporter F (right), in two scenarios: $D = 0.3[h^{-1}]$ (solid lines), and $D = 0.2[h^{-1}]$ (dashed lines).

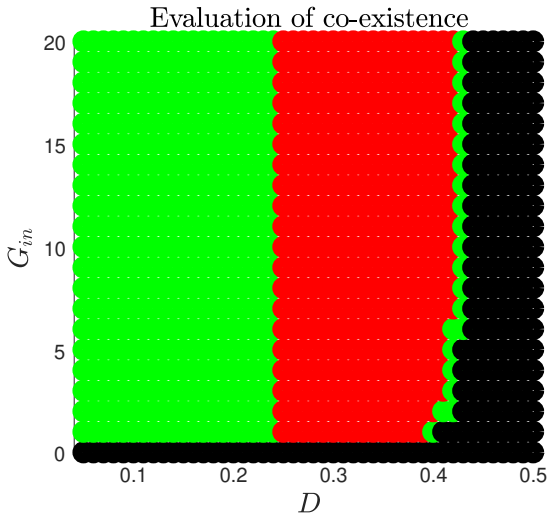

Figure 2.6: Numerical analysis of coexistence. Legend: green - only producer, red - co-existence, black - washout. This was obtained by numerical integration over a time span $T = 6000h$, having initial conditions given by $G(0) = 0.5$, $A(0) = 0.1$, $B_p(0) = 0.1$, $B_c(0) = 0.1$.

Chapter 3

Observation of Heterogeneous Communities

3.1 Introduction

In this chapter, the design of estimation algorithms is presented for the systems described in Chapter 2. First, the available measurements are introduced, then the questions addressed in this chapter are posed.

Available measurements

In this chapter, the following measurements will be considered:

1. The total biomass $y_1(t) = \sum_{i=1}^{n} x_i(t)$: obtained by methods such as *flow-cytometry* or *mass-spectrometry*. These kinds of measurement are usual in practice, although demanding a higher sampling time;

2. The fluorescent reporter $y_2(t) = F(t)$: obtained by *optical density* and obeying dynamics (2.7). Since it uses light to promote an indirect measurement, it can be sampled faster. However, the strain that produces the protein and expresses this reporter needs to be *bio-engineered*.

In this light, this chapter aims to address the following questions:

Q1- Are systems (2.1)–(2.4) *completely* or *partly* observable?

Q2- What are the necessary conditions for observability?

Q3- How do the available measurements $y_1(t)$ or $y_2(t)$ influence observability and observer design?

Q4- How to design the appropriate observers?

Preliminaries

Before discussing the questions posed above, some preliminary tools are introduced.

Observability of nonlinear systems

Observability is a property of a dynamical system indicating how well its internal states can be inferred by means of the available measurements. For nonlinear systems, the problem of observability has extensively discussed in the seminal paper by Hermann and Krener [Hermann and Krener, 1977].

Following that work, let us consider a general nonlinear system endowed with a measurement function as

$$\begin{aligned} \dot{x} &= f(x,u) \\ y &= h(x) \end{aligned} \tag{3.1}$$

where $x \in M$, a smooth connected manifold of dimension n, $y \in \mathbb{R}^p$, $u \in \Omega \subseteq \mathbb{R}^m$ and f, g being smooth functions. Let $\Sigma(x_0, u, [t_0, t_1])$ denote the solution of (3.1), in the time span $[t_0, t_1]$, with initial condition x_0 and input u. Then, a pair of points x^0, x^1 are said *indistinguishable* if they realize the same input-output map, *i.e.*, for every admissible input $u(t)$ in $[t_0, t_1]$,

$$h(\Sigma(x^0, u, [t_0, t_1])) = h(\Sigma(x^1, u, [t_0, t_1])).$$

Let $I(x_0)$ define the set of all indistinguishable points at x_0. Then, observability is defined as follows

Definition 3.1. *[Hermann and Krener, 1977] System (3.1) is said observable at $x_0 \in M$ if $I(x_0) = \{x_0\}$, and observable if $I(x) = \{x\}$ for every $x \in M$.*

The definition above is global, however, it can be also stated locally (*i.e.*, in a open neighborhood U of x_0). Furthermore, it might be only necessary to distinguish x_0 from its closest neighbors, leading to the weaker concept of observability called *weak observability*.

Definition 3.2. *[Hermann and Krener, 1977] System (3.1) is said to be (i) locally weakly observable at $x_0 \in M$ if there exists an open neighborhood $U \subset M$ of x_0 such that $I(x_0) = \{x_0\}$ for every open neighborhood $V \subset M$ of x_0 contained in U, and (ii) locally weakly observable if it is so for all $x \in M$.*

To introduce a criteria for verification of observability for (3.1), consider the following definition of the *Lie derivatives*:

Definition 3.3. *(Lie Derivative): Let $h(x)$ be a continuously differentiable function and*

$f(x,u)$ be a vector field. The Lie derivative of $h(x)$ along $f(x,u)$ is defined as

$$L_f h(x) = L_f^1 h(x) = \frac{\partial h(x)}{\partial x} f(x,u), \quad L_f^k h(x) = L_f L_f^{k-1} h(x),\ k \geq 2.$$

Then, the observation space $\mathcal{O}$ be the set formed by all linear combinations induced by the Lie derivatives of h_i (the components of h) with respect to f, *i.e.*,

$$\mathcal{O} = [h_1, \ldots, h_p, L_f h_1, \ldots, L_f h_p, L_f^2 h_1, \ldots, L_f^2 h_p, \ldots].$$

Let $d\mathcal{O}$ be the gradient of the elements of $\mathcal{O}$. The well-known *observability rank condition* is stated as follows:

Theorem 3.1. *[Hermann and Krener, 1977] The system (3.1) is (locally) weakly observable if $d\mathcal{O}$ contains n linearly independent vectors, i.e., rank$(d\mathcal{O}) = n$.*

If the system under consideration is time-varying and autonomous (as it will be the case in the following), *i.e.*,

$$\begin{aligned} \dot{x} &= A(t)x(t) \\ y &= C(t)x(t) \end{aligned}$$

and considering that $A(t), C(t)$ are analytic functions, then the following algorithm [Sontag, 1998, Ch. 6, p. 279] can be used to verify the rank condition above:

$$\operatorname{rank} \left(\begin{bmatrix} C_0(t) \\ C_1(t) \\ \vdots \\ C_{n-1}(t) \end{bmatrix} \right) = n,$$

where $C_0 = C(t)$ and $C_{i+1}(t) = \frac{d}{dt} C_i(t) + C_i(t)A(t)$ for $i = 1, \ldots, n-1$.

3.2 Estimating microbial co-cultures

3.2.1 Observability analysis

Since the structure of systems (2.1) and (2.4) are similar, the observability analysis presented in this section will be derived only for the latter [Souza et al., 2021a]. Indeed, the observability conditions for the species concentration are identical (by substituting $1 - k_h$ by k_1, and μ_p, μ_c by μ_1, μ_2, respectively). The observability condition for the nutrients are different but, nonetheless, follow the same rationale in both cases.

Consider (2.4) decomposed in two sub-systems: the first composed of the strains and products and the second composed of the nutrients. Denoting $x_1 = \text{vec}(B_p, B_c, H, F)$ and $x_2 = \text{vec}(G, A)$, the first sub-system can be obtained by rewriting (2.4) as

$$\begin{aligned} \dot{x}_1 &= \begin{bmatrix} (1-k_h)\mu_p(x_2) - (k+D) & 0 & 0 & 0 \\ 0 & \mu_c(x_2) - (k+D) & 0 & 0 \\ k_h\mu_p(x_2) & 0 & -(k+D+m) & 0 \\ 0 & 0 & m & -(k+D) \end{bmatrix} x_1 \\ y &= \begin{bmatrix} 0 & 0 & 0 & 1 \\ 1 & 1 & 0 & 0 \end{bmatrix} x_1 \end{aligned} \tag{3.2}$$

where $\mu_p(x_2), \mu_c(x_2)$ are given by (2.5). In (3.2), the variables G, A (*i.e.*, the elements of x_2) are interpreted as external inputs.

Proposition 3.1. *Assume $D > 0$ and that k, m, k_h and $\mu_p(x_2)$, $\mu_c(x_2)$ are known. Then, system (3.2) is observable in an interval $[t_0, t_1]$ if there exists a $t \in [t_0, t_1]$ such that $(1 - k_h)\mu_p(x_2(t)) \neq \mu_c(x_2(t))$.*

Proof. Since system (3.2) can be interpreted as an autonomous (without inputs) time-varying dynamics, and endowed with a constant measurement matrix, the observability condition to be satisfied in the interval $[t_0, t_1]$ is $\exists t \in [t_0, t_1]$ such that

$$\text{rank}\left(\begin{bmatrix} 0 & 0 & 0 & 1 \\ 1 & 1 & 0 & 0 \\ 0 & 0 & m & -(k+D) \\ (1-k_h)\mu_p(x_2) - (k+D) & \mu_c(x_2) - (k+D) & 0 & 0 \end{bmatrix}\right) = 4.$$

Since m, k, k_h are positive constants and $D > 0$ by assumption, this condition is verified if $(1 - k_h)\mu_p(x_2) \neq \mu_c(x_2)$. □

If the conditions given in Proposition 3.1 are verified, then B_p and B_c are observable and, therefore, can be considered as available signals. As readily seen in (2.4), the state vector x_2 and the measurement $y_2(t)$ are coupled by the functions $\mu_p(x_2)$ and $\mu_c(x_2)$ through the first

time derivative of x_1.

The fact above simplifies the observability analysis of the pair x_2 since all terms in (3.2), except the arguments of functions $\mu_p(x_2), \mu_c(x_2)$, are known. Denoting the vector-valued function $\mu(x_2) = \text{vec}(\mu_p(x_2), \mu_c(x_2))$, this brings us to the following proposition:

Proposition 3.2. *Let the conditions given in Proposition 3.1 be satisfied. Then, the state vector x_2 is observable in a neighborhood of a point x_2^0 if, for $x_1 \neq 0$, the following condition holds*

$$\det J(\mu(x_2^0)) \neq 0$$

where $J(\mu(x_2^0))$ is the Jacobian of $\mu(x_2)$ evaluated at x_2^0.

Proof. As discussed above, if x_1 and its time derivative are available, the observability problem for x_2 reduces to the invertibility of the vector-valued function $\mu(x_2)$. Evoking the *inverse function theorem* [Nijenhuis, 1974], the condition given in this proposition assures that $\mu(x_2)$ is invertible in, at least, a vicinity of the point x_2^0. □

Remark 3.1. *If only one substrate is considered, i.e., $x_2 = S$ (such as in the case of model (2.1)), then the condition given in Proposition 3.2 reduces to the invertibility of function $\mu_i(S)$.*

A question that might arise concerns the observability conditions if solely y_2 is available. To tackle this question, a weaker concept of observability, called *detectability* (or *asymptotic observability*) can be evoked. Recalling [Sontag, 1998], a system is called *detactable* if all of its unobservable states are asymptotically stable. This brings us to the following proposition:

Proposition 3.3. *If only the measurement y_2 is available, then system (2.4) is detectable.*

Proof. As it can be directly seen from (2.4), the states H and F are not observable through y_2, since no relation with this measurement or its derivatives can be directly constructed.

For the remaining states, however, the observability conditions given in propositions 3.1–3.2 remain valid. Indeed, if a subsystem composed of B_p and B_c is considered, the rank condition simply reduces to

$$\text{rank}\left(\begin{bmatrix} 1 & 1 \\ (1-k_h)\mu_p(x_2) - (k+D) & \mu_c(x_2) - (k+D) \end{bmatrix}\right) = 2$$

which does not alter the requirement stated in Proposition 3.1.

Noticing that the dynamics of the unobservable states F and H are basically first-order stable filters having B_p and x_2 as inputs, this fact implies that the unobservable states have asymptotically stable dynamics. Therefore, system (2.4) is detectable with respect to y_2. □

Using the conditions given in propositions 3.1–3.3, the observable (or detectable) states of (2.4) might be numerically estimated.

3.2.2 Estimation of H, B_p and B_c

In this subsection, the objective is to develop state observers for system (3.2). The estimation of the nutrients G, A will be addressed in the subsequent section. To construct these observers, the differentiation of the available measurements will be needed, hence it is assumed that the input D is continuously differentiable with a known and bounded derivative.

As it will be shown in the following, the first and second time derivatives of y_1, as well as the first time derivative of y_2, will be needed. Therefore, the following differentiators (see Appendix B) will be implemented:

$$\begin{cases} \dot{z}_0 = \lambda_{12} L_1^{\frac{1}{3}} |z_0 - y_1| \text{sign}(z_0 - y_1) + z_1 \\ \dot{z}_1 = \lambda_{11} L_1^{\frac{1}{2}} |z_0 - y_1| \text{sign}(z_0 - y_1) + z_2 \\ \dot{z}_2 = \lambda_{10} L_1 \text{sign}(z_0 - y_1) \end{cases} \tag{3.3}$$

$$\begin{cases} \dot{\xi}_0 = \lambda_{21} L_2^{\frac{1}{2}} |\xi_0 - y_2| \text{sign}(z_0 - y_2) + \xi_1 \\ \dot{\xi}_1 = \lambda_{20} L_2 \text{sign}(\xi_0 - y_2) \end{cases} \tag{3.4}$$

and thus, according to [Levant, 2003], if the gains L_1 and L_2 are selected such as

$$\begin{aligned} L_1 &\geq \left| m\Big(k_h \mu_1 B_p - mH - 2(k+D)H\Big) - (F+w)\Big(\dot{D} + (k+D)^2 + (k+D)m\Big)\right|, \\ L_2 &\geq \left|(1-k_h)\mu_1 B_p + \mu_2 B_c - (k+D)(B_p + B_c + w)\right|, \end{aligned} \tag{3.5}$$

then, it is guaranteed that $z_0 \to y_1$, $z_1 \to \dot{y}_1$, $z_2 \to \ddot{y}_1$, and $\xi_0 \to y_2$, $\xi_1 \to \dot{y}_2$ in a finite-time in the noise-free case, and the related discrepancies stay bounded for bounded noises. Having these estimates, an observer for H is readily obtained from the dynamics of F in (2.4) as follows:

$$\hat{H} = \frac{z_0(k+D+m) + z_1}{m}. \tag{3.6}$$

Remark 3.2. *The quantities in* (3.5) *can be estimated by determining the range of operation of the bioreactor.*

Since the dynamics of both B_p and B_c depends on G and A (which are, *a priori*, unknown), denote $\mu_p = \mu_1(G, A)B_p$ and $\mu_c = \mu_2(G, A)B_c$. Computing the second derivative of F, one gets

$$\begin{aligned} \ddot{F} &= m\dot{H} - (k+D)\dot{F} \\ &= m\left[k_h \mu_p - (k+D+m)H\right] - (k+D)\dot{F} - \dot{D}F, \end{aligned}$$

and thus, the measurement $y_1(t)$ can be used to estimate $\mu_p(G, A)$ by means of the output of

the differentiator (3.3) and the estimate (3.6):

$$\begin{aligned}\hat{\mu}_p &= \frac{z_2 + (k+D)z_1 + \dot{D}z_0}{mk_h} + \frac{(k+D+m)\hat{H}}{k_h} \\ &= \frac{z_2 + [2(k+D)+m]z_1 + \left[\dot{D} + m + (k+D)^2\right] z_0}{mk_h}.\end{aligned} \tag{3.7}$$

Now, let us investigate the dynamics of the total biomass. By summing the third and forth equations in (2.4), one gets

$$\dot{B}_p + \dot{B}_c = (1-k_h)\mu_p(G,A)B_p + \mu_c(G,A)B_c - (k+D)(B_p+B_c),$$

which allows us to use the measurement y_2, along with the output of the differentiator (3.4) and the estimate (3.7), to compute an estimate of μ_c by

$$\hat{\mu}_c = \xi_1 + (k+D)\xi_0 - (1-k_h)\hat{\mu}_p.$$

Therefore, profiting on the structure of $\dot{B}_p$ and $\dot{B}_c$, the following observers can be proposed:

$$\dot{\hat{B}}_p = (1-k_h)\hat{\mu}_p - (k+D)\hat{B}_p, \tag{3.8}$$

$$\dot{\hat{B}}_c = \hat{\mu}_c - (k+D)\hat{B}_c. \tag{3.9}$$

For the next result, consider the estimation errors given by $e_p = B_p - \hat{B}_p$ and $e_c = B_c - \hat{B}_c$.

Theorem 3.2. *Consider system (2.4), differentiators (3.3)–(3.4) with gains satisfying (3.5), and observers (3.8)–(3.9). Then, the dynamics of the estimation errors e_p and e_c are input-to-state stable with respect to the measurement noises.*

Proof. Computing the time derivatives of e_p, e_c, one gets

$$\begin{aligned}\dot{e_p} &= -(k+D)e_p + (\mu_p - \hat{\mu}_p), \\ \dot{e_p} &= -(k+D)e_c + (\mu_c - \hat{\mu}_c).\end{aligned}$$

Consider a Lyapunov function candidate given by $V = \frac{1}{2}(e_p^2 + e_c^2)$, whose time derivative is given by

$$\begin{aligned}\dot{V} &= e_p\dot{e}_p + e_c\dot{e}_c \\ &= -(k+D)(e_p^2 + e_c^2) + e_p(\mu_p - \hat{\mu}_p) + e_c(\mu_c - \hat{\mu}_c).\end{aligned}$$

Using the *Young's inequality* [Hardy et al., 1934], the term $e_p(\mu_p - \hat{\mu}_p)$ can be upper

bounded as follows:

$$e_p(\mu_p - \hat{\mu}_p) \leq \frac{\epsilon^2}{2} e_p^2 + \frac{(\mu_p - \hat{\mu}_p)^2}{2\epsilon^2}$$

for any constant $\epsilon > 0$. Applying the same idea to the term $e_c(\mu_c - \hat{\mu}_c)$, the derivative $\dot{V}$ can be upper bounded by

$$\dot{V} \leq -2(k + D - \epsilon^2)V + \frac{(\mu_p - \hat{\mu}_p)^2}{2\epsilon^2} + \frac{(\mu_c - \hat{\mu}_c)^2}{2\epsilon^2}. \tag{3.10}$$

Finally, recalling the results concerning the differentiator (see the Appendix B, Theorem B.1), the positive terms on the right-hand side of (3.10) are bounded. Then, provided that $k + D > \epsilon^2$ (which is always verified by a proper selection of ϵ), one can conclude that the function V is an ISS Lyapunov function, proving the claim. □

3.2.3 Estimation of G and A

An interesting feature of the observers proposed in the previous section is that they *do not* depend on *any* of the reaction rates r_i and, therefore, do not require the joint estimation of the nutrients G and A.

Obviously, this is not the case when G and A need to be estimated – what would be of interest when designing control algorithms for system (2.4) (or (2.1)). Indeed, real-time information of these quantities is hard to obtain in practice, making this estimation an interesting option. In this light, following hypothesis is imposed:

Assumption 3.1. *The estimates $\hat{B}_p$ and $\hat{B}_c$ have converged to the true values of B_p and B_c.*

Assumption 3.1 is technical and is needed only to simplify the analysis of the observers proposed in the following. In practice, all observers will be launched at once. Under assumption 3.1, the following observer can be proposed

$$\begin{aligned} \dot{\hat{G}} &= -r_1(\hat{G}, \hat{A})B_p - r_2(\hat{G}, \hat{A})B_c - D\hat{G} + D_g G_{in} \\ \dot{\hat{A}} &= -r_3(\hat{G}, \hat{A})B_p - r_4(\hat{G}, \hat{A})B_c - D\hat{A} + D_a A_{in}. \end{aligned} \tag{3.11}$$

For the next theorem, let the estimation errors be given by $e_g = G - \hat{G}$ and $e_a = A - \hat{A}$.

Theorem 3.3. *Let Assumption 3.1 be satisfied and consider system (2.4) and observer (3.11). If*

$$D > (B_c + B_p) \max\left\{ \frac{k_g^p + k_g^c}{\Theta_a}, \frac{k_a k_g}{\Theta_g K_g^2} \right\},$$

then the dynamics of the estimation errors e_g, e_a are globally asymptotically stable.

Proof. The dynamics of the estimation errors e_g, e_a are computed as

$$\begin{aligned}\dot{e}_g &= (-r_1(G,A) + r_1(\hat{G},\hat{A}))B_p + (-r_2(G,A) + r_2(\hat{G},\hat{A}))B_c - De_g \\ \dot{e}_a &= (-r_3(G,A) + r_3(\hat{G},\hat{A}))B_p + (-r_4(G,A) + r_4(\hat{G},\hat{A}))B_c - De_a.\end{aligned} \tag{3.12}$$

The objective here is to show that e_g is a perturbation on the dynamics of e_a (and *vice-versa*), and the overall interconnection is ultimately bounded. Considering the term proportional to B_p, summing and subtracting $r_1(\hat{G}, A)$ leads to

$$-r_1(G,A) + r_1(\hat{G},\hat{A}) = -r_1(G,A) + r_1(\hat{G},\hat{A}) + r_1(\hat{G},A) - r_1(\hat{G},A)$$

$$\begin{aligned}&= \frac{k_g^p \Theta_a}{A+\Theta_a}\left(\frac{\hat{G}}{K_g+\hat{G}} - \frac{G}{K_g+G}\right) + \frac{k_g^p \hat{G}}{K_g+\hat{G}}\Theta_a\left(\frac{1}{\Theta_a+\hat{A}} - \frac{1}{\Theta_a+A}\right) \\ &= \frac{k_g^p \Theta_a}{A+\Theta_a} K_g\left(\frac{-e_g}{(K_g+\hat{G})(K_g+G)}\right) + \frac{k_g^p \hat{G}}{K_g+\hat{G}}\Theta_a\left(\frac{e_a}{(A+\Theta_a)(\hat{A}+\Theta_a)}\right).\end{aligned}$$

Since the function r_2 is similar to r_1, an analogous result can be derived for the term proportional to B_c. Considering a Lyapunov function candidate given by $V_g = |e_g|$, a bound on its time derivative can be computed as

$$\dot{V}_g \leq -D|e_g| + \frac{B_p k_g^p + B_c k_g^c}{\Theta_a}|e_a|. \tag{3.13}$$

Now, let us focus on the dynamics of e_a in (3.12). Note that, due to the over-expression terms (*i.e.*, $r_a^{over,*}(G,A)$), r_3 and r_4 are composed of two functions each:

$$\begin{aligned}-r_3(G,A) + r_3(\hat{G},\hat{A}) &= -r_3(G,A) + r_3(\hat{G},\hat{A}) + r_3(\hat{G},A) - r_3(\hat{G},A) \\ &= r_a^{up,p}(\hat{G},\hat{A}) - r_a^{up,p}(G,A) + r_a^{over,p}(G,A) - r_a^{over,p}(\hat{G},\hat{A}).\end{aligned}$$

Consider the difference $r_a^{up,p}(\hat{G},\hat{A}) - r_a^{up,p}(G,A)$ as above. Summing and subtracting $r_a^{up,p}(\hat{G},A)$, one can write

$$\begin{aligned}r_a^{up,p}(\hat{G},\hat{A}) - r_a^{up,p}(G,A) &= \frac{k_a}{r_g^{up,p}(G,A)+\Theta_g}\left(\frac{-e_a}{(A+K_a)(\hat{A}+K_a)}\right) \\ &+ \frac{k_a\hat{A}}{\hat{A}+K_a}\Theta_g\left(\frac{r_g^{up,p}(G,\hat{A}) - r_g^{up,p}(\hat{G},\hat{A})}{(r_g^{up,p}(\hat{G},\hat{A})+\Theta_g)((r_g^{up,p}(G,\hat{A})+\Theta_g)}\right) \\ =&\frac{k_a}{r_g^{up,p}(G,A)+\Theta_g}\left(\frac{-e_a}{(A+K_a)(\hat{A}+K_a)}\right) \\ &+ \frac{k_a\hat{A}}{\hat{A}+K_a}\Theta_g\frac{\Theta_a}{\hat{A}+\Theta_a}\left(\frac{k_g^p\frac{e_g}{(\hat{G}+K_g)(G+K_g)}}{(r_g^{up,p}(\hat{G},\hat{A})+\Theta_g)((r_g^{up,p}(G,\hat{A})+\Theta_g)}\right).\end{aligned}$$

Proceeding analogously for the remaining difference $r_a^{over,p}(G,A) - r_a^{over,p}(\hat{G},\hat{A})$ one has

$$\begin{aligned} &r_a^{over,p}(G,A) - r_a^{over,p}(\hat{G},\hat{A}) = k_{over}\left(r_g^{up,p}(G,A) - r_g^{up,p}(\hat{G},\hat{A})\right) \\ &= k_{over}\left[\frac{k_g^p G}{G+K_g}\Theta_a\left(\frac{-e_a}{(A+\Theta_a)(\hat{A}+\Theta_a)}\right) + \frac{k_g^p\Theta_a}{\hat{A}+\Theta_a}K_g\left(\frac{e_g}{(K_g+G)(K_g+\hat{G})}\right)\right]. \end{aligned}$$

The last term to be analyzed is the one proportional to B_c, *i.e.*, $r_4(G,A) - r_4(\hat{G},\hat{A})$. However, due to the similarity of the concerned functions, one can profit of the developments made above to write

$$\begin{aligned} &- r_a^{up,c}(G,A) + r_a^{up,c}(\hat{G},\hat{A}) = \frac{k_a}{r_g^{up,p}(G,A)+\Theta_g}\left(\frac{-e_a}{(A+K_a)(\hat{A}+K_a)}\right) \\ &+ \frac{k_a\hat{A}}{\hat{A}+K_a}\Theta_g\frac{\Theta_a}{\hat{A}+\Theta_a}\left(\frac{k_g^c\frac{e_g}{(\hat{G}+K_g)(G+K_g)}}{(r_g^{up,c}(\hat{G},\hat{A})+\Theta_g)((r_g^{up,c}(G,\hat{A})+\Theta_g)}\right), \end{aligned}$$

and

$$\begin{aligned} &r_a^{over,c}(G,A) - r_a^{over,c}(\hat{G},\hat{A}) \\ &= k_{over}\left[\frac{k_g^c G}{G+K_g}\Theta_a\left(\frac{-e_a}{(A+\Theta_a)(\hat{A}+\Theta_a)}\right) + \frac{k_g^c\Theta_a}{\hat{A}+\Theta_a}K_g\left(\frac{e_g}{(K_g+G)(K_g+\hat{G})}\right)\right]. \end{aligned}$$

Finally, considering a Lyapunov function candidate $V_a = |e_a|$, whose time derivative can be upper-bounded using the developments made above as

$$\begin{aligned} \dot{V}_a &\leq -D|e_a| + \left[B_p\left(\frac{k_a k_g^p}{\Theta_g K_g^2} + \frac{k_g^p}{K_g}\right) + B_c\left(\frac{k_a k_g^c}{\Theta_g K_g^2} + \frac{k_g^c}{K_g}\right)\right]|e_g| \\ &\leq -D|e_a| + \left(\frac{k_a}{K_g}\frac{1+\Theta_g K_g}{\Theta_g K_g}(k_g^p B_p + k_g^c B_g^c)\right)|e_g|. \end{aligned} \tag{3.14}$$

In order to prove boundedness of the overall estimation error, let $V_{ag} = V_g + V_a$. The time derivative of this function, according to (3.13) and (3.14), is upper bounded by

$$\begin{aligned} \dot{V}_{ag} &= \dot{V}_g + \dot{V}_a \\ &\leq -D(|e_g| + |e_a|) + \frac{B_p k_g^p + B_c k_g^c}{\Theta_a}|e_a| + \left(\frac{k_a}{K_g}\frac{1+\Theta_g K_g}{\Theta_g K_g}(k_g^p B_p + k_g^c B_g^c)\right)|e_g| \\ &\leq -DV_{ag} + \frac{B_p k_g^p + B_c k_g^c}{\Theta_a}|e_a| + \left(\frac{k_a}{K_g}\frac{1+\Theta_g K_g}{\Theta_g K_g}(k_g^p B_p + k_g^c B_g^c)\right)|e_g|, \end{aligned}$$

leading us to conclude that, if $D > (k_g^p B_c + k_g^c B_p)\max\left\{\frac{1}{\Theta_a}, \frac{k_a(1+\Theta_g K_g)}{\Theta_g K_g^2}\right\}$, then $V_{a,g}$ is a Lyapunov function, proving the claim. □

The advantage of measuring y_1

As discussed in Proposition 3.3, the system (2.4) is detectable through y_2. Then, a question is raised: *why not design an observer for the observable states (in this case, the concentration of substrates and microbes) using solely this measurement?* By substituting B_p and B_c by $\hat{B}_p$ and $\hat{B}_c$ in (3.11), additional observer equations can be proposed:

$$\begin{aligned}\frac{d}{dt}\hat{B} &= \begin{bmatrix}(1-k_h)\mu_p(\hat{x}_2)-(k+D) & 0\\ 0 & \mu_c(\hat{x}_2)-(k+D)\end{bmatrix}\hat{B} + L(y_2 - C_2\hat{B}),\\ \frac{d}{dt}\hat{H} &= k_h\mu_p(\hat{x}_2) - (k+D+m)\hat{H},\end{aligned} \tag{3.15}$$

for $\hat{B} = \text{vec}(\hat{B}_p, \hat{B}_c)$, $C_2 = \begin{bmatrix}1 & 1\end{bmatrix}$, $\hat{x}_2 = \text{vec}(\hat{G}, \hat{A})$, and some gain L. In this case, the estimates $\hat{B}_p$ and $\hat{B}_c$ would be computed *jointly* with the estimates $\hat{G}$ and $\hat{A}$. Obviously, a more intricate analysis would have to be carried out to identify the stability conditions.

It is interesting to notice that, in addition to allowing the observation of H, the measurement y_1 is helpful when observing B_p and B_c in the sense that it eliminates the need of knowing the rates r_i perfectly.

Therefore, one can conclude that estimation of H, B_p and B_c using both y_1 and y_2 requires only knowledge on parameters m, k, and k_h, while the estimation of G and A requires knowledge on all parameters *except* Y_g and Y_a. In counterpart, if solely y_2 is used, then the knowledge of *all* parameters in (2.4) are required for the estimation of the (observable) state variables. Clearly, in practice, these parameters (especially those related to the functions r_i, $i \in \{1, \ldots, 4\}$) may be uncertain and, thus, the first scenario would introduce less error in the resulting estimation.

3.2.4 Numerical example

In this section, a numerical experiment is presented to illustrate the proposed methodology. For the simulation of system (2.4), the parameters are such as given given in [Mauri et al., 2020] and, arbitrarily (but realistically) $k_h = 0.2$ and $m = 1$. The initial conditions are selected as $G(0) = 5$, $A(0) = 0$, $B_p(0) = 3$, $B_c(0) = 2$, $H(0) = 0$ and $F(0) = 0$ $[gL^{-1}]$.

Furthermore, the inlet glucose concentration is taken as $G_{in} = 20$ $[gL^{-1}]$ and the dilution rate as $D = 0.3 + 0.05\sin(0.1t)$ $[h^{-1}]$. Aiming at a simulation that is closer to a real-world scenario, it is considered that all measurements are sampled at every 10 minutes by a zero-order holder. Figure 3.1 shows the sampled measurements y_1 and y_2, both corrupted by measurement noise (in contrast with the unperturbed signals, depicted by the black curves).

In the following, the simulation results will be presented for two scenarios: using both measurements and applying observers (3.6), (3.8) and (3.9), and using only the measurement

of the total biomass (*i.e.*, y_2), applying observers (3.15). A discussion on the estimation error introduced by parametric uncertainty is then provided.

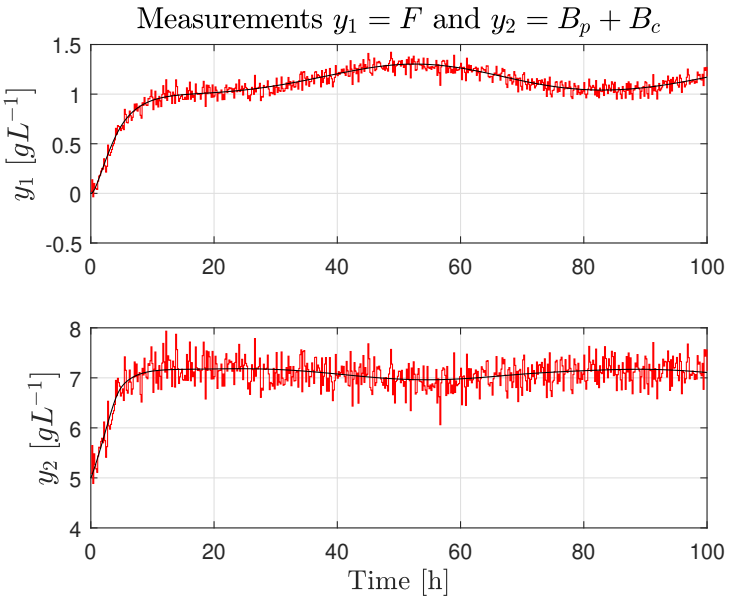

Figure 3.1: Measurements y_1 and y_2 (in red), in contrast to the output of the differentiators (3.3)–(3.4) (in black).

Estimation using both measurements

First, simulation results are presented considered observers (3.6), (3.8) and (3.9). The gains of the differentiators (3.3)–(3.4) are taken as $L_1 = 0.05$ and $L_2 = 1$, respectively. Finally, the initial conditions for the observers are taken as $\hat{G}(0) = 0$, $\hat{A}(0) = 0$, $\hat{B}_p(0) = 0$ and $\hat{B}_c(0) = 0$.

Figures 3.3 and 3.4 illustrate the real trajectories of B_p, B_c and G, A, respectively, as well as their respective estimates. Finally, Figure 3.2 shows the estimation of the heterologous protein H. Although the estimate $\hat{H}$ shows more sensitivity to noise than the other estimates, which are obtained through integration, it does not require any knowledge of the rates r_i.

Using only the total biomass

Now, the same scenario described previously will be considered, but using observers given by (3.15). These observers will be initialized with $\hat{G}(0) = 0$, $\hat{A}(0) = 0$, $\hat{B}_p(0) = 0$, $\hat{B}_c(0) = 0$ and $\hat{H}(0) = 0$. The observer gain will be selected as $L = 10$.

Figures 3.5 and 3.6 illustrate, respectively, the estimation of the nutrients G and A, and biomasses B_p and B_c. As it can be seen, since all parameters are perfectly known, all estimates converge to the true values. Also, since they undergo integration, the influence of

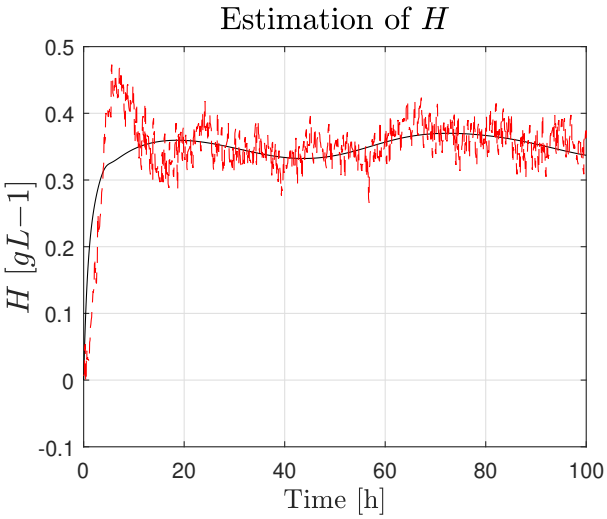

Figure 3.2: Estimation of $H(t)$.

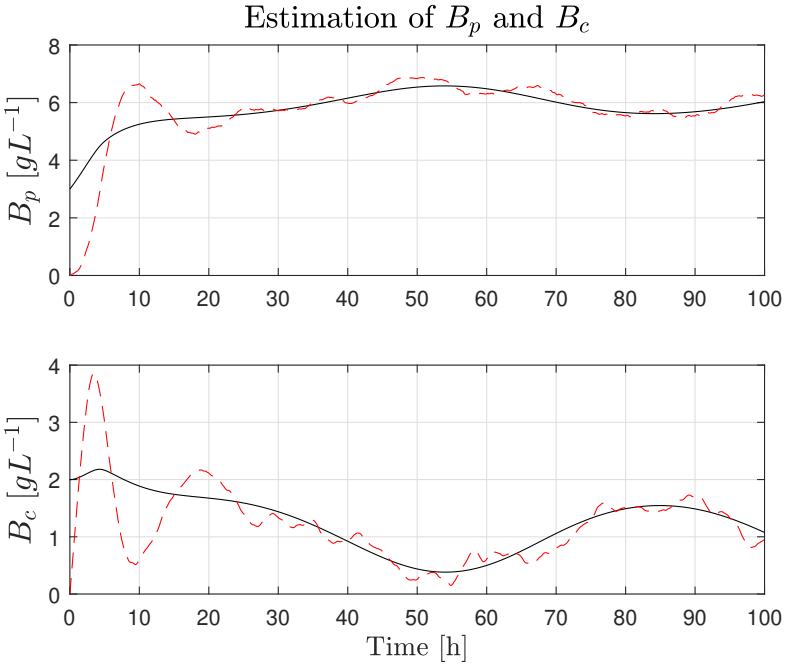

Figure 3.3: Estimation of $B_p(t)$ and $B_c(t)$.

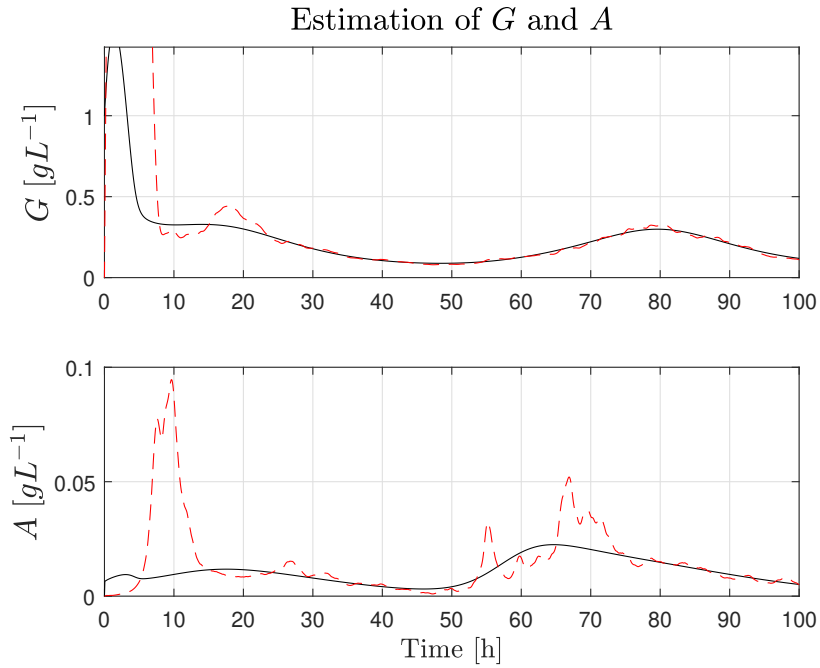

Figure 3.4: Estimation of $G(t)$ and $A(t)$.

measurement noise is attenuated. The same conclusion is drawn for the estimate of H, as shown in Figure 3.7.

3.2.5 Part conclusion

In this chapter, the observation problem for systems (2.4) (and also for (2.1), thanks to their similarities) has been discussed. First, an analysis has been carried out to identify their conditions of observability considering the total biomass and the fluorescent reporter as available measurements. It has been shown that the system is observable with both measurements, but merely detectable if only the first is available.

Second, considering the two available measurements, state observers were proposed for each variable, and the stability properties are discussed for the case in which the two measurements are available. Finally, the advantage of measuring the fluorescent reporter is highlighted, in the sense that it not only enables observability of the system, but also alleviates the dependence on the parameters of the system.

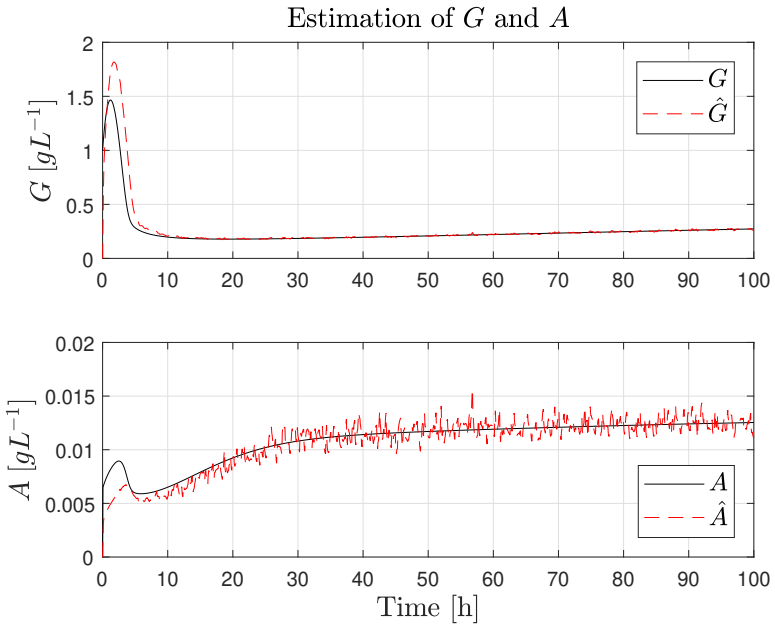

Figure 3.5: Estimation of $G(t)$ and $A(t)$ using observers (3.15).

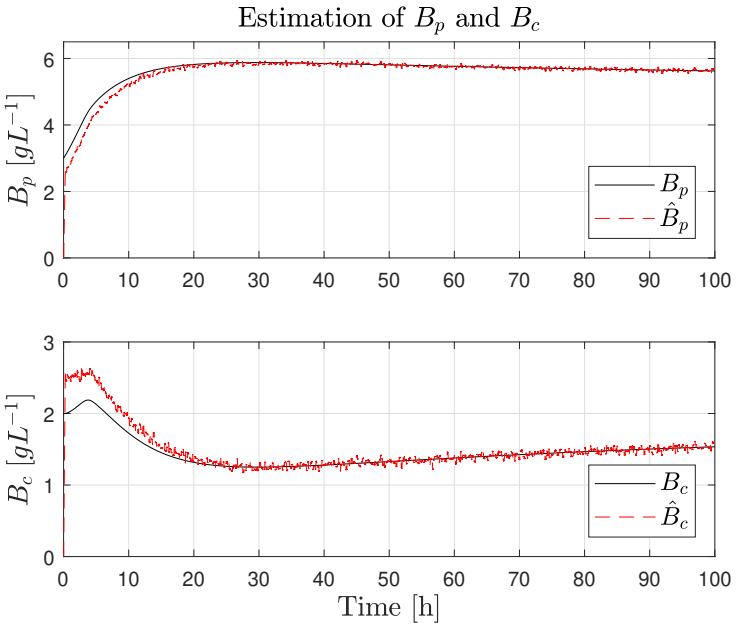

Figure 3.6: Estimation of $B_p(t)$ and $B_c(t)$ using observers (3.15).

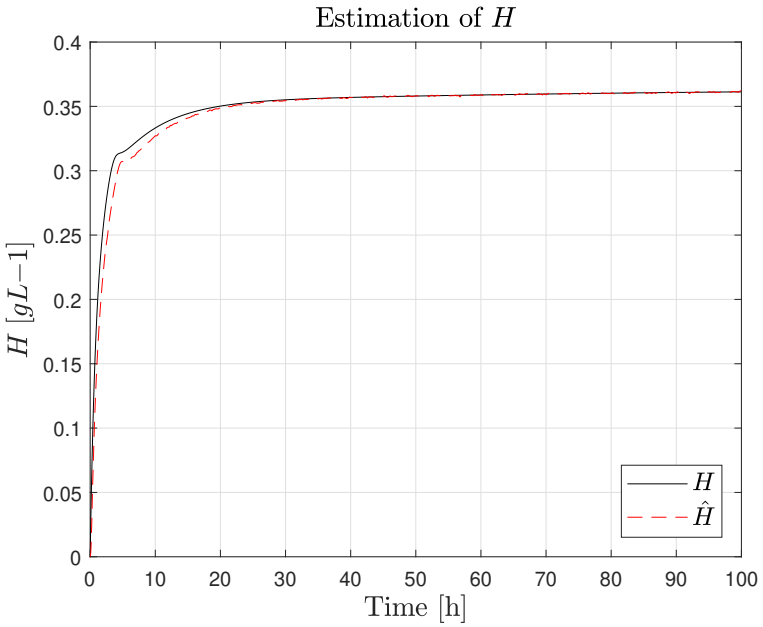

Figure 3.7: Estimation of $H(t)$ using observers (3.15).

Chapter 4

Control of Heterogeneous Communities

4.1 Introduction

In this chapter, the generic bioreactor model (2.1) and the COSY model (2.4) are reconsidered to address the control design for a co-culture of microbes. Mainly, the interest of designing a controller for a heterogeneous community is to ensure their *co-existence*, *i.e.*, avoiding that one goes extinct. It has also been shown that an oscillating chemostat [Smith, 1981], or the use of feedback control [Leenheer and Smith, 2003], might induce the coexistence of two different species.

Also, another control objective relates to the stabilization (or the optimization) of the production on the bioreactor. Indeed, controlling production requires, in some sense, avoiding that the producing species are outcompeted and that the required nutrient is depleted from the bioreactor (if there is no nutrient, there is no metabolism).

Therefore, the main questions to be tackled in this chapter are:

Q1- Are these systems controllable (or stabilizable) taking into account the control constraints?

Q2- How can the co-population be (robustly) stabilized at desired concentration levels?

Q3- How can the production of the bioreactor be (robustly) stabilized? Is it possible to cast an optimization problem?

These questions are going to be discussed in the sequel, by considering both the generic model (2.1) and also the COSY model (2.4). Before starting to tackle these objectives, a discussion on the available control inputs are presented in the following.

The available control inputs

In both models (2.1) and (2.4), there are two controlled variables, both physically altering the composition of the environment in the bioreactor:

1. $D(t)$: describing the dilution rates, *i.e.*, the rates of transfer (inflow or outflow) of medium in the bioreactor (in unit h^{-1}). This variable is often actuated by an electromechanical pump.

2. $S_{in}(t)$: describing the concentration of substrates diluted in the inflow of medium (in unit gL^{-1}). In the COSY model (2.4), this variable is represented by G_{in} and A_{in} are, respectively, the concentration of glucose and acetate.

It is plausible to have the inflow of different media, for instance, containing or not diluted nutrients ($D_s(t)$ and $D_0(t)$, respectively). By considering a continuous bioreactor of constant volume, the outflow is equal to total inflow, *i.e.*, $D(t) = D_s(t) + D_0(t)$.

The concentration $S_{in}(t)$ (or, analogously, $G_{in}(t)$ and $A_{in}(t)$) can be modulated by properly selecting the rates D_0 and D_s, which indicates that it also might be actuated by electromechanical pumps, as illustrated in Figure 4.1. Considering that D_s relates to the transfer of medium with a high concentration $S_{in}^{\max}$, the inflow concentration S_{in} can be determined by

$$S_{in}(t) = \frac{S_{in}^{\max} D_s(t)}{D_s(t) + D_0(t)}$$

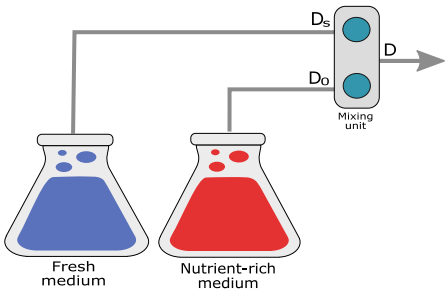

Figure 4.1: Mixing unit to modulate the concentration $S_{in}(t)$

This is interesting since it allows the design of a control considering variables of similar nature. Furthermore, the time constant of a electromechanical device is much smaller than the one of a biological process.

4.2 A discussion on controllability

Thanks to its physical meaning, systems (2.1) and (2.4) are time-varying, positive systems. Furthermore, they have constrained controls, since $D(t)$ and $S_{in}(t)$ (or $G_{in}(t)$ and $A_{in}(t)$ for the COSY model (2.4)) are also non-negative and possibly upper bounded. In such a case, deriving a rank condition for controllability is not applicable since it cannot be investigated by utilizing Lie algebra, as discussed for general nonlinear systems in [Hermann and Krener, 1977].

Nevertheless, an analysis can still be performed by profiting the structure of (2.1) and (2.4) and it is possible to evaluate the *reachability* of such a system, according to the following

definition:

Definition 4.1. *A state x_1 is called reachable if there exist a finite time t_1 and an admissible control $u(t)$ on $[t_0, t_1]$ such that $x(t_0)$ can be steered to x_1.*

Consider the competition model (2.1). If the nutrient inflow concentration S_{in} can be made sufficiently high, it is possible to prevent the nutrients of being depleted from the bioreactor (*i.e.*, $S \to 0$). Then, the sign of the derivative of each x_i can be assigned by a proper selection of D.

Consider the sub-system for x_1 and x_2 in (2.1). Clearly, it can be rewritten as autonomous time-varying linear system, whose solution is

$$\begin{aligned} x_1(t) &= e^{f_1(t-t_0)} B_p(t_0), \\ x_2(t) &= e^{f_2(t-t_0)} B_c(t_0), \end{aligned} \tag{4.1}$$

where $f_i = \int_{t_0}^{t} k_h \mu_i(S(s)) - (k + D(s))ds$, for $i = 1, 2$. From these expressions and information on the functions μ_i, it is possible to estimate the reachable set for the sub-system above.

Consider now the COSY model (2.4). Although three inputs are considered available (*i.e.*, the dilution rate D and the inflow substrate concentrations G_{in} and A_{in}), a similar analysis is more intricate due to the presence of two substrates. Also, considering $D = D_a = D_g$ and recalling the dynamics for the substrates:

$$\begin{aligned} \dot{G} &= DG_{in} - DG - r_1(G, A)B_p - r_2(G, A)B_c \\ \dot{A} &= DA_{in} - DA - r_3(G, A)B_p - r_4(G, A)B_c \end{aligned}$$

the two right-most terms on the dynamics of G are *always* negative. This is important since the input DG_{in}, being always non-negative, can be used to compensate these terms and assign the sign of $\dot{G}$.

However, the same does not apply to the two right-most terms on the dynamics of A: thanks to the metabolic overflow, acetate is excreted by the species (mostly by the producer strain) after a certain threshold depending on G, A (see (2.6)). Therefore, it can be seen as an *extra input* of acetate, what might eventually change the sign of these terms.

Clearly, it would be possible to compensate this by a proper selection of D. Nevertheless, if D is fixed (or used for another purposes, as it will be the case in this chapter), it would be impossible to freely assign the sign of $\dot{A}$ and drive the concentration of A by using solely the input DA_{in}, since it is always non-negative.

4.3 Controlling competing species

4.3.1 A gentle motivation for a robust approach

Before presenting the proposed control architecture, the nuances of the problems are stressed. Consider (2.1) with a single limiting substrate S. As early pointed out by [Leenheer and Smith, 2003], coexistence is possible if $\mu_1(S)$ and $\mu_2(S)$ intersect at a point S_i. Selecting $D(t) = \mu(S_i)$ implies that

$$\dot{x}_i = (\mu_i(S(t)) - D(t))x_i = 0.$$

However, if each of the competing species are to be stabilized at given concentration levels x_i^d, $i = \{1, 2\}$, the control problem becomes more complex. Indeed, this problem can be seen as the stabilization of the origin of the auxiliary dynamics $\sigma(x_i) = x_i(t) - x_i^d$. Computing the time derivative of $\sigma(x_i)$, one has

$$\dot{\sigma}(x_i) = (\mu_i(S(t)) - D(t))x_i.$$

Evidently, it is possible to steer only one of the species to a certain point in the state-space by setting $D(t) = \mu_i(S)$. The other species, depending on the functions $\mu_i(S(t))$, will be driven to another point and might even be extinct. However, consider that $D(t)$ is set such that one of the species (henceforth, arbitrarily, x_1) is stabilized at a given point. Denoting $\xi(S) = \mu_1(S) - \mu_2(S)$ and computing the first and the second time derivative of $\sigma(x_2)$, one has that

$$\begin{aligned} \dot{\sigma}(x_2) &= (\mu_2(S) - \mu_1(S))x_2 \\ &= -\xi(S)x_2 \end{aligned} \tag{4.2}$$

$$\begin{aligned} \ddot{\sigma}(x_2) &= \left(-\frac{\partial \xi}{\partial S}\dot{S} + \xi^2\right) x_2 \\ &= x_2 \left(-\frac{\partial \xi}{\partial S}\left[\mu_1(S)(S_{in} - S) - k_1\mu_1(S)x_1 - k_2\mu_2(S)x_2\right] + \xi^2(S)\right), \end{aligned} \tag{4.3}$$

which indicates that S_{in} can be utilized to stabilize the surface $\sigma(x_2) = 0$. In this light, the following challenges are met:

1. $\sigma(x_2)$ possesses a relative degree 2 w.r.t. the input S_{in};
2. Controllability of (4.3) w.r.t. S_{in} is lost at a point S_o satisfying $\frac{\partial \xi}{\partial S}(S_o) = 0$;
3. From (4.3) one observes a heavy dependence on the parameters of $\mu_i(S)$, which, as discussed previously, are uncertain. This fact motivates the need for a robust approach.

In the remainder of this section, the design of a control architecture aiming to solve this problem is proposed. This control architecture is composed of two phases: in the first moment, the control $D(t)$ is used to stabilize x_1 at the desired position $x_1^d > 0$ and, simultaneously, the substrate concentration will be shifted to a positive value ensuring the system controllability using the control $S_{in}(t)$. Once these goals are reached, the control goal for $S_{in}(t)$ will commute to the stabilization of x_2 at a constant level.

In this section we will assume that

$$\mu_i(S) = \frac{a_i}{b_i + S}, \quad i = 1, 2,$$

and the sets of admissible values A_i and B_i are given for a_i and b_i, respectively, then the following hypotheses are imposed:

Assumption 4.1. *For any $a_i \in A_i$ and $b_i \in B_i$, $i = 1, 2$, let there exist a constant $S_{a,b}$ such that $\xi(S_{a,b}) = 0$ and $\xi(S) > 0$ for $S > S_{a,b}$.*

Assumption 4.2. *For any $a_i \in A_i$ and $b_i \in B_i$, $i = 1, 2$, the equality $\frac{\partial \xi(S_o)}{\partial S} = 0$ is satisfied for some $S_o < S_{a,b}$.*

Hypothesis 4.1 states that the kinetic rates intersect, which is an obligatory requirement to have co-existence of the species (see [Leenheer and Smith, 2003] for an extensive discussion), while the latter property can be guaranteed by a proper numbering of each species. Hypothesis 4.2 implies that the function $\xi(S)$ and its derivative with respect to S are not zero at the same point. As it will be shown in the design of the control architecture, the distinction of these points is needed to achieve the stabilization of $x_2(t)$. For further reference, define

$$\underline{\mu}_i(S) = \min_{\substack{a_i \in A_i, \\ b_i \in B_i}} \mu_i(S), \quad \text{and} \quad \overline{\mu}_i(S) = \max_{\substack{a_i \in A_i, \\ b_i \in B_i}} \mu_i(S).$$

4.3.2 Design of the control architecture

Stabilization of x_1

This subsection will report the results of [Souza et al., 2020]. Consider the following decision variable:

$$\sigma_1(x_1) = x_1 - x_1^d \tag{4.4}$$

where $x_1^d > 0$ is an arbitrary point for x_1 to be stabilized. As it can be seen from equation (2.1), if the concentration x_i is in a steady-state value, *i.e.*, $\dot{x}_i(t) = 0$ for $t \geq 0$, then there are two possibilities: either $x_i = 0$ or $D(t) = \mu_i(S(t))$. With the latter case in mind, the following proposition is stated:

Proposition 4.1. *Consider model (2.1) and the surface (4.4). If the dilution rate is selected*

such as

$$D(t) = \begin{cases} \overline{\mu_1}(S) + \chi, & \text{if } \sigma_1 \geq 0 \\ \underline{\mu_1}(S) - \chi, & \text{if } \sigma_1 < 0 \end{cases} \tag{4.5}$$

where $\chi \in (0, \underline{\mu_1}(S(0)))$ *is a tuning parameter and, then the closed-loop system is globally finite-time stable with respect to the output* σ_1*, provided that* $S(t) \geq S(0) \quad \forall t \geq 0$.

Proof. Consider the following Lyapunov function candidate for (4.4), which is proper and positive definite with respect to σ_1:

$$V_1 = \tfrac{1}{2}\sigma_1^2 \tag{4.6}$$

whose time derivative is given by $\dot{V}_1 = \sigma_1 \dot{\sigma}_1$. By noticing that $\sigma_1 = \sqrt{2V_1}$, this relation can rewritten such that D appears explicitly:

$$\dot{V}_1 = \sigma_1(\mu_1(S) - D(t))x_1(t)$$

and hence, selecting $D(t)$ as given by (4.5) and stressing that $x_1(0)$ can be either lower or greater than x_1^d, then $\dot{V}_1 \leq -\chi\sqrt{2V_1}\min\{x_1(0), x_1^d\}$ holds, proving the claim. □

An immediate consequence of this choice on D is the fact that, when x_1 is stabilized at level x_1^d, the equivalent control is given by $D_{eq} = \mu_1(S)$. Furthermore, control law (4.5) uses information on x_1 and S, and the latter has to be bigger than zero (bigger than $S(0) > 0$ to have $D(t) > 0$ for the selected value of χ). Hence, it is necessary to design a control law for S, which can be done using $S_{in}(t)$.

First Control Law – $S_{in}^{[1]}$

The first control strategy is to be active whenever $x_1(t)$ is not stabilized in the surface (4.4) or its vicinity. The objective here is to keep S away from zero, otherwise, it would cause $D(t) = 0$ (due to $\mu_1(0) = \mu_2(0) = 0$) and no control action on $x_1(t)$ will be possible. Moreover, it is also necessary to realize the condition imposed in Proposition 4.1 that $S(t) \geq S(0)$ for all $t \geq 0$.

In order to design a control law for $S_{in}(t)$, it is necessary to note that the point S_o, defined in Assumption 4.2, corresponds to the value of S at which the system loses its controllability for the variable x_2 with respect to the control input $S_{in}(t)$ (see below the analysis of control for the second phase: at S_o the dynamics of $\ddot{x}_2$ is independent in S_{in}, hence, the system is not controllable). In addition, the system is not controllable at all if $S = 0$. Then the goal is to shift S out of this dangerous region.

To this end, let us introduce three special points: $\underline{S_{a,b}}$, $\overline{S_o}$ and S_m, which are given by

$$\overline{S_o} = \max_{\substack{a_i \in A_i \\ b_i \in B_i}} S_o, \qquad \underline{S_{a,b}} = \min_{\substack{a_i \in A_i \\ b_i \in B_i}} S_{a,b}$$

hence, S_m is selected such as $S_m > \overline{S_o}$.

Remark 4.1. *An option for selection is* $S_m = \frac{\overline{S_o} + \underline{S_{a,b}}}{2}$.

Thus stabilization of S at S_m will ensure that, at least at the instant of commutation to regulate $x_2(t)$, the latter variable is controllable, avoiding the issue remarked above. Hence, in this light, the following result is stated:

Proposition 4.2. *Consider model (2.1) with an output* $\sigma(S) = S - S_m$. *By means of a switching law given by*

$$S_{in}^{[1]} = \frac{1}{D} \begin{cases} S_{\max}, & \text{if } \sigma(S) < 0 \\ 0, & \text{if } \sigma(S) \geq 0 \end{cases} \tag{4.7}$$

where

$$S_{\max} = DS + \sum_{i=1}^{2} \rho_i x_i \overline{\mu_i}(S) + \epsilon, \quad \epsilon > 0,$$

the output $\sigma(S)$ *is globally finite-time stabilized provided that* $D(t) > 0$, *for all* $t \geq 0$.

Proof. : Consider a Lyapunov function candidate given by $V_S(S) = \frac{1}{2}(S - S_m)^2$, whose time derivative is given by

$$\dot{V}_S = (S - S_m)\dot{S} = (S - S_m)\left(D(S_{in}^{[1]} - S) - \sum_{i=1}^{2} \rho_i x_i \mu_i(S) \right)$$

Then, taking (4.7) into account, one has $\dot{V}_S \leq -\varepsilon\sqrt{2V_s}$ for some $\varepsilon \in (0, \epsilon]$ dependent on initial conditions, implying the stated result. □

Theorem 4.1. *Let* $S(0) \leq S_m$. *Then controls (4.5), (4.7) with* $\chi \in (0, \underline{\mu_1}(S(0)))$ *and* $\epsilon > 0$ *ensure that* $x_1(t) = x_1^d$ *and* $S(t) = S_m$ *for all* $t \geq T$, *where* $T > 0$ *is a finite time dependent on the initial conditions.*

Proof. First, note that such a selection of χ induces $D(t) > 0$. Furthermore, as proven in Proposition 4.2 by means of Lyapunov function (4.6), the origin of (4.4) is globally finite-time stable after a time $T_1 > 0$ bounded by

$$T_1 \leq \frac{V_1^{0.5}(x_1(0))}{\min\{x_1(0), x_1^d\}\chi\sqrt{2}}$$

Consequently, control law (4.7) is well-posed (since $D(t) > 0$ guarantees that no division by zero will occur). If $\epsilon > 0$, as proven in Proposition 4.2 by means of the Lyapunov function V_S, control law (4.7) renders the system with output $S - S_m$ globally finite-time stable after

a time $T_2 > 0$ bounded by

$$T_2 \leq \frac{V_S^{0.5}(S(0))}{\varepsilon\sqrt{2}}$$

Finally, control laws (4.5) and (4.7) render $x_1(t) = x_1^d$ and $S(t) = S_m$ after a time $T = T_1 + T_2 \leq \frac{1}{\sqrt{2}}(\min\{x_1(0), x_1^d\}\chi^{-1}V_1^{0.5}(x_1(0)) + \varepsilon^{-1}V_S^{0.5}(S(0)))$, as claimed. □

Second Control Law – $S_{in}^{[2]}$

The second control has to be active once x_1 is stabilized on the surface (4.4). The objective here is then to stabilize the remaining species x_2 at an arbitrary point $x_2^d > 0$, which can be done by means of S_{in}, as discussed previously.

Remark 4.2. *As x_1 is in sliding motion due to the discontinuous control laws developed previously, an immediate consequence is that after the establishment of the sliding motion for the variable σ_1, the control D can be considered in its equivalent form [Utkin, 1992] $D_{eq} = \mu_1(S)$, which is assumed in this subsection.*

As it can be seen from the model (2.1), if concentration x_2 is in steady-state, *i.e.*, $\dot{x}_2 = 0$, the equivalent control on D implies that stabilization can be achieved if S is steered to a certain level in which $\xi(S) = 0$ holds, *i.e.*, $S = S_{a,b}$. Indeed, if all parameters of the kinetic rates were perfectly known, then the intersection point $S_{a,b}$ would be readily available and the stabilization is easily solved. However, as aforementioned, these parameters are uncertain and therefore the control law designed in this section must provide a robust stabilization of x_2.

Before stating the main results of this subsection, let us define the bounds on ξ as follows:

$$\overline{\xi}(S) = \overline{\mu_1}(S) - \underline{\mu_2}(S), \qquad \underline{\xi}(S) = \underline{\mu_1}(S) - \overline{\mu_2}(S),$$

and also, the bounds on the derivatives of ξ with respect to S are given by

$$\frac{\partial\overline{\xi}}{\partial S} = \frac{\overline{a_1}\overline{b_1}}{(\underline{b_1}+S)^2} - \frac{\underline{a_2}\underline{b_2}}{(\overline{b_2}+S)^2}, \qquad \frac{\partial\underline{\xi}}{\partial S} = \frac{\underline{a_1}\underline{b_1}}{(\overline{b_1}+S)^2} - \frac{\overline{a_2}\overline{b_2}}{(\underline{b_2}+S)^2}$$

In this sense, recalling (4.2)–(4.3) and following the idea of the sub-optimal control (see the Appendix B for the definition of the functional Δ), the control input $S_{in}^{[2]}$ can be selected such as

$$S_{in}^{[2]} = S + \frac{1}{D}\left(\sum_{i=1}^{2}\rho_i x_i\tilde{\mu}_i(S) - k_1\text{sign}[\Delta(y(t))]\right) \tag{4.8}$$

where $\tilde{\mu}_i(S) = \frac{\overline{\mu}_i(S)+\underline{\mu}_i(S)}{2}$ is a middle point estimate of the uncertain function $\mu_i(S)$ that

appears in (4.3). Then, by plugging control law (4.8) in the dynamics (4.3), one has that

$$\begin{aligned}\ddot{\sigma}(x_2) &= x_2\left(\xi^2(S) - \frac{\partial \xi}{\partial S}\left(\sum_{i=1}^{2}\rho_i x_i\left(\tilde{\mu}_i(S) - \mu_i(S)\right) - k_1 \text{sign}[\Delta(y(t))]\right)\right), \\ &= a(t) + b(t)k_1\text{sign}[\Delta(y(t))]\end{aligned} \tag{4.9}$$

where the terms $a(t)$ and $b(t)$ are given by

$$\begin{aligned}a(t) &= x_2\left(\xi^2(S) - \frac{\partial \xi}{\partial S}\sum_{i=1}^{2}\rho_i x_i(\tilde{\mu}_i(S) - \mu_i(S))\right) \\ b(t) &= x_2\frac{\partial \xi}{\partial S}\end{aligned} \tag{4.10}$$

and hence this last expression clearly has the same form as (B.4). Also, in order to eliminate the uncertain term $\mu_i(S)$, the bounds of functions $a(t)$ and $b(t)$ in (4.10) can be written as

$$\begin{aligned}|a(t)| &\leq x_2\left(\overline{\xi}^2(S) + \frac{\partial \overline{\xi}}{\partial S}\sum_{i=1}^{2}\rho_i x_i\left(\frac{\overline{\mu}_i(S) - \underline{\mu}_i(S)}{2}\right)\right) = a_{\max}(x_1, x_2, S) \\ b_{\min}(x_2, S) &= x_2\frac{\partial \underline{\xi}}{\partial S}(S) \leq b(t) \leq x_2\frac{\partial \overline{\xi}}{\partial S}(S) = b_{\max}(x_2, S)\end{aligned} \tag{4.11}$$

and it is worth noticing that $b_{\min}(x_2, S) > 0$ while $S > \overline{S_o}$.

Proposition 4.3. *The selection of control law (4.8) renders S_{in} non-negative, for all $t \geq 0$, provided that $k_1 \leq DS + \sum_{i=1}^{2}\rho_i x_i \tilde{\mu}_i(S)$.*

Proof. The proof is straightforward by noticing that k_1 is the only tunable parameter in (4.8) and, to assure positiveness of S_{in}, the term $k_1\text{sign}[\Delta(y(t))]$ must not compensate all other (positive) terms. Since $\text{sign}[\Delta(y(t))] \in [-1, 1]$ it is obvious that the selection of k_1 such as

$$k_1 \leq DS + \sum_{i=1}^{2}\rho_i x_i \tilde{\mu}_i(S) \tag{4.12}$$

renders $S_{in} \geq 0$ for all $t > 0$, as claimed. □

As discussed previously, since the control S_{in} is multiplied by the term $\frac{\partial \xi}{\partial S}$ in (4.3), it implies that if S reaches the interval $S \leq \overline{S_o}$, the stabilization of surface (4.3) might be no longer possible (actually the system loses its controllability at S_o but, since this value is uncertain, it is prudent to keep $S > \overline{S_o}$). Clearly, control law (4.8) does not guarantee *a priori* that S will not reach this interval.

In order to state conditions to overcome such a problem and also to ensure a proper selection of k_1, a deeper understanding of what happens in such a control phase is discussed in the sequel. Assume that k_1 is properly tuned and that t_2 is the time instant in which this control phase is activated. Since the previous control phase has stabilized S at a level $S_m > \overline{S_o}$, then $\dot{x}_2(t_2) > 0$ and hence two different scenarios are possible:

1. If $x_2(t_2) > x_2^d$, then S must increase in order to have $\dot{x}_2 < 0$;

2. If $x_2(t_2) < x_2^d$, then S must decrease in order to have $\dot{x}_2 > 0$;

Obviously, the second case is troublesome since, depending on the selected gain, S might reach the region in which the stabilization is compromised. Hence, the stabilization of surface (4.3) will proceed for $x_2^d = x_2(t_2)$ is assumed. With this assumption, the problem of having $S \leq \overline{S_o}$ may be alleviated.

In the following, an interval $I = [\underline{S}, \overline{S}] \times x_1^d \times [x_2^d - \delta, x_2^d + \delta]$ for all $t \geq t_2$ and some $\overline{S_o} < \underline{S} < \overline{S} < +\infty$ and $\delta > 0$ is considered. Due to functioning of the suboptimal control, the dynamics of the closed-loop system will be governed by the equation $\ddot{y}(t) = a(t) - b(t)k_1$. If the choice of k_1 imposes that $a(t) < b(t)k_1$, then $\ddot{y}(t) = -r$ gives the worst-case trajectory estimate. Since in this case $y(t_2) = 0$ and $\dot{y}(t_2) > 0$, let us define, for $(S(t),\ x_1(t)\ x_2(t)) \in I$, the minimum value of $\ddot{y}(t)$ as $r = a_{\max}(x_1, x_2, S) - b_{\min}(x_2, S)k_1$ for the time interval $[t_2, t_3]$, where $t_3 > t_2$ is the instant of time that $\dot{y}(t_3) = 0$. Omitting all arguments for the sake of readability, this estimate can be expressed as follows:

$$r = -\left[(x_2^d + \delta)\left(\xi(\overline{S})^2 + \xi'_{\max}\left(x_1^d \rho_1 \frac{\overline{\mu}_1(\overline{S}) - \underline{\mu}_1(\underline{S})}{2} + (x_2^d + \delta)\rho_2 \frac{\overline{\mu}_2(\overline{S}) - \underline{\mu}_2(\underline{S})}{2}\right)\right) - (x_2^d - \delta)\xi'_{\min} k_1\right] \tag{4.13}$$

where $\xi'_{\min} = \min_I \frac{\partial \xi}{\partial S}$ and $\xi'_{\max} = \max_I \frac{\partial \overline{\xi}}{\partial S}$ (this notation will be also used in the following).

In this light, let us state the following result:

Lemma 4.1. *If there exists a compact interval I in which the following inequalities hold:*

(a) $\frac{1}{\xi'_{\min}}\left(\overline{\xi}^2(\overline{S}) + \xi'_{\max}\sum_{i=1}^{2}\rho_i \overline{x_i}\frac{\overline{\mu}_i(\overline{S}) - \underline{\mu}_i(\underline{S})}{2}\right) < D\underline{S} + \sum_{i=1}^{2}\rho_i \overline{x_i}\tilde{\mu}_i(\underline{S})$,

(b) $|\xi(S)| \leq \frac{|x_2^d \xi(S_m)|}{x_2^d - \delta}$ *and*

(c) $\frac{1}{2r}(x_2^d \xi(S_m))^2 \leq \delta$

for all $(S(t), x_1(t), x_2(t)) \in I$, $\overline{x_1} = x_1^d$ and $\overline{x_2} = x_2^d + \delta$, then there is a choice of constant gain k_1 in (4.8) that assures both positiveness of S_{in} and the permanence of trajectories of S and x_2 inside the domain of attraction of the origin of (4.3).

Proof. The idea here is to show that, under the conditions presented in this lemma, it is possible to select a constant value of k_1 that satisfies all constraints of non-negativeness and stabilizability of (4.3), during all transients.

First, the right-hand side of inequality (a) is immediate from Proposition 4.4, corresponding directly to the choice of k_1 that yields S_{in} non-negative. The left-hand side, however, relates to the choice of k_1 that stabilizes these dynamics. Indeed, one can easily see that

control law (4.8) renders the dynamics (4.3) as

$$\ddot{y} = a(t) + b(t)k_1 \text{sign}[\Delta(y(t))]$$

where $a(t)$ and $b(t)$ are given by (4.10). Noticing that this last expression has the same form as (B.4), the stabilization by the suboptimal control is therefore possible if $b_{\min}k_1 > |a_{\max}|$, hence

$$k_1 > \frac{|a_{\max}|}{b_{\min}}$$

which, recalling (4.11) and the constraint of set I, leads us to

$$k_1 > \frac{1}{\xi'_{\min}} \left(\overline{\xi}^2(\overline{S}) + \xi'_{\max} \sum_{i=1}^{2} \rho_i \overline{x_i} \frac{\overline{\mu}_i(\overline{S}) - \underline{\mu}_i(\underline{S})}{2} \right) \tag{4.14}$$

where, for simplicity, $\overline{x_1} = x_1^d$ and $\overline{x_2} = x_2 + \delta$.

Inequalities (b) and (c) are imposed in order to guarantee that $(S(t), x_1(t),\ x_2(t)) \in I$. According to the design of the control on the first step, at the instant of commutation $x_2^d = x_2(t_2)$, $y(t_2) = 0$ and $\dot{y}_2(t_2) = -x_2^d\xi(S_m) > 0$. Hence, estimates on the behaviour of trajectories of S and x_2 can be obtained by solving analytically the equation $\ddot{y}(t) = -r$ (note that $r > 0$) for $t \in [t_2, t_3]$, where the instant t_3 corresponds to the first time instant in which $\dot{y}(t_3) = 0$.

Consequently, due to properties of the suboptimal control algorithm as shown in Corollary B.1, the following relations hold true:

$$\begin{aligned} |y(t)| &\leq y(t_3) \\ |\dot{y}(t)| &\leq y(t_2) \end{aligned} \tag{4.15}$$

and hence, by integration of $\ddot{y}(t) = -r$ in the aforementioned time window, one has that

$$\dot{y}(t) = \dot{y}(t_2) - rt$$

and, as $\dot{y}(t_3) = 0$ and $\dot{y}(t_2) = -x_2^d\xi(S_m)$, it is immediate that $t_3 = \frac{-1}{r}x_2^d\xi(S_m)$. Integrating once again in the same interval:

$$y(t) = y(t_2) + \dot{y}(t_2) - \frac{r}{2}t^2$$

which, if evaluated at t_3, results in inequality (c), i.e. $y(t_3) = \frac{1}{2r}\left(x_2^d\xi(S_m)\right)^2 \leq \delta$.

Finally, inequality (b) is obtained from the second equation in (4.15), which states that

$$|x_2(t)\xi(S(t))| \leq x_2(t_2)\xi(S(t_2)) = x_2^d\xi(S_m)$$

and, due to monotonicity of $\xi(S)$ for $S > \overline{S_o}$, leads us to

$$\frac{-|x_2^d\xi(S_m)|}{x_2^d + \delta} \leq |\xi(S)| \leq \frac{|x_2^d\xi(S_m)|}{x_2^d - \delta}$$

which, due to the modulus and the positive nature of the constants x_2^d and δ, reduces to

$$|\xi(S)| \leq \frac{|x_2^d\xi(S_m)|}{x_2^d - \delta}$$

completing the proof. □

This last lemma gives us a way to perform a choice of a certain constant gain k_1 satisfying the aforementioned constraints and to evaluate the domain of attraction I. Supposing that there exist the values of δ, $\underline{S}$ and $\overline{S}$ that verify the constraints in Lemma 4.1, and that the gain k_1 is selected to satisfy (a), then, the final result of this section can be stated as the following theorem:

Theorem 4.2. *Consider the dynamics (4.3) and control law (4.8). If the constraints described in Lemma 4.5 are satisfied, then the origin of (4.3) is stabilized in I for all $t > T_3$, where $T_3 > 0$ is a finite-time depending on x_1^d, x_2^d and S_m.*

Proof. This proof is straightforward by the preliminaries given on the suboptimal control (see Appendix B). From (B.10), then (omitting arguments for readability):

$$T_3 \leq t_3 + \alpha p\sqrt{|y(t_3)|}$$

where $\alpha(S, x_1, x_2) = \max_I \frac{b_{\max}(x_2,S)k_1 + a_{\max}(x_1,x_2,S)}{-r}$ and p is defined in Subsection 3.2. Hence, profiting the computations performed in the proof of Lemma 4.1, the relation for T_3 above becomes

$$T_3 \leq \frac{-x_2^d\xi(S_m)}{r} + \alpha p\sqrt{\left|\frac{1}{2r}\left(x_2^d\xi(S_m)\right)^2\right|}$$

as stated. □

Remark 4.3. *For the sake of simplicity, the possibility of having time-varying parameters a and b has not been made explicit in the development. However, it can be tackled by the same control architecture in a very natural manner. Recalling formula (4.3), the influence of these*

time-varying parameters would appear such as

$$\ddot{y} = x_2 \left(\xi^2(S) - \frac{\partial \xi}{\partial S} \left(D(S_{in} - S) - \sum_{i=1}^{2} \rho_i x_i \mu_i(S) \right) - \frac{\partial \xi}{\partial a} \dot{a} - \frac{\partial \xi}{\partial b} \dot{b} \right)$$

where the two right-most new terms can be seen as a perturbation (especially because $\dot{a}$ *and* $\dot{b}$ *are supposed to be small, given the slow nature of the system) and, taking the uncertainty into account, they can be added to* $a_{\max}$*. The design of the control law then proceeds as explained in this subsection.*

4.3.3 Numerical example

In this section, a numerical experiment is presented to illustrate the proposed methodology. Consider model (2.1) with the reaction rates given as the Monod equation (2.2) as follows:

$$\mu_1(S) = \frac{4S}{20 + S}, \quad \mu_2(S) = \frac{2S}{6 + S}$$

and with initial conditions $S(0) = 1$ $[gL^{-1}]$ and $x_1(0) = x_2(0) = 1.5$ $[gL^{-1}]$. The control inputs are constrained such as $D \in [0, 2]$ (in h^{-1}) and $S_{in} = [0, 30]$ (in $\frac{g}{L}$). Also, for simplicity, $k_1 = k_2 = 1$.

The objective is to stabilize x_1 at $x_1^d = 2$ $[gL^{-1}]$ and x_2 at $x_2^d = 1.5$ $[gL^{-1}]$. The uncertainty will be considered as $\pm 20\%$ on each parameter. However, for the control synthesis, it is assumed that the parameter uncertainties satisfy the following intervals:

$$A_1 = [3.40, 4.60], \qquad A_2 = [1.70, 2.30]$$
$$B_1 = [17.00, 23.00], \qquad B_2 = [4.80, 7.20]$$

To assess the robustness of the controller, four parameter sets will be considered for simulation purposes (i.e., the controller does not have such an information). These sets are shown in Table 4.1 as follows.

Table 4.1: Random Parameter Sets

	$[\mu_{\max,1}, K_{m,1}]$	$[\mu_{\max,2}, K_{m,2}]$
Parameter set 1	[4.00, 20.00]	[2.00, 6.00]
Parameter set 2	[3.80, 24.00]	[2.40, 7.20]
Parameter set 3	[3.60, 22.00]	[2.20, 5.40]
Parameter set 4	[4.60, 23.00]	[1.80, 4.80]

Analyzing the impact of these uncertainties in $S_{a,b}$ and S_o, one can arbitrarily select

$S_m = 7.5$. Also, in accordance with Lemma 4.5, the selection of gain k_1 as

$$k_1 = \frac{1}{4}\left(\frac{\bar{\xi}^2(S_m)}{\xi'_{\min}(S_m)} + \underline{\mu}_1(S_m)\right)$$

satisfies all constraints on stabilizability, non-negativeness of S_{in} and transient behavior of all trajectories will be satisfied for this simulated scenario.

First, let us analyze the whole performance of the control law concerning the parameters given in Table 4.1, as illustrated in Figure 4.2. As can be seen, both phases successfully stabilizes both species in a finite-time despite of the parametric uncertainties.

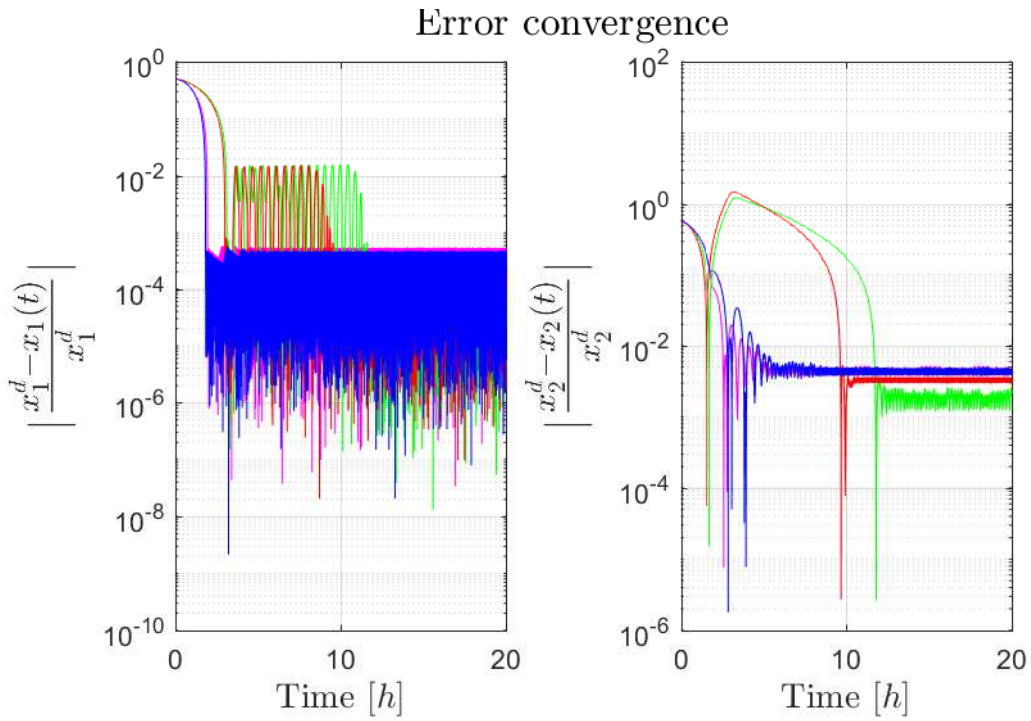

Figure 4.2: Convergence of the error (logarithmic scale). Legend: magenta – parameter set 1, green – parameter set 2, red – parameter set 3, blue – parameter set 4. The second-order nature of the control used for the variable x_2 is clearly seen in the behaviour of the convergence error.

Now, for clarity and depth, let us focus only on parameter set 1. As can be seen in Figure 4.3, the first control phase is activated in $t \in [0, 3]$. In this interval, one can easily see the stabilization of S at S_m and x_1 at x_1^d. Immediately after this step, the second phase is initiated and successfully stabilizes x_2 at $x_2(t_2) = 1.2$. Also, one can see that the control architecture successfully stabilized $S = S_{a,b}$, even though $S_{a,b}$ belongs to an uncertain interval. This fact shows the usefulness of this methodology since it allows a robust solution to the stated stabilization problem.

In Figure 4.4, one can see the time evolution of the control inputs $S_{in}(t)$ and $D(t)$. Clearly,

one can see the high frequency switching on both control laws, which is natural to the sliding-mode control. This phenomenon is called *ideal sliding-mode*, where the actuators are supposed to allow this high frequency.

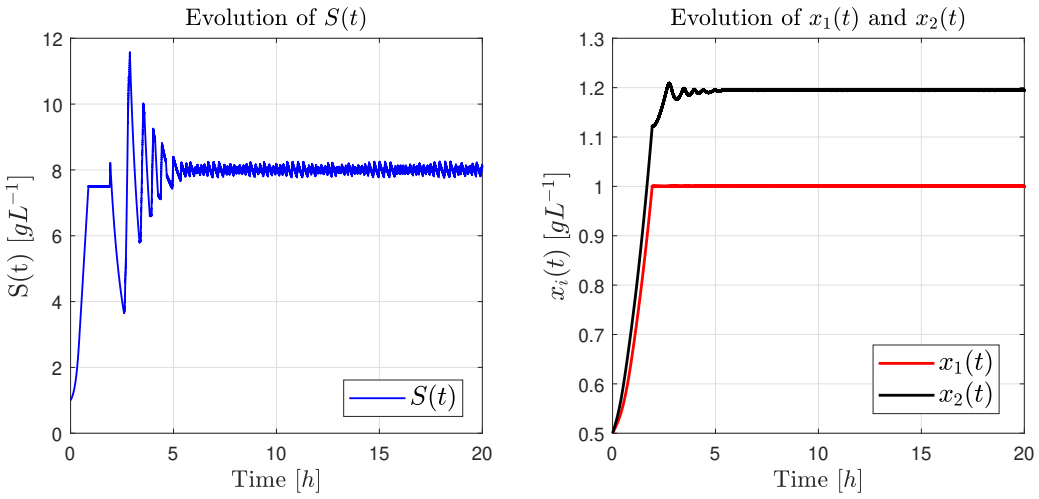

Figure 4.3: Stabilization at $x_1 = 1$ and $x_2 = 1.2$

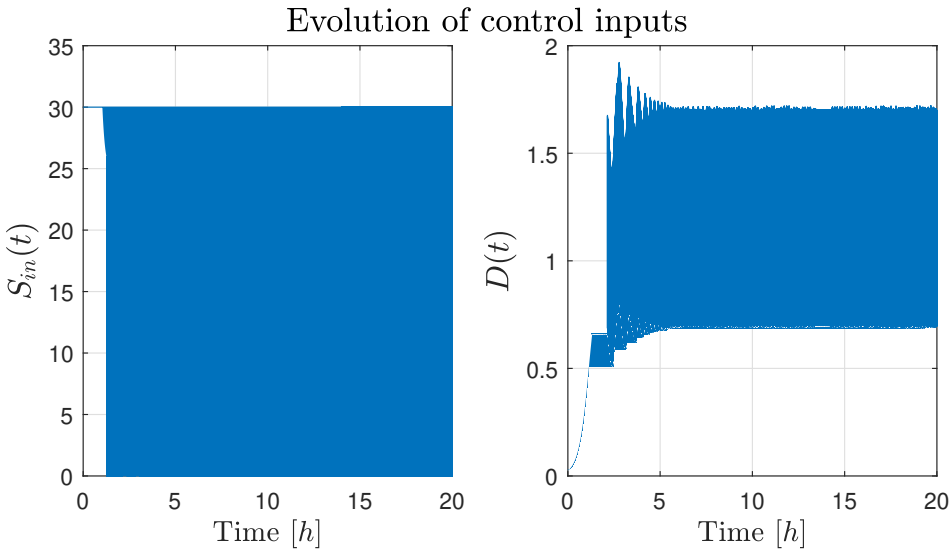

Figure 4.4: Control inputs $S_{in}(t)$ and $D(t)$

In order to investigate this control architecture in a numerical experiment that is closer to the real-world, the same scenario will be simulated considering dynamics on the actuators: a first-order filter and a sampler will be introduced to the output of the proposed controllers. This means that the pumping rates are not perfect and can only be changed at sampling times $\tau \approx 30$ seconds.

As it can be seen in Figure 4.5, even under these new circumstances, the system can still be stabilized at the desired positions. However, a larger discrepancy is observed for the variable

$x_2(t)$. Figure 4.6 illustrates the control inputs after the actuator dynamics. Clearly, it still oscillates but at much smaller frequencies. It is worth noticing that this is possible thanks to the fact that the actuator is *much faster* than the dynamics of the controlled system.

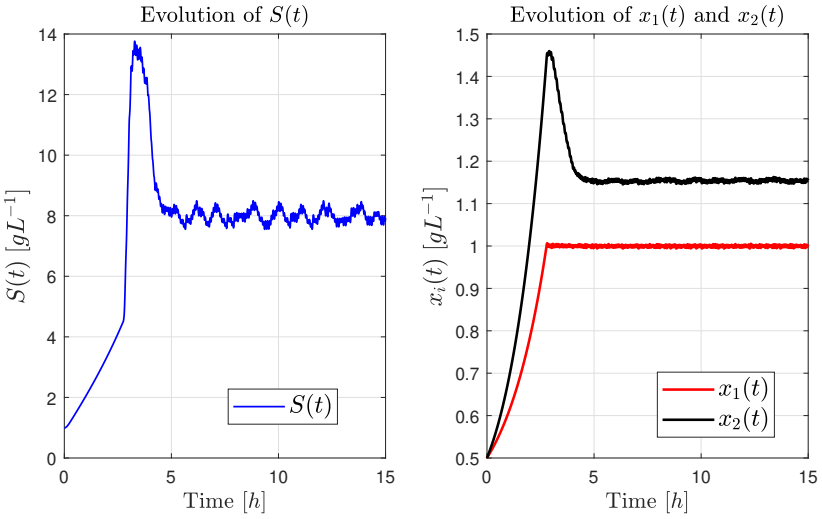

Figure 4.5: Stabilization considering actuator dynamics.

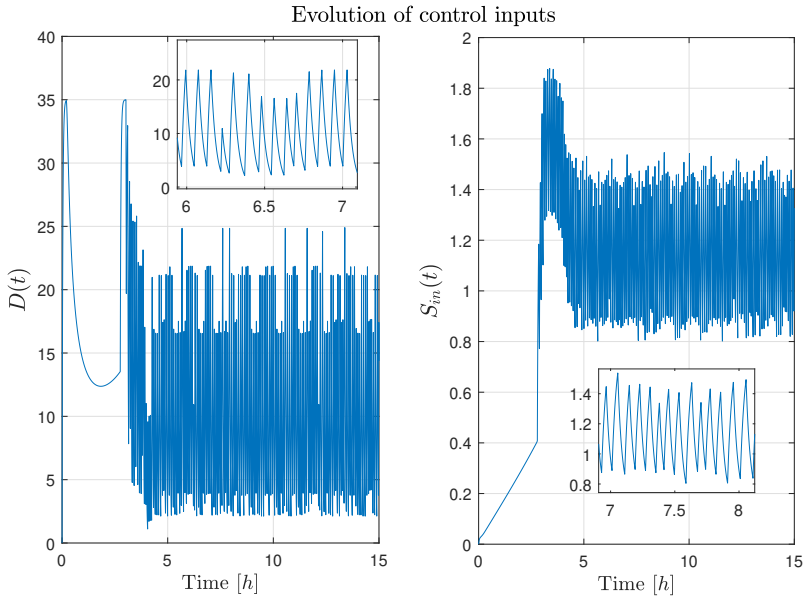

Figure 4.6: Evolution of the control inputs (output of the actuator). The small boxes zooms the signal on a 1 hour time-window.

4.4 Control of the COSY model

In this section, particular attention is drawn to the control problem concerning the COSY model (2.4). For all simulations and numerical results throughout this section, the model parameters will be selected as the ones given by [Mauri et al., 2020] and, arbitrarily (but still realistically), $k_h = 0.2$ and $m = 1$.

For simplicity, the (multiplying) control inputs will be denoted $u_1 = D_g G_{in}$ and $u_2 = D_a A_{in}$. Note that these inputs are constrained such as

$$u_1 \geq 0, \quad u_2 \geq 0. \tag{4.16}$$

4.4.1 Ensuring coexistence through state feedback

Although the ultimate objective is to stabilize the production of H, the first challenge tackled in this section is *how to ensure the coexistence of both producer and cleaner strains*. As it will be shown, this ultimate objective will be attained by using the same control law proposed in this subsection.

First, a control law for the dilution rate D will be proposed. As clearly seen from (2.4), controlling the concentration of B_p allows one to control the concentration of H. Defining an error variable σ_p as

$$\sigma_p = B_p - B_p^\star \tag{4.17}$$

where $B_p^\star$ is a desired concentration level for B_p, the control law for the dilution rate is selected as follows:

$$D = \max\{D_{\min}, (1 - k_h)\mu_p(G, A) - k + \varphi(\sigma_p)\} \tag{4.18}$$

where $D_{\min} > 0$ is a (predefined) minimum value for the dilution rate, $\varphi(\sigma_p)$ is any function satisfying $\varphi(\sigma_p)\sigma_p > 0$ for $\sigma_p \neq 0$ and $\mu_p(G, A)$ is as given in (2.5). As this control law depends on the concentration of the substrates, before stating the result concerning stability of σ_p, several conditions (in terms of G and A) will be imposed.

First, as readily seen by computing the dynamics of σ_p, the saturation $D = D_{\min}$ does not ensure the stability of the origin of (4.17). To remedy this issue, the following constraint is needed:

$$(1 - k_h)\mu_p(G^\star, A^\star) \geq k + D_{\min}$$

which basically imposes that, by selecting proper values of required levels $G^\star$ and $A^\star$ for G and A, respectively, the saturation shown in (4.18) will not be reached at the desired equilibrium.

Figure 4.7 illustrates this constraint as a function of G and A, highlighting that it is only transgressed for very low values of A.

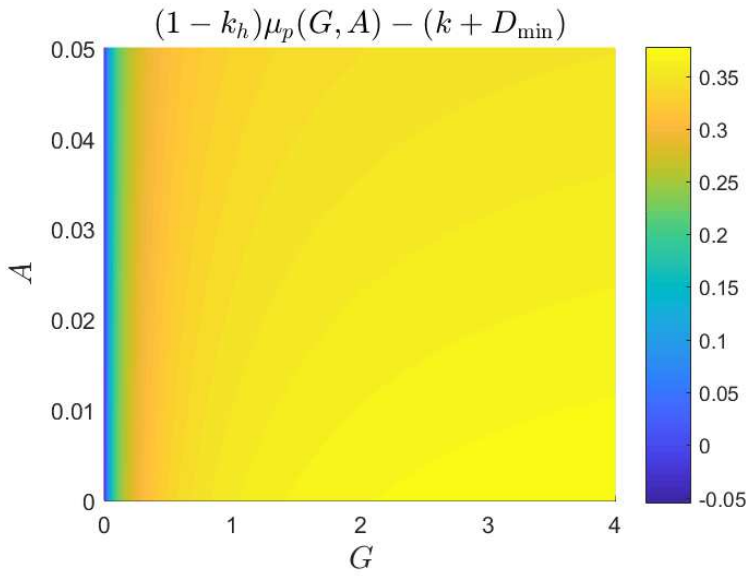

Figure 4.7: Illustration of the constraint $(1-k_h)\mu_p(G,A) \geq k + D_{\min}$ as a function of G and A and for $D_{\min} = 0.05$.

Now, let us consider the dynamics of B_c, which is also affected by the selection of the dilution rate as given by (4.18). As readily seen from (2.4), the possible steady-states of B_c under control (4.18) are either $B_c = 0$ or $B_c > 0$ with the constraint that $\mu_c(G,A) - (k+D) = 0$. Obviously, the former scenario is of no interest since coexistence is envisaged. With the latter scenario in mind and considering that B_c, G and A are in their respective steady-states, the dynamics of B_c becomes

$$\dot{B}_c = h(G^\star, A^\star)B_c$$

where $h(G,A) = \mu_c(G,A) - (1-k_h)\mu_p(G,A)$. Therefore, in order to keep the value of B_c constant in a positive value in the equilibrium, the choice of $G^\star$ and $A^\star$ also needs to satisfy

$$h(G^\star, A^\star) = 0.$$

Figure 4.4.1 illustrates the surface obtained by plotting the function $h(G,A)$. The line rendering $h(G,A) = 0$ (and, consequently, the appropriate selection of G and A) is also shown.

Now, let us investigate how steer the concentrations of G and A through the state-space. Consider two other error variables given by

$$\sigma_g = G - G^\star, \quad \sigma_a = A - A^\star.$$

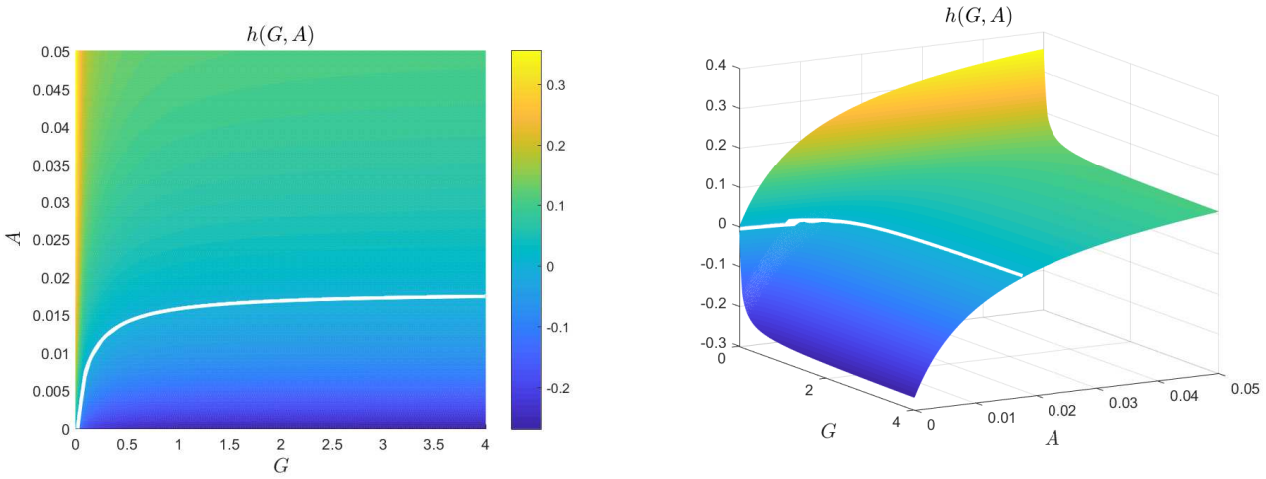

Figure 4.8: Surface of $h(G, A)$. The white line represents the values of G and A rendering $h(G, A) = 0$.

The idea is then to drive these variables to zero. Since D is already fixed (*i.e.*, selected as (4.18) aiming at the stabilization of B_p), this can only be done through the remaining inputs u_1 and u_2 (*i.e.*, through the actuation of G_{in} and A_{in}, respectively).

In this light, consider the following control laws for u_1 and u_2:

$$u_1 = \max\left\{0, r_1(G, A)B_p + r_2(G, A)B_c + DG - \varphi(\sigma_g)\right\} \tag{4.19}$$

$$u_2 = \max\left\{0, r_3(G, A)B_p + r_4(G, A)B_c + DA - \varphi(\sigma_a)\right\} \tag{4.20}$$

Proposition 4.4. *Consider system (2.4) with ouputs σ_g and σ_a. If u_1 and u_2 can be chosen arbitrarily large, then the surfaces $\sigma_g = 0$ and $\sigma_a = 0$ are asymptotically stable under control laws (4.19), provided that $r_1(G, A) < l$ and $r_2(G, A) < l$.*

Proof. The restrictions $r_1(G, A)$ and $r_2(G, A)$ imply that the terms proportional to B_p and B_c in the dynamics of A are sign-defined (*i.e.*, the extra acetate input discussed in Section 4.2 will not disrupt controllability of A through the positive control). Under this condition, the dynamics of G and A are similar, therefore this proof will consider only the former. For simplicity, the dynamics of G is rewritten as

$$\dot{G} = -f_1 - DG + u_1,$$

where $f_1 = f_1(G, A, B_p, B_c) = r_1(G, A)B_p + r_2(G, A)B_c \geq 0$. Considering a candidate Lyapunov function $V_g = \frac{1}{2}\sigma_g^2$, whose time derivative is computed as follows:

$$\begin{aligned}\dot{V}_g &= \sigma_g \dot{\sigma}_g \\ &= \sigma_g \left(u_1 - f_1 - DG\right).\end{aligned}$$

Consider the control u_1 as given by (4.19). Recalling that $\varphi(\sigma_g)\sigma_g > 0$ by definition, the derivative $\dot{V}_G$ becomes

$$\dot{V}_g = -\varphi(\sigma_g)\sigma_g \leq 0.$$

provided that $\sigma_g \leq 0$, or $\varphi(\sigma_g) \leq DG + f_1$.

However, $\sigma_g > 0$ may lead to $u_1 = 0$ and the time-derivative $\dot{V}_g = \sigma_g(-f_1 - DG) < 0$. This implies that V_g is a Lyapunov function and the claimed stability property for σ_g. □

Remark 4.4. *It is worth noticing that no upper bounds on G_{in} and A_{in} (and, consequently, on u_1 and u_2) are imposed. If this is the case, then the result of Proposition 4.4 are merely local: depending on D, B_p and B_c, the upper bound of u_1 and u_2 might not be sufficient to ensure that $\dot{V}_g < 0$.*

Now, since (4.19) allows one to steer the concentrations of G and A through the state-space, it is possible to finally state the stability results of σ_p. For the next result, let the constraint set be denoted as

$$\mathcal{C} = \Big\{(G, A) \in \mathbb{R}^2_+ \ : \ r_1(G, A) < l, r_2(G, A) < l, (1 - k_h)\mu_p(G, A) - (k + D_{\min}) > 0 \text{ and } h(G, A) = 0\Big\}. \tag{4.21}$$

Theorem 4.3. *Consider system (2.4) with an output σ_p as given by (4.17). Let $(G^\star, A^\star) \in \mathcal{C}$ and the conditions of Proposition 4.4 hold true. Then, by selecting D as given by (4.18), the closed-loop system is locally asymptotically stable with respect to the output σ_p. Furthermore, if $B_c(0) > 0$, then $B_c > 0$ for all time.*

Proof. Consider a Lyapunov function candidate given by $V_p = \frac{1}{2}\sigma_p^2$ and assume that G and A have converged to the desired steady-states $G^\star$ and $A^\star$, respectively. Computing the time derivative of V_p, one gets

$$\begin{aligned}\dot{V}_p &= \sigma_p\dot{\sigma}_p \\ &= \sigma_p((1 - k_h)\mu_p(G^\star, A^\star) - (k + D))B_p.\end{aligned}$$

By selecting D as given by (4.18) and thanks to the selection of the pair $(G^\star, A^\star)$, this derivative becomes

$$\dot{V}_p = \sigma_p\varphi(\sigma_p)B_p < 0.$$

which characterizes V_p as a Lyapunov function. Assume now that G and A have not converged (due to, for instance, some transient response) and, therefore, the condition $(1-k_h)\mu_p(G, A) - (k + D_{\min}) \geq 0$ is not satisfied. This would enforce $D = D_{\min}$ and lead the time-derivative of

V_p to be

$$\dot{V}_p < -D_{\min}\sigma_p \leq 0,$$

indicating that σ_p is, at least, bounded. Once G and A reaches their steady-state, the previous conclusion concerning $\dot{V}_p$ will be valid and asymptotic stability is assured. □

An interesting fact emerges when applying control law (4.18): the concentration of the product H, in its steady-state, becomes a monotonic function of $\mu_p(G, A)B_p$. Indeed, plugging control law (4.18) into the dynamics of H and setting it to zero, the steady-state is readily computed as:

$$H^\star = \frac{k_h B_p^\star}{1 - k_h} \frac{\mu_p(G^\star, A^\star)}{\mu_p(G^\star, A^\star) + \frac{m}{1-k_h}}.$$

Therefore, stabilizing H at a desired concentration level basically sums up to choosing proper values of $B^\star$, $G^\star$ and $A^\star$. Clearly, the control laws proposed in this section are suitable for such an objective. Figure 4.9 illustrates the heatmap of $H^\star$ as a function of G and A.

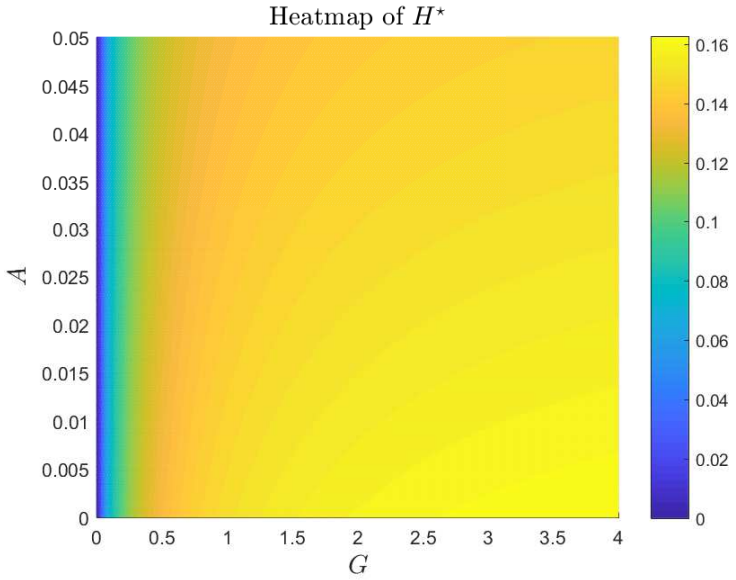

Figure 4.9: Heatmap of $H^\star$ as a function of G and A (considering $B_p^\star = 1$).

4.4.2 Numerical example

In this section, numerical experiments will be presented to illustrate the control methodology developed in this chapter. The COSY model (2.4) will be simulated considering the initial conditions for the biomasses as $B_p(0) = B_c(0) = 0.1$ $[gL^{-1}]$, for the nutrients as $G(0) = A(0) = 1$ $[gL^{-1}]$ and for the heterologous protein as $H(0) = 0$ $[gL^{-1}]$. Arbitrarily, the

saturation in (4.18) is selected as $D_{\min} = 0.05$ and, for simplicity, the functions $\varphi(\cdot)$ where simply selected as $\varphi(s) = s$.

The desired steady-states for B_p and G are, respectively, $B_p^\star = 0.5$ $[gL^{-1}]$ and $G^\star = 3$ $[gL^{-1}]$. According to Figure 4.4.1, in order to have $h(G, A) = 0$ in the steady-state, one must select $A^\star = 0.0175$ $[gL^{-1}]$.

Figure 4.10 shows the trajectories of the concentrations of G and A. As it can be seen, both desired levels were attained roughly after $t = 20h$. Figure 4.11 then illustrates the trajectories of B_p and B_c, where one sees that the desired steady-state for $B_p = 0.3$ $[gL^{-1}]$ was attained, while the B_c converged to a positive level ($\approx B_c = 1.73$ $[gL^{-1}]$), as expected. Finally, Figure 4.12 shows the computed control inputs, reaching their steady-states at $D = 0.414$ $[h^{-1}]$, $G_{in} = 6.22$ and $A_{in} = 3.25$ (both in $[gL^{-1}]$).

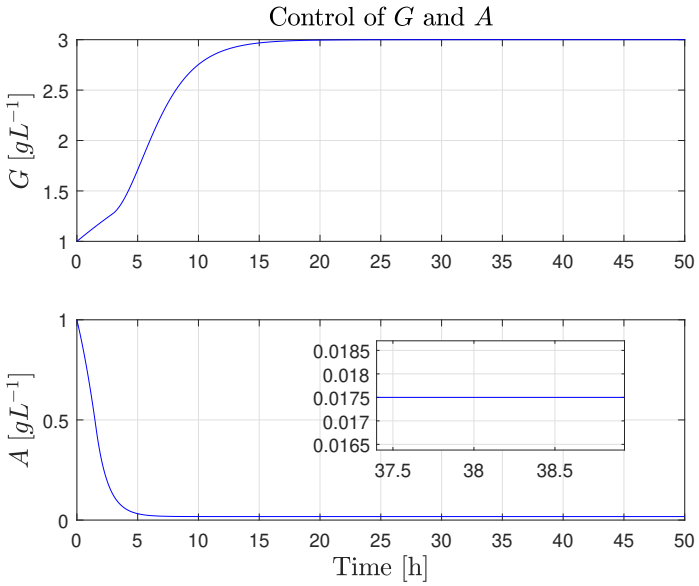

Figure 4.10: Control of the concentrations of G and A.

4.5 Part conclusion

In this chapter, the control problem for systems (2.1) and (2.4) has been investigated. As it was discussed, controllability of such systems is a complicated task, due to their non-negative, nonlinear nature and bounded control inputs.

First, for the competition model (2.1), a gentle motivation for the need of a robust approach is presented. In this light, a robust control architecture composed of two phases (each one with a control objective concerning the input S_{in}) is proposed, allowing the explicit consideration of parametric uncertainty in the reaction rates, and its stabilizing features are proven.

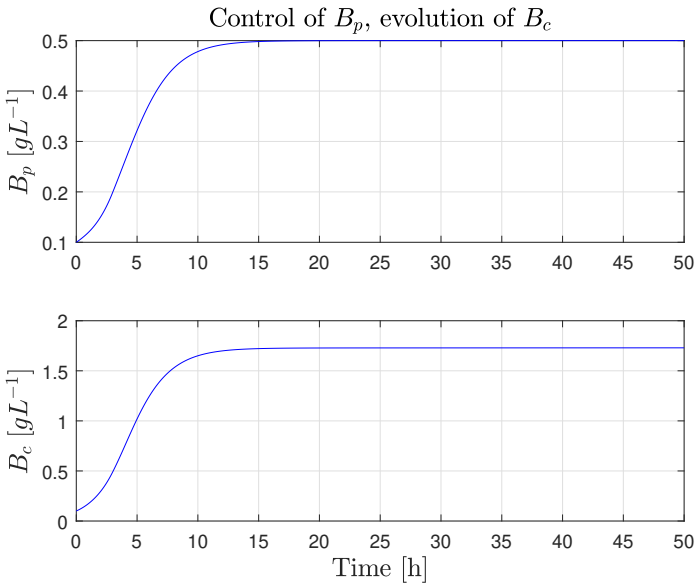

Figure 4.11: Control of the concentrations of B_p at 0.5 $[gL^{-1}]$ and the consequent evolution of B_c.

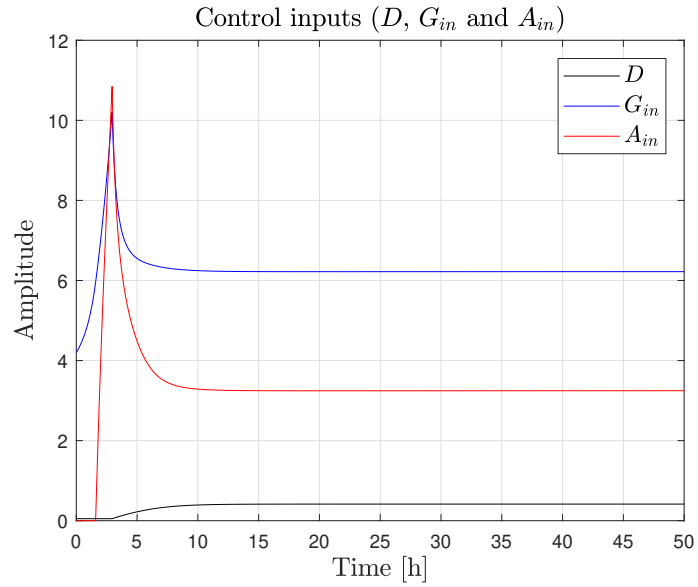

Figure 4.12: Computed control inputs for D (in $[h^{-1}]$), and for G_{in}, A_{in} (both in $[gL^{-1}]$).

These control laws are based on switching controllers, guaranteeing both non-negativity of the inputs and controllability of the system. A numerical example illustrates the methodology.

Considering the COSY model (2.4), the control problem becomes more complicated. Indeed, the excretion of acetate by the producer strain can be considered as an extra input, which further restrain the controllability of the system. Therefore, in order to stabilize H (which can be done simply by stabilizing the concentration of the producer strain B_p), a control law using the dilution rate was proposed. However, to guarantee controllability and also the permanence of the cleaner strain, several constraints concerning the concentrations of glucose and acetate were imposed. Therefore, two more control laws using the inflow concentration of each substrate were proposed, allowing the values of glucose and acetate to be stabilized at proper values that respect such constraints. A numerical experiment illustrate the efficacy of this methodology.

Part 3:

Robust Output Feedback Model Predictive Control

Chapter 5

MPC using interval estimators

5.1 Introduction

Problem statement

Consider a general discrete-time system given by

$$\begin{aligned} x_{k+1} &= f(x_k, u_k, w_k, \theta_k) \\ y_k &= Cx_k + v_k \end{aligned} \tag{5.1}$$

where $x_k \in \mathbb{R}^n$ is the state vector, $u_k \in \mathbb{R}^m$ is the input vector and $y_k \in \mathbb{R}^p$ is the available measurement vector. The measurement matrix $C \in \mathbb{R}^{p\times n}$ is known and constant and $f : \mathbb{R}_+^{2n+m+r} \to \mathbb{R}^n$. The signals $w \in \ell_\infty^n$ and $v \in \ell_\infty^p$ are, respectively, process and measurement noise. The time-varying signal $\theta_k \in \Theta \subset \mathbb{R}^r$ represent some parametric dependence (such as scheduling or uncertain parameters).

Assumption 5.1. *Initial conditions of* (5.1) *are bounded such as* $\underline{x}_0 \leq x_0 \leq \overline{x}_0$*, for some known* $\underline{x}_0, \overline{x}_0 \in \mathbb{R}^n$*. Furthermore, the additive perturbations* $w_k \in [\underline{w}_k, \overline{w}_k]$ *and* $v_k \in [\underline{v}_k, \overline{v}_k]$ *for all* $k \in \mathbb{Z}_+$*, where* $\underline{w}, \overline{w} \in \ell_\infty^n$ *and* $\underline{v}, \overline{v} \in \ell_\infty^p$ *are known signals.*

Assumption 5.2. *Let* $C \geq 0$*.*

Assumption 5.1 imposes that the three sources of uncertainties in (5.8), *i.e.*, x_0, w_k and v_k are enclosed in given intervals, which is a classic hypothesis on the design of interval observers (IOs), whereas Assumption 5.2 is technical and can always be achieved by a proper change of coordinates.

The objective of this chapter is to address the following problem statement:

Problem 5.1. (OF-MPC) *Let* $[\underline{x}_0, \overline{x}_0] \in \mathbb{X}$ *and assumptions 5.1 be satisfied. The objective is to design an output feedback controller stabilizing system* (5.1) *in a vicinity of the origin while robustly satisfying state and control constraints*

$$x_k \in \mathbb{X}, \quad u_k \in \mathbb{U}, \quad \forall k \in \mathbb{Z}_+$$

for any admissible realization of θ_k*,* w_k *and* v_k*, where* $\mathbb{X} \subset \mathbb{R}^n$ *and* $\mathbb{U} \subset \mathbb{R}^m$ *are given bounded convex sets.*

Roughly speaking, Problem 5.1 requires *robust constraint satisfaction*, which means that

the constraints imposed in both state and control input must be respected *even* if the system is plagued by disturbances and uncertainties. The main rationale of the solutions proposed for such a problem relies on interval estimators. These estimators, while having a simple structure, provide information on the set-membership of the states (*i.e.*, in the form of intervals), with guaranteed convergence and low computational complexity. Their design is achieved by using the bounds on the uncertainties, and under some conditions on cooperativity (or non-negativeness).

Roughly speaking, an IO uses the available measurement to generate, at every instant k, signals $\underline{x}_k, \overline{x}_k \in \mathbb{R}^n$ that satisfy the following relation:

$$\underline{x}_k \leq x_k \leq \overline{x}_k, \quad \forall k \in \mathbb{Z}_+. \tag{5.2}$$

On the other hand, an interval predictor (IP, also called a *framer* [Mazenc and Bernard, 2011]) can be seen as an open-loop estimator, since it does not depend on the measurements y_k. For this reason, it can be used to predict an envelope, where all the trajectories of the considered system are enclosed. In this light, the IP generates signals $\underline{z}_t, \overline{z}_t \in \mathbb{R}^n$ such that

$$\underline{z}_t \leq x_t \leq \overline{z}_t, \quad \forall t \in \{k, k+1, \ldots, k+N\}. \tag{5.3}$$

where $N \in \mathbb{Z}_+$ is the finite prediction horizon. Therefore, the main idea is to use this information to check the fulfillment of constraints in the MPC, since

$$[\underline{z}_k, \overline{z}_k] \subset \mathbb{X} \Rightarrow x_k \subset \mathbb{X},$$

and, obviously, the same property can be checked from (5.2).

5.1.1 Preliminaries

Preliminaries on MPC

A standard MPC algorithm solves a constrained optimization problem, by predicting the behaviour of the system over a prediction horizon N (see Figure 5.1 below), to determine a control input sequence $\mathcal{S}_N = \{s_0, \ldots, s_{N-1}\}$ that minimizes a cost function V_N (assuming, for simplicity, that the whole state vector is available as exact measurements). This algorithm is summarized as the following minimization problem:

$$\mathcal{S}_N := \arg\min_{\mathcal{S}_N} V_N(x_{k,0}, \ldots, x_{k,N}, \mathcal{S}_N) \tag{5.4}$$

subject to the following constraints

$$x_{k,0} = x_k, \tag{5.5a}$$
$$x_{k,i+1} = f(x_{k,i}, s_i, 0, 0), \tag{5.5b}$$
$$x_{k,i+1} \subset \mathbb{X}, \qquad s_i \subset \mathbb{U}, \tag{5.5c}$$
$$x_{k,N} \in \mathbb{X}_f, \tag{5.5d}$$

where $\mathbb{X}_f \subset \mathbb{X}$ is the terminal set.

Constraint (5.5a) imposes the initialization of the prediction with the measured x_k, constraint (5.5b) states that the predicted states are obtained using the available dynamical model, constraint (5.5c) requires that the prediction respects the constraints on state and control, and (5.5d) is a *stabilizing constraint*, imposing the endpoint of the prediction to be in a terminal set (the features of this set will be discussed in the sequel).

The cost function V_N is defined as follows

$$V_N = V_f(x_{k,N}) + \sum_{i=0}^{N-1} \ell(x_{k,i+1}, s_i).$$

where $V_f(x)$ is the terminal cost and $\ell(x, s)$ is the stage cost.

Applying the philosophy of the *receding-horizon control*, a sequence $\mathcal{S}_N$ is obtained at every decision instant k and only its first element, s_0, is applied to the system from the instant k to $k+1$. This algorithm is then applied for all subsequent time instants.

Concerning the stability of an MPC algorithm, an important requirement is *recursive feasibility*:

Definition 5.1. *The MPC algorithm is recursive feasible iff, for all initially feasible x_0, it remains feasible for all subsequent times.*

Indeed, the stability of an MPC controller can be evoked by the classic results reviewed in [Mayne et al., 2000] to establish *stabilizing ingredients* for recursive feasibility. These ingredients are the *terminal set* $\mathbb{X}_f$, the *terminal cost* V_f and the *terminal controller* $\kappa_f(x)$, which satisfy the following definition:

Definition 5.2. *The stabilizing ingredients are such that the following axioms are verified:*

1. $\mathbb{X}_f \subset \mathbb{X}$, *closed and* $0 \in \mathbb{X}_f$*: the state constraint is satisfied in* $\mathbb{X}_f$*;*
2. $\kappa_f(x) \in \mathbb{U}$, $\forall x \in \mathbb{X}_f$*: the control constraint is satisfied in* $\mathbb{X}_f$*;*
3. $f(x, \kappa_f(x)) \in \mathbb{X}_f$, $\forall x \in \mathbb{X}_f$*:* $\mathbb{X}_f$ *is positively invariant under* $\kappa_f(x)$*;*
4. $[V_f + \ell](x, \kappa_f(x)) \leq 0$, $\forall x \in \mathbb{X}_f$*:* V_f *is a local Lyapunov function.*

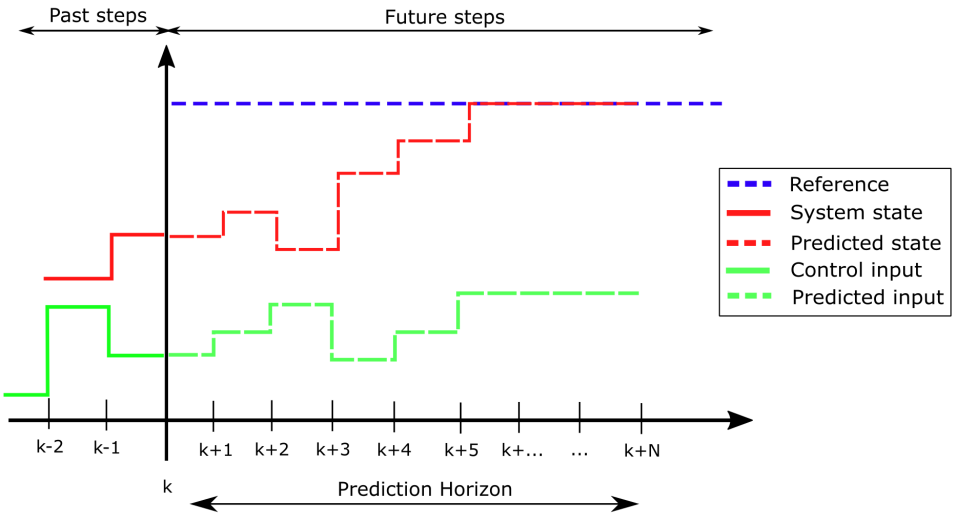

Figure 5.1: Illustration of the MPC algorithm.

Preliminaries on interval arithmetic

The design of the interval estimators presented in this chapter will require some results on interval arithmetic. To this end, we evoke the following:

Lemma 5.1. *[Efimov et al., 2013] Let $x \in \mathbb{R}^n$ be a vector variable, $\underline{x} \leq x \leq \overline{x}$ for some $\underline{x}, \overline{x} \in \mathbb{R}^n$. Then,*
(1) if $A \in \mathbb{R}^{m\times n}$ is a constant matrix, then

$$A^+\underline{x} - A^-\overline{x} \leq Ax \leq A^+\overline{x} - A^-\underline{x}. \tag{5.6}$$

(2) if $A \in \mathbb{R}^{m\times n}$ is a matrix variable and $\underline{A} \leq A \leq \overline{A}$ for some $\underline{A}, \overline{A} \in \mathbb{R}^{m\times n}$, then

$$\underline{A}^+\underline{x}^+ - \overline{A}^+\underline{x}^- - \underline{A}^-\overline{x}^+ + \overline{A}^-\overline{x}^- \leq Ax \leq \overline{A}^+\overline{x}^+ - \underline{A}^+\overline{x}^- - \overline{A}^-\underline{x}^+ + \underline{A}^-\underline{x}^-. \tag{5.7}$$

Lemma 5.2. *[Efimov and Raïssi, 2016] For $A \in \mathbb{R}_+^{n\times n}$, the system*

$$x_{k+1} = Ax_k + \omega_k,\ \omega : \mathbb{Z}_+ \to \mathbb{R}_+^n,\ \omega \in \ell_\infty^n,\ k \in \mathbb{Z}_+$$

has a non-negative solution $x_k \in \mathbb{R}_+^n$ for all $k \in \mathbb{Z}_+$ provided that $x_0 \geq 0$.

Definition 5.3. *A system satisfying Lemma 5.2 is called cooperative or monotone.*

Lemma 5.3. *[Farina and Rinaldi, 2000] A matrix $A \in \mathbb{R}_+^{n\times n}$ is Schur stable iff there exists a diagonal matrix $P \in \mathbb{R}^{n\times n}$, $P \succ 0$, such that $A^\top PA - P \prec 0$.*

5.2 OF-MPC for LTI systems

In this section, a solution for Problem 5.1 will be investigated for the case in which system (5.1) is an LTI one [Souza et al., 2021d], *i.e.*,

$$x_{k+1} = Ax_k + Bu_k + w_k \tag{5.8}$$

in which the (constant) matrices $A \in \mathbb{R}^{n\times n}$ and $B \in \mathbb{R}^{n\times m}$ are known.

5.2.1 Design of interval estimators

Interval observer

First, by using output injection of the available measurement, system (5.8) can be rewritten as

$$x_{k+1} = (A - LC)x_k + Bu_k + Ly_k - Lv_k + w_k \tag{5.9}$$

for any $L \in \mathbb{R}^{n\times p}$. Under Assumption 5.1, an IO for such a system can be constructed by introducing a gain L_o to be determined (which replaces L above), and using (5.6) to replace the uncertain terms (*i.e.*, $w_k - Lv_k$) by their interval bounds. The resulting IO [Efimov et al., 2013] is given as follows:

$$\begin{aligned}\overline{x}_{k+1} &= D_o\overline{x}_k + Bu_k + L_oy_k - L_o^+\underline{v}_k + L_o^-\overline{v}_k + \overline{w}_k\\ \underline{x}_{k+1} &= D_o\underline{x}_k + Bu_k + L_oy_k - L_o^+\overline{v}_k + L_o^-\underline{v}_k + \underline{w}_k\end{aligned} \tag{5.10}$$

where $D_o = A - L_oC$, and having $\underline{x}_0, \overline{x}_0$ as specified in Assumption 5.1. Note that the precision of (5.10) can be evaluated by the width of its interval, *i.e.*, $\delta x_k = \overline{x}_k - \underline{x}_k$, whose dynamics are given by:

$$\delta x_{k+1} = D_o\delta x_k + \delta w_k + |L_o|\delta v_k, \tag{5.11}$$

where $\delta w_k = \overline{w}_k - \underline{w}_k$ and $\delta v_k = \overline{v}_k - \underline{v}_k$ determine the uncertainty size of the state and the output disturbances, respectively. Since $\delta x_0 = \overline{x}_0 - \underline{x}_0$, the solution of (5.11) is obtained by

$$\delta x_k = D_o^k(\overline{x}_0 - \underline{x}_0) + \sum_{i=0}^{k-1} D_o^{k-1-i}(\delta w_i + |L_o|\delta v_i)$$

for all $k \in \mathbb{Z}_+$. Hence, the values of δx_k are completely determined by the choice of the gain L_o and the uncertainty levels given in Assumption 5.1. Our first result shows a procedure to compute this gain.

Theorem 5.1. *Let Assumption 5.1 be satisfied. If the following inequalities are verified for*

a scalar $\rho > 0$*, a diagonal matrix* $P \in \mathbb{R}^{n\times n}$ *and matrices* $W^+, W^- \in \mathbb{R}_+^{n\times p}$*:*

$$\begin{gathered}\min_{\rho,P,W^+,W^-} \rho \\ P > 0,\ PA - (W^+ - W^-)C \geq 0, \\ \begin{bmatrix} P - \mathcal{I}_n & 0 & A^\top P - C^\top (W^+ - W^-)^\top \\ \star & \rho\mathcal{I}_n & E^\top \\ \star & \star & P \end{bmatrix} \succeq 0, \\ E = \begin{bmatrix} P & W^+ + W^- \end{bmatrix},\end{gathered}$$

then system (5.10) *with gains* $L_o^+ = P^{-1}W^+$ *and* $L_o^- = P^{-1}W^-$ *is an IO for system* (5.8)*, i.e., relation* (5.2) *holds and* $\delta x_k \in \ell_\infty^n$*. Furthermore, the transfer* $(\delta w_k, \delta v_k) \longmapsto \delta x$ *has a gain lesser than* $\sqrt{\rho}$*.*

Proof. Let the estimation errors be given by $\overline{e}_k = \overline{x}_k - x_k$ and $\underline{e}_k = x_k - \underline{x}_k$, whose increments have the following form:

$$\begin{aligned}\overline{e}_{k+1} &= D_o\overline{e}_k + \overline{w}_k - w_k + L_o v_k - L_o^+ \underline{v}_k + L_o^- \overline{v}_k, \\ \underline{e}_{k+1} &= D_o\underline{e}_k + w_k - \underline{w}_k - L_o v_k - L_o^+ \overline{v}_k + L_o^- \underline{v}_k.\end{aligned} \tag{5.12}$$

Then, under Assumption 5.1 and Lemma 5.1, all exogenous inputs (*i.e.*, the independent right-most terms) in (5.12) are non-negative. Consequently, if D_o is also non-negative, we have that $\underline{e}_k, \overline{e}_k \geq 0$ for all $k \in \mathbb{Z}_+$ under Lemma 5.2. This requirement is imposed by the first inequality on this theorem and implies relation (5.2).

Note that, under Assumption 1, the asymptotic stability of (5.11) and (5.12) sums up to the Schur stability of D_o. In this light, let $\nu_k = \mathrm{vec}(\delta w_k, \delta v_k)$ and consider a candidate Lyapunov function $V_k = \delta x_k^\top P \delta x_k$, whose increments for (5.11) are given by

$$V_{k+1} - V_k = \begin{bmatrix} \delta x_k \\ \nu_k \end{bmatrix}^\top \underbrace{\begin{bmatrix} D_o^\top P D_o - P & D_o^\top E \\ E^\top D_o & E^\top P^{-1} E \end{bmatrix}}_{\Pi} \begin{bmatrix} \delta x_k \\ \nu_k \end{bmatrix}. \tag{5.13}$$

Thus, a sufficient condition for Schur stability of D_o is $\Pi \preceq 0$. Now, by introducing a performance index given by $J = \sum_{k=0}^\infty \delta x_k^\top \delta x_k - \gamma^2 \nu_k^\top \nu_k + (V_{k+1} - V_k)$, the desired ℓ_∞ performance is achieved by rendering $J < 0$, while minimizing γ. Taking (5.13) into account, this condition is equivalent to

$$\begin{bmatrix} D_o^\top P D_o - P + \mathcal{I}_n & D_o^\top E \\ E^\top D_o & E^\top P^{-1} E - \gamma^2 \mathcal{I}_n \end{bmatrix} \preceq 0.$$

Since P is diagonal, we can decompose the relation above as follows:

$$\begin{bmatrix} D_o^\top P \\ E^\top \end{bmatrix} P^{-1} \begin{bmatrix} PD_o & E \end{bmatrix} - \begin{bmatrix} P - \mathcal{I}_n & 0 \\ 0 & \gamma^2 \mathcal{I}_n \end{bmatrix} \preceq 0$$

and hence, by applying the Schur complement in the inequality above, and by introducing the variables $\rho = \gamma^2$, $W^+ = PL_o^+$ and $W^- = PL_o^-$, the inequalities given in this theorem are obtained, proving the claim. □

Interval predictor

To avoid confusion with the IO developed in the previous section, $\overline{z}_k$ and $\underline{z}_k$ will denote the predicted upper and lower bounds for x_k, respectively, for all $k \in \mathbb{Z}_+$. Also, the predictor gain (which replaces L in (5.9)) will be denoted as L_p.

By definition, $L_p = L_p^+ - L_p^-$ for some $L_p^+, L_p^- \in \mathbb{R}_+^{n\times p}$. Then, under (5.2), Assumption 5.2 and Lemma 5.1, we can state that

$$L_p^+ C\underline{x}_k - L_p^- C\overline{x}_k \leq L_p C x_k \leq L_p^+ C\overline{x}_k - L_p^- C\underline{x}_k$$

which allows us to substitute the terms which are unavailable for prediction in (5.9) (*i.e.*, $Ly_k - Lv_k + w_k = LCx_k + w_k$), with their respective bounds. The following IP is then obtained:

$$\begin{aligned} \overline{z}_{k+1} &= D_p\overline{z}_k + Bu_k + L_p^+ C\overline{z}_k - L_p^- C\underline{z}_k + \overline{w}_k, \\ \underline{z}_{k+1} &= D_p\underline{z}_k + Bu_k + L_p^+ C\underline{z}_k - L_p^- C\overline{z}_k + \underline{w}_k, \end{aligned} \tag{5.14}$$

where $D_p = A - L_pC$. As readily seen, (5.14) is composed only by known terms (under Assumption 5.1 and assuming that u_k is to be computed in the control algorithm).

Introducing a change of coordinates describing the center of the interval, $z_k^\star = \frac{\overline{z}_k + \underline{z}_k}{2}$, and the width of the interval, $\delta z_k = \overline{z}_k - \underline{z}_k$, one gets the following equivalent representation of dynamics of (5.14):

$$z_{k+1}^\star = Az_k^\star + Bu_k + w_k^\star, \tag{5.15}$$

$$\delta z_{k+1} = (A + 2L_p^- C)\delta z_k + \delta w_k \tag{5.16}$$

where, similarly, $w_k^\star = \frac{\overline{w}_k + \underline{w}_k}{2}$ and $\delta w_k = \overline{w}_k - \underline{w}_k$. Two interesting features are to be noted: *(i)* the dynamics of the center of the predicted interval $z_k^\star$ is independent of L_p, but it is controlled by u_k and, hence, (5.15) can be used in MPC algorithm, and *(ii)* the dynamics of the interval width δz_k is governed by the (known) interval width of the state disturbance δw_k, and its stability can be assured by a proper choice of the gain L_p. The following theorem

offers a procedure to compute such a gain.

Theorem 5.2. *Let assumptions 5.1–5.2 be satisfied, and there exist a diagonal matrix* $P \in \mathbb{R}^{n\times n}$*, matrices* $Q, \Gamma \in \mathbb{R}^{n\times n}$ *and* $U^-, U^+ \in \mathbb{R}_+^{n\times p}$ *such that the following linear matrix inequalities are verified:*

$$PA - U^+C + U^-C \geq 0, \tag{5.17}$$
$$\begin{bmatrix} P-Q & 0 & A^\top P + 2C^\top U^{-\top} \\ 0 & \Gamma & P \\ PA + 2U^-C & P & P \end{bmatrix} \succeq 0$$
$$P \succ 0,\ Q \succ 0,\ \Gamma \succ 0.$$

Then, system (5.14) with gains $L_p^- = P^{-1}U^-$*,* $L_p^+ = P^{-1}U^+$ *and* $\underline{z}_0 = \underline{x}_0$*,* $\overline{z}_0 = \overline{x}_0$ *is an IP for system (5.8), i.e., the relation (5.3) is satisfied and* $\delta z \in \ell_\infty^n$*.*

Proof. Assume that the gain L_p is selected such that the matrix D_p is non-negative. Then, the realization of relation (5.3) for system (5.8), (5.14) (under substitution of $\underline{z}_k, \overline{z}_k$ instead of $\underline{x}_k, \overline{x}_k$, respectively) can be proven following the same arguments as in Theorem 5.1. Recalling that $L_p = L_p^+ - L_p^-$ with $L^+, L^- \in \mathbb{R}_+^{n\times p}$, then

$$A - L_pC = A - L_p^+C + L_p^-C \geq 0$$

is the condition to verify under Assumption 5.2. The stability of (5.16) implies the stability of the IP (5.14). In this sense, note that

$$0 \leq A - L_p^+C + L_p^-C \leq A + 2L_p^-C$$

since $L_p^-C \geq 0$ and $L_p^+C \geq 0$ under Assumption 5.2. Then $A + 2L_p^-C \in \mathbb{R}_+^{n\times n}$ and according to Lemma 5.3, we can select a diagonal matrix $P \in \mathbb{R}^{n\times n}$ considering $V_k = \delta z_k^\top P \delta z_k$ as a Lyapunov function candidate (with $P \succ 0$), whose increment takes, for any $Q \in \mathbb{R}^{n\times n}$ and $\Gamma \in \mathbb{R}^{n\times n}$, the following form:

$$V_{k+1} - V_k = \begin{bmatrix} \delta z_k \\ \delta w_k \end{bmatrix}^\top \overbrace{\begin{bmatrix} D^\top P D - P + Q & D^\top P \\ PD & P - \Gamma \end{bmatrix}}^{\Sigma} \begin{bmatrix} \delta z_k \\ \delta w_k \end{bmatrix} - \delta z_k^\top Q \delta z_k + \delta w_k^\top \Gamma \delta w_k$$

where $D = A + 2L^-C$. If $Q \succ 0$, $\Gamma \succ 0$ and $\Sigma \preceq 0$, then the stability conditions are fulfilled and the system (5.16) is ISS with respect to the input δw_k:

$$V_{k+1} - V_k \leq -\delta z_k^\top Q \delta z_k + \delta w_k^\top \Gamma \delta w_k.$$

The first LMI in this theorem relates to the condition $A-(L^+-L^-)C \geq 0$ and is obtained by defining $U^- = PL^- \in \mathbb{R}_+^{n\times p}$ and $U^+ = PL^+ \in \mathbb{R}_+^{n\times p}$. The second condition concerns the Schur stability of Σ. Decomposing the matrix Σ, similarly as in Theorem 5.1, and taking its Schur complement, the second LMI is readily obtained by recalling that $PD = PA+2PL^-C$. This proves the theorem. □

Remark 5.1. *Similarly to Proposition 1, an additional optimization problem can be posed for the maximization of Q and minimization of Γ while solving the LMIs of Theorem 5.2, aiming an optimal accuracy in the interval prediction.*

5.2.2 Control design

Before discussing the MPC algorithm to be proposed, we stress the stabilization of the IP through a (static) state feedback. Note that IP (5.14) can be stabilized by designing a feedback for its completely known center dynamics (5.15)

$$z^\star_{k+1} = (A + BK_f)z^\star_k + (\mathcal{I}_n + BS_f)w^\star_k, \tag{5.18}$$

using the following control law:

$$u_k = S_f w^\star_k + K_f z^\star_k \tag{5.19}$$

with the gains $K_f \in \mathbb{R}^{m\times n}$ and $S_f \in \mathbb{R}^{m\times n}$ guaranteeing input-to-state stability of the closed-loop system and minimizing the influence of $w^\star_k$, respectively. These gains can be selected as follows:

Theorem 5.3. *Let $S_f = \Sigma P^{-1}$ and $K_f = \Upsilon P^{-1}$, where $P \in \mathbb{R}^{n\times n}$ and $\Sigma, \Upsilon \in \mathbb{R}^{m\times n}$ are solutions of a linear optimization problem:*

$$\max_{Q,\Gamma_1,\Gamma_2\in\mathbb{R}^{n\times n}} Q - \Gamma_1 - \Gamma_2,$$

$$Q = Q^\top \succ 0,\ \Gamma_1 = \Gamma_1^\top \succ 0,\ \Gamma_2 = \Gamma_2^\top \succ 0,\ P = P^\top \succ 0,\ \Pi \succeq 0$$

$$\Pi = \begin{bmatrix} P-Q & 0 & 0 & PA^\top + \Upsilon^\top B^\top \\ 0 & \Gamma_1 & 0 & P + \Sigma^\top B^\top \\ 0 & 0 & \Gamma_2 & P \\ AP + B\Upsilon & P + B\Sigma & P & P \end{bmatrix}.$$

Then the center dynamics (5.15) with the control (5.19) is ISS (from the input $(w^\star_k)$ to the state $z^\star_k$) with the optimal attenuation of the disturbances and with an ISS-Lyapunov function $V(z^\star_k) = z^{\star\top}_k P^{-1} z^\star_k$.

Proof. Substituting the control (5.19) into the (5.15) yields the closed-loop dynamics (5.18).

Consider the increment of the candidate Lyapunov function $V(z_k^\star)$:

$$V(z_{k+1}^\star) - V(z_k^\star) =$$
$$\begin{bmatrix} z_k^\star \\ w_k^\star \end{bmatrix}^\top \overbrace{\begin{bmatrix} \tilde{A}^\top P^{-1}\tilde{A} - P^{-1} + \tilde{Q} & \tilde{A}^\top P^{-1}\tilde{D} \\ \tilde{D}^\top P^{-1}\tilde{A} & \tilde{D}^\top P^{-1}\tilde{D} - \tilde{\Gamma}_1 \end{bmatrix}}^{\tilde{\Pi}} \begin{bmatrix} z_k^\star \\ w_k^\star \end{bmatrix} - z_k^{\star\top}\tilde{Q}z_k^\star + w_k^{\star\top}\tilde{\Gamma}_1 w_k^\star,$$

where $\tilde{A} = A + BK_f$, $\tilde{D} = \mathcal{I}_n + BS_f$ and for any $\tilde{Q}, \tilde{\Gamma}_1 \in \mathbb{R}^{n\times n}$. If $\tilde{\Pi} \preceq 0$, then

$$V(z_{k+1}^\star) - V(z_k^\star) \leq -\alpha V(z_k^\star) + w_k^{\star\top}\tilde{\Gamma}_1 w_k^\star \tag{5.20}$$

meaning that the system is ISS, provided that $\tilde{Q} \succeq \alpha P^{-1}$ and $\tilde{\Gamma}_1 \succ 0$, where $\alpha > 0$ always exists if $\tilde{Q} \succ 0$. Note that

$$\tilde{\Pi} = -\begin{bmatrix} P^{-1} - \tilde{Q} & 0 \\ 0 & \tilde{\Gamma}_1 \end{bmatrix} + \begin{bmatrix} \tilde{A}^\top P^{-1} \\ \tilde{D}^\top P^{-1} \end{bmatrix} P \begin{bmatrix} P^{-1}\tilde{A} & P^{-1}\tilde{D} \end{bmatrix}$$

is such that, by applying the Schur complement, the LMIs given in the formulation of this proposition are verified for $\Sigma = S_f P$, $\Upsilon = K_f P$, $\tilde{Q} = P^{-1}QP^{-1}$, $\tilde{\Gamma}_1 = P^{-1}\Gamma_1 P^{-1}$. □

Remark 5.2. *Additional constraint can be imposed on P, in order to guarantee some optimal performance for the terminal cost under the control (5.19).*

Remark 5.3. *If $w_k^\star = 0$ for $k \in \mathbb{Z}_+$ then an obvious choice is $S_f = 0$, which can be imposed as a constraint on the optimization problem given by Proposition 5.3.*

As a consequence of property (5.20), the following ellipsoid is a positively invariant set for (5.8) under control (5.19):

$$\tilde{\mathbb{X}} = \left\{ z^\star \in \mathbb{R}^n : z^{\star\top} P^{-1} z^\star \leq \alpha^{-1} \sup_{k\geq 0} w_k^{\star\top}\tilde{\Gamma}_1 w_k^\star \right\}, \tag{5.21}$$

for the α obtained in Theorem 5.3. The following assumption, which is conventionally imposed in MPC [Mayne et al., 2000], is introduced:

Assumption 5.3. *Let the terminal set $\mathbb{X}_f \subseteq \tilde{\mathbb{X}} \subseteq \mathbb{X}$ and $u_k \in \mathbb{U}$ for all $z_k^\star \in \mathbb{X}_f$ in (5.19).*

Assumption 5.3 may be relaxed by further constraining the conditions given in Theorem 5.3, as suggests the following corollary:

Corollary 5.1. *Let there exist symmetric and positive definite matrices $\mathcal{U} \in \mathbb{R}^{m\times m}$ and $Z \in \mathbb{R}^{2n\times 2n}$ such that $\mathbb{U} = \{u \in \mathbb{R}^m : u^\top \mathcal{U} u \leq 1\}$ and $\mathcal{W}_k \in \{\mathcal{W} \in \mathbb{R}^{2n} : \mathcal{W}^\top Z \mathcal{W} \leq 1\}$, and*

the conditions of Theorem 5.3 be satisfied with additional inequalities:

$$\begin{gathered}\frac{\eta}{\alpha\kappa}\Gamma \leq \min\{\kappa^{-1}Z, P\},\ P \geq \kappa Z^{-1},\\ \begin{bmatrix} \frac{\eta}{3}P & 0 & \Upsilon^\top \\ 0 & \frac{\kappa}{3}P & \Sigma^\top \\ \star & \star & \mathcal{U}^{-1} \end{bmatrix} \geq 0\end{gathered} \tag{5.22}$$

for some constants $\eta > 0$ and $\kappa > 0$, then control (5.19) satisfies the constraint $u_k \in \mathbb{U}$ for all $z_k^\star \in \mathbb{X}_f$.

Proof. First of all, the imposed inequalities on Z and Γ imply:

$$\begin{gathered}Z \geq \kappa P^{-1},\ \frac{\eta}{\alpha}\Gamma_1 \leq Z,\\ \frac{\eta}{\alpha}\Gamma_1 \leq \kappa P \leq PZP \Rightarrow \frac{\eta}{\alpha}\tilde{\Gamma}_1 = \frac{\eta}{\alpha}P^{-1}\Gamma_1 P^{-1} \leq Z,\end{gathered}$$

consequently,

$$\eta z_k^{\star\top} P^{-1} z_k^\star \leq \frac{\eta}{\alpha} w_k^{\star\top}\tilde{\Gamma}_1 w_k^\star \leq w_k^{\star\top} Z w_k^\star \leq 1$$

for $z_k^\star \in \tilde{\mathbb{X}}$. Next, note that the condition $u_k \in \mathbb{U}$ takes the form:

$$\begin{bmatrix} z_k^\star \\ w_k^\star \end{bmatrix}^\top \begin{bmatrix} K_f \\ S_f \end{bmatrix} \mathcal{U} \begin{bmatrix} K_f \\ S_f \end{bmatrix}^\top \begin{bmatrix} z_k^\star \\ w_k^\star \end{bmatrix} \leq 1.$$

If $z_k^\star \in \tilde{\mathbb{X}}$, then the ellipsoid (5.21) can be evoked to rewrite the previous inequality as

$$\begin{bmatrix} K_f \\ S_f \end{bmatrix} \mathcal{U} \begin{bmatrix} K_f \\ S_f \end{bmatrix}^\top \leq \frac{1}{2}\begin{bmatrix} \eta P^{-1} & 0 \\ 0 & Z \end{bmatrix}.$$

Applying Schur complement the latter property is equivalent to

$$\begin{bmatrix} \frac{\eta}{2}P^{-1} & 0 & K_f^\top \\ 0 & \frac{1}{2}Z & S_f^\top \\ K_f & S_f & \mathcal{U} \end{bmatrix} \geq 0,$$

then multiplying this inequality from both sides by $\mathrm{diag}\{P, P, I_m\}$ and taking into account that $PZP \geq \kappa P$ we get the LMI of the corollary. □

5.2.3 An extension to linear time-delayed systems

The idea developed in this section was also applied to linear time-delayed systems [Souza et al., 2021c], whose dynamics are given by the following retarded difference equation:

$$x_{k+1} = A_0 x_k + A_1 x_{k-h} + B u_k + w_k,$$

where $x_{k-h} \in \mathbb{R}^n$ is the delayed state, with a known and fixed delay $h > 0$.

For brevity of exposition, these results are not reported in this thesis. In such a case, each interval estimator has two gains (for illustration, L_0 and L_1), one relating to the actual state, and another relating to the delayed one. Due to this new term, the stability analysis must be then carried out using the *Lyapunov-Krasovskii* framework [Fridman, 2014].

Interestingly, the proposed methodology easily encompasses delays in states, inputs and outputs, features that were not entirely reported on the robust MPC literature. The challenge in this scenario, however, remains in the fact the two gains must be designed to render both $A_0 - L_0 C$ and $A_1 - L_1 C$ non-negative (in order to ensure non-negativity of the estimation errors), instead of only one as discussed in this section.

5.2.4 Numerical illustration

Consider the (linearized) continuous stirred tank reactor (CSTR), where an exothermic and irreversible reaction $S \to P$ occurs [Henson and Seborg, 1997]. The model is composed of two states, the concentration of reactant C_S and the temperature of the reactor T, and one controlled input, the coolant stream T_C. The resulting linear system is as follows:

$$\begin{aligned} x_{k+1} &= \begin{bmatrix} 0.745 & -0.002 \\ 5.610 & 0.780 \end{bmatrix} x_k + \begin{bmatrix} 5.6 \times 10^{-6} \\ 0.464 \end{bmatrix} u_k + w_k, \\ y_k &= \begin{bmatrix} 0 & 1 \end{bmatrix} x_k + v_k. \end{aligned} \tag{5.23}$$

where the disturbances are considered to be enclosed in $\mathbb{W} = [-0.02, 0.02] \times [-0.2, 0.2]$ and $\mathbb{V} = [-0.2, 0.2]$. The initial conditions are assumed to be bounded such as $x_0 \in [-1.1, -1] \times [6, 7]$.

Solving the conditions given in this section, the following gains are obtained for the IO and IP:

$$L_o = \begin{bmatrix} -0.02 \\ 0.78 \end{bmatrix}, \quad L_p = \begin{bmatrix} -0.02 \\ 0.39 \end{bmatrix}$$

while for the control (considering $S_f = 0$ due to the symmetry of the disturbances bounds), the feedback gain obtained was $K_f = \begin{bmatrix} -6.99 & -0.50 \end{bmatrix}$. The IO/IP are initialized according to the initial conditions given above.

In the following, Figures 5.2 and 5.3 depict, respectively the evolution of the states of the real system and the pair IO/IP, and the evolution of the computed control signal. As it can be seen, the stabilization of the interval center is successful. Since the pair IP/IO has stable widths and thanks to relations (5.2) and (5.3), the real trajetories of (5.23) is also stabilized in a vicinity of the origin (which evidences the practical ISS).

However, in Figure 5.2, one can see that the IP is much more conservative than the IO.

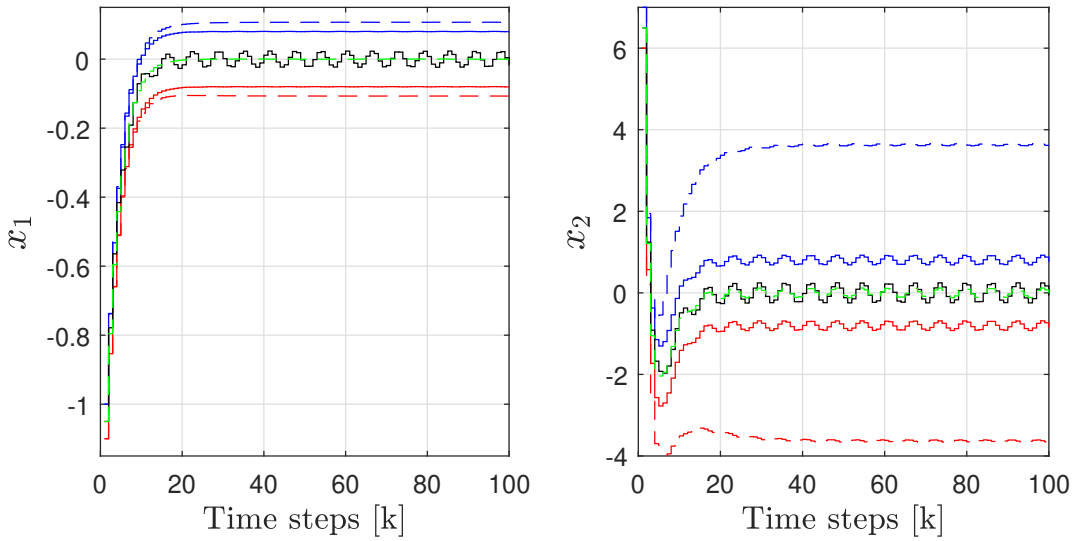

Figure 5.2: Evolution of the states. Legend – continuous lines: IO, dashed lines: IP, black lines: real system, blue lines: upper estimates, red lines: lower estimates, green lines: interval center.

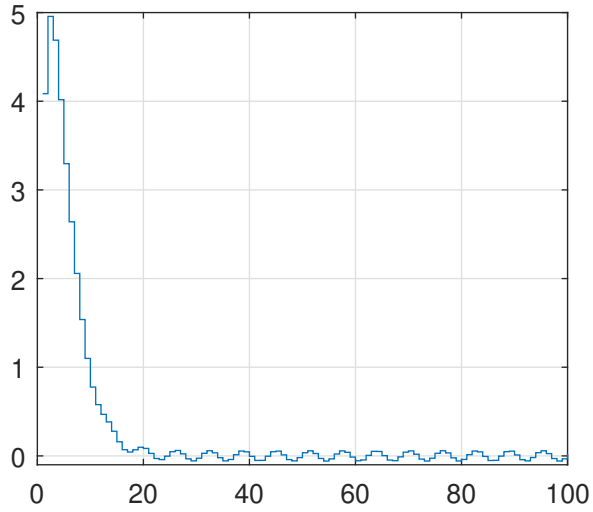

Figure 5.3: Evolution of the control input.

5.3 OF-MPC for LPV systems

In this section, a solution for Problem 5.1 will be investigated for the case in which system (5.1) is described by linear parameter-varying model [Souza et al., 2021b], *i.e.*,

$$x_{k+1} = A(\theta_k)x_k + B(\theta_k)u_k + w_k \tag{5.24}$$

It is assumed that θ_k is not measured, but its set of admissible values Θ is known. Furthermore, the matrix functions $A : \Theta \to \mathbb{R}^{n\times n}$ and $B : \Theta \to \mathbb{R}^{n\times m}$ are locally bounded and known. The measurement matrix $C \in \mathbb{R}^{p\times n}$ is assumed to be known.

Assumption 5.4. *There exist matrices $A_0 \in \mathbb{R}^{n\times n}, B_0 \in \mathbb{R}^{n\times m}$ and $\Delta A_i \in \mathbb{R}^{n\times n}, \Delta B_i \in \mathbb{R}^{n\times m}$, $i = 1, \dots, \nu$ for some $\nu \in \mathbb{Z}_+$, such that the following relations are satisfied for all $\theta \in \Theta$:*

$$A(\theta) = A_0 + \sum_{i=1}^{\nu} \lambda_i(\theta)\Delta A_i, \quad B(\theta) = B_0 + \sum_{i=1}^{\nu} \lambda_i(\theta)\Delta B_i,$$
$$\sum_{i=1}^{\nu} \lambda_i(\theta) = 1, \quad \lambda_i(\theta) \in [0, 1].$$

Assumption 5.5. *It is assumed that $\Delta B_i \geq 0$.*

Assumption 5.4 (which is technical and it is introduced to simplify the writing) states that system (5.24) admits a convex embedding in a polytope defined by ν known vertices ΔA_i and ΔB_i with known centers A_0, B_0. Note that, since functions A, B and the set Θ are known, then there exists matrices $\underline{A}, \overline{A}, \underline{B}, \overline{B}$ such that

$$\underline{A} \leq A(\theta) \leq \overline{A}, \quad \underline{B} \leq B(\theta) \leq \overline{B}, \quad \forall \theta \in \Theta.$$

5.3.1 Design of interval estimators

Interval observer

In this section, the objective is to design an IO for (5.24) by exploiting the available measurement. To this end, let us evoke Assumption 5.4 and rewrite (5.24) as

$$x_{k+1} = (A_0 - LC)x_k + \sum_{i=1}^{\nu} \lambda_i(\theta)\Delta A_i x_k + Ly_k + (B_0 + \sum_{i=1}^{\nu} \lambda_i(\theta)\Delta B_i)u_k - Lv_k + w_k \tag{5.25}$$

for any $L \in \mathbb{R}^{n\times p}$. First, let us denote

$$\Delta A_+ = \sum_{i=1}^{\nu} \Delta A_i^+, \quad \Delta A_- = \sum_{i=1}^{\nu} \Delta A_i^-, \quad \text{and} \quad \Delta B = \sum_{i=1}^{\nu} \Delta B_i^+.$$

Then, under assumptions 5.4–5.5 and Lemma 5.1, replacing the uncertain terms in (5.24)

by their interval bounds leads to the following IO:

$$\begin{aligned}\overline{x}_{k+1} =& D_o\overline{x}_k + \Delta A_+\overline{x}_k^+ + \Delta A_-\underline{x}_k^- + B_0u_k + \Delta Bu_k^+ + L_oy_k - L_o^+\underline{v}_k + L_o^-\overline{v}_k + \overline{w}_k\\ \underline{x}_{k+1} =& D_o\underline{x}_k - \Delta A_+\underline{x}_k^- - \Delta A_-\overline{x}_k^+ + B_0u_k - \Delta Bu_k^- + L_oy_k - L_o^+\overline{v}_k + L_o^-\underline{v}_k + \underline{w}_k\end{aligned} \tag{5.26}$$

where $D_o = A_0 - L_oC$, $L_o \in \mathbb{R}^{n\times p}$ being the observer gain to be determined. The fulfillment of relation (5.2) follows the cooperativity of the estimation errors $\overline{e}_k = \overline{x}_k - x_k$ and $\underline{e}_k = x_k - \underline{x}_k$, the respective conditions are given in the following lemma:

Lemma 5.4. *Let assumptions 5.4–5.5 be satisfied. Then, provided that $A_0 - L_oC$ is non-negative, the estimation errors are non-negative, i.e., $\underline{e}_k, \overline{e}_k \geq 0$ for all $k > 0$.*

Proof. First, by applying (5.7) in $\lambda_i x_k$, one obtains

$$\underline{\lambda}_i^+\underline{x}_k^+ - \overline{\lambda}_i^+\underline{x}_k^- - \underline{\lambda}_i^-\overline{x}_k^+ + \overline{\lambda}_i^-\overline{x}_k^- \leq \lambda_i x_k \leq \overline{\lambda}_i^+\overline{x}_k^+ - \underline{\lambda}_i^+\overline{x}_k^- - \overline{\lambda}_i^-\underline{x}_k^+ + \underline{\lambda}_i^-\underline{x}_k^-$$

Since $\lambda_i \in [0,1]$, then $\overline{\lambda}_i^+ = 1$ and $\underline{\lambda}_i^+ = \overline{\lambda}_i^- = \underline{\lambda}_i^- = 0$, by definition. Under this, the relation $-\underline{x}_k^- \leq \lambda_i(\theta_k)x_k \leq \overline{x}_k^+$ holds. Then, since the vertices of the polytopic system are known, relation (5.6) can be applied to obtain the following inequalities

$$-\Delta A_+\underline{x}_k^- - \Delta A_-\overline{x}_k^+ \leq \sum_{i=1}^N \lambda_i(\theta_k)\Delta A_i x_k \leq \Delta A_+\overline{x}_k^+ + \Delta A_-\underline{x}_k^-. \tag{5.27}$$

Finally, the same idea applies to the term proportional to u_k, leading to the following relation:

$$-\Delta B_iu_k^- \leq -(\Delta B_iu_k)^- \leq \lambda_i\Delta B_iu_k \leq (\Delta B_iu_k)^+ \leq \Delta B_iu_k^+ \tag{5.28}$$

Now, computing the increments of the estimation errors $\overline{e}_k, \underline{e}_k$ and taking (5.27)–(5.28) into account, one gets

$$\overline{e}_{k+1} = D_o\overline{e}_k + r_{1,1} + r_{1,2}, \quad \underline{e}_{k+1} = D_o\underline{e}_k + r_{2,1} + r_{2,2}$$

where

$$\begin{aligned}r_{1,1} &= \Delta A_+\overline{x}_k^+ + \Delta A_-\underline{x}_k^- - \sum_{i=1}^N \lambda_i(\theta_k)\Delta A_i x_k + \Delta Bu_k^+ - \sum_{i=1}^N \lambda_i(\theta_k)\Delta B_iu_k,\\ r_{1,2} &= L_ov_k - L_o^+\underline{v}_k + L_o^-\overline{v}_k + \overline{w}_k - w_k,\\ r_{2,1} &= \sum_{i=1}^N \lambda_i(\theta_k)\Delta A_i x_k - (-\Delta A_+\underline{x}_k^- - \Delta A_-\overline{x}_k^+) + \sum_{i=1}^N \lambda(\theta_k)\Delta B_iu_k + \Delta Bu_k^-,\\ r_{2,2} &= L_o^+\overline{v}_k - L_o^-\underline{v}_k - L_ov_k + w_k - \underline{w}_k.\end{aligned} \tag{5.29}$$

From assumptions 5.1 and 5.4 and relations (5.27)–(5.28), the quantities given in (5.29) are positive. Hence, if D_o is non-negative, then $\overline{e}_k, \underline{e}_k > 0$ for all $k > 0$ under Lemma 5.2, and

thus satisfying relation (5.3). □

Now, it is needed to derive stability conditions for IO (5.26). First, let us denote $\chi_k = \text{vec}(\overline{x}_k, \underline{x}_k)$ and rewrite (5.26) as

$$\chi_{k+1} = \left(\mathcal{A}_0 - \tilde{L}_o C_1\right)\chi_k + \mathcal{A}_+\chi_k^+ + \mathcal{A}_-\chi_k^- + \delta_k \tag{5.30}$$

where $\mathcal{A}_0 = \text{diag}\,(A_0, A_0) \in \mathbb{R}^{2n\times 2n}$, $\tilde{L}_o = \text{diag}(L_o, L_o) \in \mathbb{R}^{2n\times 2p}$, $C_1 = \text{diag}\,(C, C) \in \mathbb{R}^{2p\times 2n}$, $\delta_k = \text{vec}(\overline{\delta}_k, \underline{\delta}_k)$, and

$$\mathcal{A}_+ = \begin{bmatrix} \Delta A_+ & 0 \\ -\Delta A_- & 0 \end{bmatrix}, \quad \mathcal{A}_- = \begin{bmatrix} 0 & \Delta A_- \\ 0 & -\Delta A_+ \end{bmatrix},$$
$$\overline{\delta}_k = B_0 u_k + \Delta B u_k^+ + L_o y_k - L_o^+ \underline{v}_k + L_o^- \overline{v}_k + \overline{w}_k,$$
$$\underline{\delta}_k = B_0 u_k - \Delta B u_k^- + L_o y_k - L_o^+ \overline{v}_k + L_o^- \underline{v}_k + \underline{w}_k.$$

For ease of notation in the sequel, let us denote $\tilde{U} = \text{diag}\,(U, U)$ and $\tilde{P} = \text{diag}\,(P, P)$ for some decision variables $P \in \mathbb{R}^{n\times n}$ and $U \in \mathbb{R}^{n\times p}$. A gain L_o that stabilizes (5.26) and satisfies the restrictions of Lemma 4 can be computed by verifying the following conditions:

Theorem 5.4. *Let assumptions 5.1–5.4 be satisfied. If there exist diagonal matrices $\tilde{P}$, Q_1, Q_2, Q_3, Ω_+, Ω_-, $\Psi \in \mathbb{R}^{2n\times 2n}$, matrices $\Gamma \in \mathbb{R}^{2n\times 2n}$ and $\tilde{U} \in \mathbb{R}^{2n\times p}$, such that the following LMIs are verified:*

$$\tilde{P}\mathcal{A}_0 - \tilde{U}C_1 \geq 0$$
$$\begin{bmatrix} \tilde{P} - Q_1 & -\Omega_+ & -\Omega_- & 0 & \mathcal{A}_0^\top \tilde{P} - C_1^\top \tilde{U}^\top \\ \star & -Q_2 & -\Psi & 0 & \mathcal{A}_+^\top \tilde{P} \\ \star & \star & -Q_3 & 0 & \mathcal{A}_-^\top \tilde{P} \\ \star & \star & \star & \Gamma & \tilde{P} \\ \star & \star & \star & \star & \tilde{P} \end{bmatrix} \succeq 0 \tag{5.31}$$
$$\tilde{P} > 0, \quad \Gamma \succ 0, \quad Q_1, Q_2, Q_3, \Omega_+, \Omega_- \geq 0,$$
$$Q_1 + \min\{Q_2, Q_3\} + 2\min\{\Omega_+, \Omega_-\} > 0$$

then system (5.26) with a gain $L_o = P^{-1}U$ is an IO for system (5.24), i.e., relation (5.2) is satisfied and, in addition, $\chi \in \ell_\infty^{2n}$ provided that $\delta \in \ell_\infty^{2n}$.

Proof. Let us consider a Lyapunov function candidate $V_k = \chi_k^\top \tilde{P}\chi_k$, whose increments are

given by

$$V_{k+1}-V_k=\begin{bmatrix}\chi_k\\ \chi_k^+\\ \chi_k^-\\ \delta_k\end{bmatrix}^\top \overbrace{\begin{bmatrix}\mathcal{D}_o^\top\tilde{P}\mathcal{D}_o-\tilde{P}+Q_1 & \mathcal{D}_o^\top\tilde{P}\mathcal{A}_+ +\Omega_+ & \mathcal{D}_o^\top\tilde{P}\mathcal{A}_- +\Omega_- & \mathcal{D}_o^\top\tilde{P}\\ \star & \mathcal{A}_+^\top\tilde{P}\mathcal{A}_+ +Q_2 & \mathcal{A}_+^\top\tilde{P}\mathcal{A}_- +\Psi & \mathcal{A}_+^\top\tilde{P}\\ \star & \star & \mathcal{A}_-^\top\tilde{P}\mathcal{A}_- +Q_3 & \mathcal{A}_-^\top\tilde{P}\\ \star & \star & \star & \tilde{P}-\Gamma\end{bmatrix}}^{\Sigma}\begin{bmatrix}\chi_k\\ \chi_k^+\\ \chi_k^-\\ \delta_k\end{bmatrix}$$
$$-{\chi_k}^\top Q_1\chi_k-{\chi_k^+}^\top Q_2\chi_k^+-{\chi_k^-}^\top Q_3\chi_k^- -2\chi_k^\top\Omega_+\chi_k^+-2\chi_k^\top\Omega_-\chi_k^- -2\chi_k^{+\top}\Psi\chi_k^- +\delta_k^\top\Gamma\delta_k.$$

If $Q=Q_1+\min\{Q_2,Q_3\}+2\min\{\Omega_+,\Omega_-\}\succ 0,\Gamma\succ 0$ and $\Sigma\preceq 0$ and provided that $\delta\in\ell_\infty^{2n}$, then the stated stability conditions are fulfilled and system (5.26) is input-to-state stable (ISS) with respect to the input δ_k (the diagonal matrix Ψ can be sign indefinite since $\chi_k^{+\top}\Psi\chi_k^-=0$ by definition):

$$V_{k+1}-V_k=-\chi_k^\top Q\chi_k+\delta_k^\top\Gamma\delta_k$$

Hence, it is needed to show that the above stability conditions can be formulated as LMIs. First, since $\tilde{P}>0$, then Σ can be decomposed as

$$\Sigma=\begin{bmatrix}\mathcal{D}_o^\top\tilde{P} & \mathcal{A}_+^\top\tilde{P} & \mathcal{A}_-^\top\tilde{P} & \tilde{P}\end{bmatrix}\tilde{P}^{-1}\begin{bmatrix}\tilde{P}\mathcal{D}_o\\ \tilde{P}\mathcal{A}_+\\ \tilde{P}\mathcal{A}_-\\ \tilde{P}\end{bmatrix}^\top-\begin{bmatrix}\tilde{P}-Q_1 & -\Omega_+ & -\Omega_- & 0\\ -\Omega_+ & -Q_2 & -\Psi & 0\\ -\Omega_- & -\Psi & -Q_3 & 0\\ 0 & 0 & 0 & \Gamma\end{bmatrix}$$

then, by applying the Schur complement, the condition $\Sigma\preceq 0$ can be equivalently written as

$$\begin{bmatrix}\tilde{P}-Q_1 & -\Omega_+ & -\Omega_- & 0 & \mathcal{D}_o^\top\tilde{P}\\ \star & -Q_2 & -\Psi & 0 & \mathcal{A}_+^\top\tilde{P}\\ \star & \star & -Q_3 & 0 & \mathcal{A}_-^\top\tilde{P}\\ \star & \star & \star & \Gamma & \tilde{P}\\ \star & \star & \star & \star & \tilde{P}\end{bmatrix}\succeq 0 \tag{5.32}$$

Denote $U=PL_o\in\mathbb{R}_+^{n\times p}$. Recalling that $PD_o=PA_0-PL_oC$, then inequality (5.32) becomes linear in P, Q_1, Q_2, Q_3, Γ, Ω_+, Ω_-, Ψ and U:

$$\begin{bmatrix} \tilde{P}-Q_1 & -\Omega_+ & -\Omega_- & 0 & \mathcal{A}_0^\top \tilde{P} - C_1^\top \tilde{U}^\top \\ \star & -Q_2 & -\Psi & 0 & \mathcal{A}_+^\top \tilde{P} \\ \star & \star & -Q_3 & 0 & \mathcal{A}_-^\top \tilde{P} \\ \star & \star & \star & \Gamma & \tilde{P} \\ \star & \star & \star & \star & \tilde{P} \end{bmatrix} \succeq 0$$

Finally, since $\tilde{P} > 0$ and diagonal, the constraint $A_0 - L_o C \geq 0$ follows from $\tilde{P}\mathcal{A}_0 - \tilde{U}C_1 \geq 0$, which is also linear in $\tilde{P}$ and $\tilde{U}$, finalizing the proof. □

Interval predictor

Let the predictor gain (which replaces L in (5.24)) be L_p. By definition, $L_p = L_p^+ - L_p^- \in \mathbb{R}^{n\times p}$, for $L_p^-, L_p^+ \in \mathbb{R}_+^{n\times p}$. Then, under Assumption 5.2, let us denote $\overline{z}_k, \underline{z}_k$ as, respectively, the upper and lower predictive bounds of x_k, and evoke Lemma 5.1 and Assumption 5.2 to write

$$L_p^+ C\underline{z}_k - L_p^- C\overline{z}_k \leq L_p C z_k \leq L_p^+ C\overline{z}_k - L_p^- C\underline{z}_k \tag{5.33}$$

Hence, the relation above allows us to rewrite (5.26) by replacing the terms unavailable for prediction (*i.e.*, $Ly_k - Lv_k + w_k = LCx_k + w_k$) by their respective bounds:

$$\begin{aligned} \overline{z}_{k+1} =& D_p\overline{z}_k + \Delta A_+\overline{z}_k^+ + \Delta A_-\underline{z}_k^- + L_p^+C\overline{z}_k - L_p^-C\underline{z}_k + B_0u_k + \Delta B u_k^+ + \overline{w}_k \\ \underline{z}_{k+1} =& D_p\underline{z}_k - \Delta A_+\underline{z}_k^+ - \Delta A_-\overline{z}_k^- + L_p^+C\underline{z}_k - L_p^-C\overline{z}_k + B_0u_k - \Delta B u_k^- + \underline{w}_k \end{aligned} \tag{5.34}$$

where $D_p = A_0 - L_pC$. Hence, under assumptions 5.4–5.2, the IP (5.34) is composed solely by known terms.

In order to show that system (5.34) is cooperative, let us consider the prediction errors $\overline{\epsilon}_k = \overline{z}_k - z_k$ and $\underline{\epsilon}_k = z_k - \underline{z}_k$ and state the following result:

Lemma 5.5. *Let assumptions 5.1–5.4 be satisfied. Then, provided that $A_0 - L_pC$ is non-negative, the prediction errors are non-negative, i.e., $\underline{\epsilon}_k, \overline{\epsilon}_k \geq 0$ for all $k \in \mathbb{Z}_+$.*

Proof. The increments of the prediction errors $\overline{\epsilon}_k$ and $\underline{\epsilon}_k$ are given by

$$\overline{\epsilon}_{k+1} = D_p\overline{\epsilon}_k + r_{1,1} + \tilde{r}_{1,2}, \quad \underline{\epsilon}_{k+1} = D_p\underline{\epsilon}_k + r_{2,1} + \tilde{r}_{2,2} \tag{5.35}$$

where $r_{1,1}$ and $r_{2,1}$ are as in (5.29) and

$$\begin{aligned} \tilde{r}_{1,2} &= L_p^+C\overline{z}_k - L_p^-C\underline{z}_k - L_pCz_k + \overline{w}_k - w_k \\ \tilde{r}_{2,2} &= L_pCz_k - L_p^+C\underline{z}_k + L_p^-C\overline{z}_k + w_k - \underline{w}_k. \end{aligned}$$

Then, according to relations (5.27), (5.28) and (5.33), all inputs (the terms independent on $\underline{\epsilon}$ and $\overline{\epsilon}$) in (5.35) are non-negative. Thus, if $A_0 - L_pC$ is also non-negative, then $\overline{\epsilon}_k, \underline{\epsilon}_k \geq 0$ for all $k \in \mathbb{Z}_+$ under Lemma 5.2. □

Now, let us address the conditions for the stability of system (5.34). Since this system is nonlinear, these conditions will be derived by denoting $\mathcal{Z}_k = \text{vec}(\overline{z}_k, \underline{z}_k)$, which allows us to rewrite (5.34) as:

$$\mathcal{Z}_{k+1} = \left(\mathcal{A}_0 + \tilde{L}_p C_2\right)\mathcal{Z}_k + \mathcal{A}_+\mathcal{Z}_k^+ + \mathcal{A}_-\mathcal{Z}_k^- + \varrho_k, \tag{5.36}$$

where $\mathcal{A}_+$ and $\mathcal{A}_-$ are the same as in (5.30), $\tilde{L}_p = \text{diag}(L_p^-, L_p^-) \in \mathbb{R}^{2n\times 2p}$, $\varrho_k = \text{vec}(\overline{\varrho}_k, \underline{\varrho}_k)$ and

$$C_2 = \begin{bmatrix} C & -C \\ -C & C \end{bmatrix}, \qquad \begin{aligned} \overline{\varrho}_k &= B_0 u_k + \Delta B u_k^+ + \overline{w}_k, \\ \underline{\varrho}_k &= B_0 u_k - \Delta B u_k^- + \underline{w}_k. \end{aligned}$$

The next theorem presents conditions that any gain L_p has to fulfill in order to render IP (5.36) stable:

Theorem 5.5. *Let assumptions 5.4–5.2 be satisfied and let L_p be a given gain. If there exist a matrix $\tilde{P}_1 \in \mathbb{R}^{2n\times 2n}$, diagonal matrices $Q_1, Q_2, Q_3, \Omega_+, \Omega_-, \Psi, \Gamma \in \mathbb{R}^{2n\times 2n}$, such that the following linear matrix inequalities are verified:*

$$\begin{bmatrix} \tilde{P}_1 - Q_1 & -\Omega_+ & -\Omega_- & 0 & (\tilde{P}_1\mathcal{A}_0 + \tilde{P}_1\tilde{L}_pC_2)^\top \\ \star & -Q_2 & -\Psi & 0 & (\tilde{P}_1\mathcal{A}_+)^\top \\ \star & \star & -Q_3 & 0 & (\tilde{P}_1\mathcal{A}_-)^\top \\ \star & \star & \star & \Gamma & \tilde{P}_1 \\ \star & \star & \star & \star & \tilde{P}_1 \end{bmatrix} \succeq 0$$

$$\tilde{P}_1 \succ 0, \quad \Gamma \succ 0, \quad Q_1, Q_2, Q_3, \Omega_+, \Omega_- \geq 0,$$

$$Q = Q_1 + \min\{Q_2, Q_3\} + 2\min\{\Omega_+, \Omega_-\} > 0,$$

then system (5.36) is ISS with respect to the input $\varrho \in \ell_\infty^{2n}$.

Proof. The proof follows the same rationale as in Theorem 5.4 and is only sketched. By considering a Lyapunov function candidate given by $V_k = \mathcal{Z}_k^\top \tilde{P}_1 \mathcal{Z}_k$, one can show input-to-state stability, *i.e.*,

$$V_{k+1} - V_k = -\mathcal{Z}_k^\top Q \mathcal{Z}_k + \varrho_k^\top \Gamma \varrho_k$$

and the LMI conditions are stated by applying the Schur complement in the resulting stability conditions. □

Finally, sufficient conditions for the existence of a gain L_p providing non-negativity of

the matrix $A_0 - L_pC$ and stability of (5.36) simultaneously are obtained by the following corollary:

Corollary 5.2. *Let assumptions 5.1–5.4 be satisfied. If there exist diagonal matrices* $\tilde{P}_2$, Q_1, Q_2, Q_3, Ω_+, Ω_-, Ψ, $\Gamma \in \mathbb{R}^{2n\times 2n}$ *and* $U^+, U^- \in \mathbb{R}^{n\times p}$ *such that the following linear matrix inequalities are verified:*

$$
\begin{gathered}
\tilde{P}_2\mathcal{A}_0 - \tilde{U}^+C_1 + \tilde{U}^-C_1 \geq 0 \\
\begin{bmatrix}
\tilde{P}_2 - Q_1 & -\Omega_+ & -\Omega_- & 0 & (\tilde{P}_2\mathcal{A}_0 + \tilde{U}^-C_2)^\top \\
\star & -Q_2 & -\Psi & 0 & (\tilde{P}_2\mathcal{A}_+)^\top \\
\star & \star & -Q_3 & 0 & (\tilde{P}_2\mathcal{A}_-)^\top \\
\star & \star & \star & \Gamma & \tilde{P}_2 \\
\star & \star & \star & \star & \tilde{P}_2
\end{bmatrix} \succeq 0 \\
P_2 > 0, \quad \tilde{P}_2 = diag(P_2, P_2), \\
U^+ \geq 0, \quad \tilde{U}^+ = diag(U^+, U^+), \\
U^- \geq 0, \quad \tilde{U}^- = diag(U^-, U^-), \\
Q_1, Q_2, Q_3, \Omega_+, \Omega_- \geq 0, \quad \Gamma \succ 0 \\
Q = Q_1 + \min\{Q_2, Q_3\} + 2\min\{\Omega_+, \Omega_-\} > 0
\end{gathered}
\tag{5.37}
$$

then system (5.36) with gains $L_p^- = P_2^{-1}U^-$ *and* $L_p^+ = P_2^{-1}U^+$, *is an IP for system (5.24), i.e., the relation* $\underline{z}_k \leq x_k \leq \overline{z}_k$ *is satisfied for all* $k \in \mathbb{Z}_+$. *Furthermore, the system (5.36) is ISS with respect to the input* $\varrho \in \ell_\infty^{2n}$.

Proof. This proof follows directly from the implications of Lemma 5.5 and Theorem 5.5. Indeed, evoking [Efimov et al., 2013], the first constraint makes $A_0 - L_pC$ non-negative, thus satisfying the conditions on cooperativity imposed on Lemma 5.5.

Then, by introducing a new variable $U = P_2L_p$ and recalling that $U = U^+ - U^-$ by definition, this search for L_p is additionally constrained by the conditions stated in Theorem 2. This guarantees stability of (5.34), concluding the proof. □

5.3.2 Control design

In this section, the control design for the IP (5.34) is addressed. To this end, the following simplifying assumption is needed:

Assumption 5.6. *Let* $\Delta B = 0$.

Remark 5.4. *Assumption 5.6 is imposed to streamline the presentation. Indeed, if system (5.24) is polytopic with* $\Delta B \neq 0$, *the design conditions given in the following are affine and have to be checked over all of its vertices. This scenario requires an intricated presentation, which is to be avoided here.*

Then, if the control u_k in (5.36) is selected such as

$$u_k = K\mathcal{Z}_k + K_+\mathcal{Z}_k^+ + K_-\mathcal{Z}_k^- + R\mathcal{W}_k \tag{5.38}$$

where $\mathcal{W}_k = \text{vec}(\overline{w}_k, \underline{w}_k)$ and for some $K, K_-, K_+, R \in \mathbb{R}^{m\times 2n}$, the resulting dynamics is given by

$$\mathcal{Z}_{k+1} = \mathcal{K}\mathcal{Z}_k + \mathcal{K}_+\mathcal{Z}_k^+ + \mathcal{K}_-\mathcal{Z}_k^- + \tilde{D}\mathcal{W}_k \tag{5.39}$$

where $\tilde{D} = \mathbb{I}_{2n} + \mathcal{B}_0 R$, $\mathcal{K} = \mathcal{D}_z + \mathcal{B}_0 K$, $\mathcal{K}_+ = \mathcal{A}_+ + \mathcal{B}_0 K_+$ and $\mathcal{K}_- = \mathcal{A}_- + \mathcal{B}_0 K_-$, in which, for ease of notation, denote $\mathcal{B}_0 = [B_0^\top, B_0^\top]^\top$. This brings us to the following result:

Theorem 5.6. *Let assumptions 5.4–5.6 be satisfied. If there exist diagonal matrices P, Q_1, Q_2, Q_3, Γ, Ω_+, Ω_-, $\Psi \in \mathbb{R}^{2n\times 2n}$ and W_1, W_2, W_3, $W_4 \in \mathbb{R}^{m\times 2n}$ such that the following inequalities are verified*

$$\begin{bmatrix} P-Q_1 & -\Omega_+ & -\Omega_- & 0 & W_1^\top\mathcal{B}_0^\top + PD_z^\top \\ \star & -Q_2 & -\Psi & 0 & W_2^\top\mathcal{B}_0^\top + P\mathcal{A}_+^\top \\ \star & \star & -Q_3 & 0 & W_3^\top\mathcal{B}_0^\top + P\mathcal{A}_-^\top \\ \star & \star & \star & \Gamma & W_4^\top\mathcal{B}_0^\top + P \\ \star & \star & \star & \star & P \end{bmatrix} \succ 0$$

$$P > 0, \quad \Gamma \succ 0,$$

$$Q_1, Q_2, Q_3, \Omega_+, \Omega_- \geq 0,$$

$$Q = Q_1 + \min\{Q_2, Q_3\} + 2\min\{\Omega_+, \Omega_-\} > 0$$

then system (5.36) under control (5.38) with gains $K = W_1P^{-1}, K_+ = W_2P^{-1}, K_- = W_3P^{-1}, R = W_4P^{-1}$ is input-to-stable stable with respect to the inputs $\mathcal{W}_k$.

Proof. Let us consider a Lyapunov function candidate given by $V_k = \mathcal{Z}_k^\top P^{-1}\mathcal{Z}_k$, whose increments are given by

$$\begin{aligned} V_{k+1} - V_k = \\ = \begin{bmatrix} \mathcal{Z}_k \\ \mathcal{Z}_k^+ \\ \mathcal{Z}_k^- \\ \mathcal{W}_k \end{bmatrix}^\top \overbrace{\begin{bmatrix} \mathcal{K}^\top P^{-1}\mathcal{K} - P^{-1} + \tilde{Q}_1 & \mathcal{K}^\top P^{-1}\mathcal{K}_+ + \tilde{\Omega}_+ & \mathcal{K}^\top P^{-1}\mathcal{K}_- + \tilde{\Omega}_- & \mathcal{K}^\top P^{-1}\tilde{D} \\ \star & \mathcal{K}_+^\top P^{-1}\mathcal{K}_+ + \tilde{Q}_2 & \mathcal{K}_+^\top P^{-1}\mathcal{K}_- + \tilde{\Psi} & \mathcal{K}_+^\top P^{-1}\tilde{D} \\ \star & \star & \mathcal{K}_-^\top P^{-1}\mathcal{K}_- + \tilde{Q}_3 & \mathcal{K}_-^\top P^{-1}\tilde{D} \\ \star & \star & \star & \tilde{D}^\top P^{-1}\tilde{D} - \tilde{\Gamma} \end{bmatrix}}^{\tilde{\Pi}} \begin{bmatrix} \mathcal{Z}_k \\ \mathcal{Z}_k^+ \\ \mathcal{Z}_k^- \\ \mathcal{W}_k \end{bmatrix} \\ - \mathcal{Z}_k^\top\tilde{Q}_1\mathcal{Z}_k - \mathcal{Z}_k^{+\top}\tilde{Q}_2\mathcal{Z}_k^+ - \mathcal{Z}_k^{-\top}\tilde{Q}_3\mathcal{Z}_k^- + \mathcal{W}_k^\top\tilde{\Gamma}\mathcal{W}_k - 2\mathcal{Z}_k^\top\tilde{\Omega}_+\mathcal{Z}_k^+ - 2\mathcal{Z}_k^\top\tilde{\Omega}_-\mathcal{Z}_k^- - 2\mathcal{Z}_k^+\tilde{\Psi}\mathcal{Z}_k^-, \end{aligned}$$

for any $\tilde{\Psi} \in \mathbb{R}^{2n\times 2n}$, non-negative definite $\tilde{Q}_i, \tilde{\Omega}_+, \tilde{\Omega}_- \in \mathbb{R}^{2n\times 2n}$, $i = \overline{1,3}$, and positive definite

$\tilde{\Gamma}$. Then, if $\tilde{\Pi} \preceq 0$, we have that

$$V_{k+1} - V_k = -\alpha V_k + \mathcal{W}_k^\top \tilde{\Gamma} \mathcal{W}_k \tag{5.40}$$

meaning that V_k is an ISS Lyapunov function, provided that $\tilde{Q} = \tilde{Q}_1 + \min\{\tilde{Q}_2, \tilde{Q}_3\} + 2\min\{\tilde{\Omega}_+, \tilde{\Omega}_-\} \succeq \alpha P^{-1}$ (such an α always exists if $\tilde{Q} \succ 0$).

Decomposing $\tilde{\Pi}$ and applying the Schur complement (similarly as done for matrix Σ in the proof of Theorem 5.1), the LMIs presented in this theorem are obtained by multiplying the resulting inequality by $\mathrm{diag}\{P, P, P, P, P\}$ from the left and right, and by introducing slack variables $\Gamma = P\tilde{\Gamma}P$, $\Omega_+ = P\tilde{\Omega}_+P$, $\Omega_- = P\tilde{\Omega}_-P$, $\Psi = P\tilde{\Psi}P$, $\tilde{Q}_i = PQ_iP$, for $i = \overline{1,3}$, and by introducing new decision variables $W_1 = KP$, $W_2 = K_+P, W_3 = K_-P$ and $W_4 = RP$. □

As a direct implication of property (5.40), the following invariant set can be estimated:

$$\tilde{\mathbb{X}} = \left\{ x \in \mathbb{R}^{2n} : x^\top P^{-1} x \leq \alpha^{-1} \sup_{k \geq 0} \mathcal{W}_k^\top \tilde{\Gamma} \mathcal{W}_k \right\}$$

for $\alpha > 0$ given in the proof of Theorem 5.6, and is an invariant set for (5.39).

In accordance with item 4 in 5.2, the following assumption (which is conventional in MPC) is imposed:

Assumption 5.7. *Let $\mathbb{X}_f \times \mathbb{X}_f \subseteq \tilde{\mathbb{X}} \subseteq \mathbb{X} \times \mathbb{X}$ and in (5.38) $u_k \in \mathbb{U}$ provided that $\mathcal{Z}_k \in \mathbb{X}_f \times \mathbb{X}_f$.*

However, if the set $\mathbb{U}$ is ellipsoidal, one may relax Assumption 5.7 by adding additional LMIs:

Corollary 5.3. *Let there exist symmetric and positive definite matrices $\mathcal{U} \in \mathbb{R}^{m \times m}$ and $Z \in \mathbb{R}^{2n \times 2n}$ such that $\mathbb{U} = \{u \in \mathbb{R}^m : u^\top \mathcal{U} u \leq 1\}$ and $\mathcal{W}_k \in \{\mathcal{W} \in \mathbb{R}^{2n} : \mathcal{W}^\top Z \mathcal{W} \leq 1\}$, and the conditions of Theorem 4 be satisfied with additional inequalities:*

$$\begin{gathered} \frac{\eta}{\alpha\kappa}\Gamma \leq \min\{\kappa^{-1}Z, P\}, \; P \geq \kappa Z^{-1}, \\ \begin{bmatrix} \frac{\eta}{3}P & 0 & 0 & W_1^\top + W_2^\top \\ 0 & \frac{\eta}{3}P & 0 & W_3^\top - W_1^\top \\ 0 & 0 & \frac{\kappa}{3}P & W_4^\top \\ W_1 + W_2 & W_3 - W_1 & W_4 & \mathcal{U}^{-1} \end{bmatrix} \geq 0 \end{gathered} \tag{5.41}$$

for some constants $\eta > 0$ and $\kappa > 0$, then control (5.38) satisfies the constraint $u_k \in \mathbb{U}$ for all $\mathcal{Z}_k \in \mathbb{X}_f \times \mathbb{X}_f$.

Proof. This proof follows the same lines as the one of Corollary 5.1. However, in this case, the control law is designed for $\mathcal{Z}_k$ instead of the interval center. To highlight the different steps, note that $\mathcal{Z}_k = \mathcal{Z}_k^+ - \mathcal{Z}_k^-$. Therefore, the control (5.38) can be rewritten as

$$u_k = (K + K_+)\mathcal{Z}_k^+ + (K_- - K)\mathcal{Z}_k^- + R\mathcal{W}_k,$$

and thus the condition $u_k \in \mathbb{U}$ takes the form:

$$\begin{bmatrix} \mathcal{Z}_k^+ \\ \mathcal{Z}_k^- \\ \mathcal{W}_k \end{bmatrix}^\top \begin{bmatrix} K + K_+ \\ K_- - K \\ R \end{bmatrix} \mathcal{U} \begin{bmatrix} K + K_+ \\ K_- - K \\ R \end{bmatrix}^\top \begin{bmatrix} \mathcal{Z}_k^+ \\ \mathcal{Z}_k^- \\ \mathcal{W}_k \end{bmatrix} \leq 1.$$

If $\mathcal{Z}_k \in \tilde{\mathbb{X}}$, then obviously $\mathcal{Z}_k^+, \mathcal{Z}_k^- \in \tilde{\mathbb{X}}$. The remainder of the proof remains identical. □

5.3.3 Numerical illustration

To illustrate the developments of this section, consider the following LPV system:

$$\begin{aligned} x_{k+1} &= \begin{bmatrix} 0.5 & 0.6 + \theta_k \\ \theta_k & 0.3 \end{bmatrix} x_k + \begin{bmatrix} 0 \\ 1 \end{bmatrix} u_k + w_k \\ y_k &= \begin{bmatrix} 0 & 1 \end{bmatrix} x_k + v_k \end{aligned} \tag{5.42}$$

where $x_k = \text{vec}(x_1, x_2) \in \mathbb{R}^2$, $\theta_k \in \Theta = [-0.2, 0]$ and the disturbances are assumed to be enclosed in $\mathbb{W} = [-0.1, 0.1]^2$, $\mathbb{V} = [-0.5, 0.5]$.

Solving the conditions presented in this chapter, the following gains are obtained for the pair IO/IP:

$$L_o = \begin{bmatrix} 0.4856 \\ 0.2501 \end{bmatrix}, \quad L_p = \begin{bmatrix} 0.3182 \\ 0.1481 \end{bmatrix},$$

while the controller gains were obtained as

$$K_0 = \begin{bmatrix} 0.0004 & -0.3034 \end{bmatrix}, \quad K_1 = \begin{bmatrix} 0.0999 & 0.0008 \end{bmatrix}, \quad K_2 = \begin{bmatrix} -0.1011 & 0.0015 \end{bmatrix}.$$

For simulation purposes, the IO is initialized with $\underline{x}_0 = [-10, 9]$ and $\overline{x}_0 = [-9, 10]$ (for simplicity, the IP is initialized with the same values), and $\theta_k = -|0.2 \sin(k)|$. Figures 5.4 and 5.5 illustrate, respectively, the evolution of the states of (5.42) and the pair IO/IP, and the evolution of the control input.

As it can be seen, the stabilization of (5.42) is successful and the computed bounds, for both IO and IP, respect relations (5.2) and (5.3).

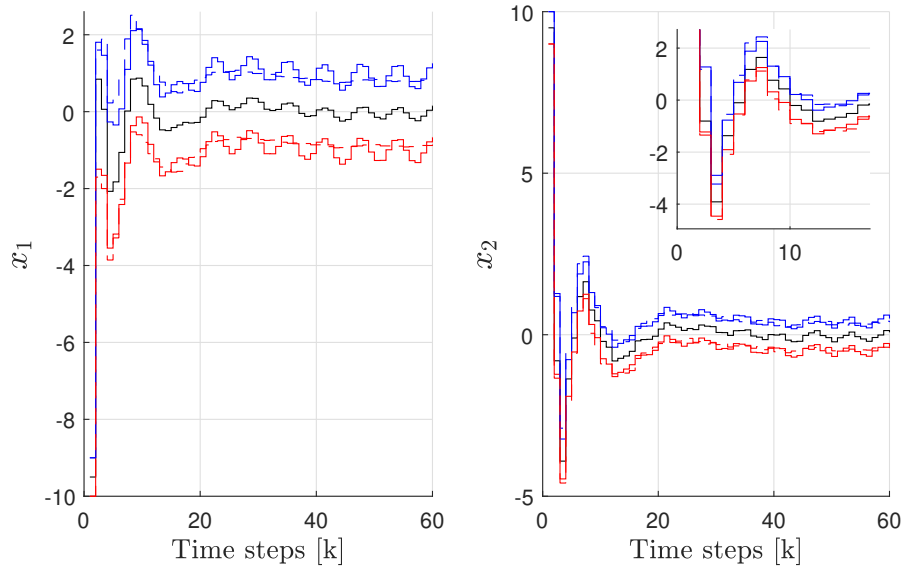

Figure 5.4: Evolution of the states. Legend – continuous lines: IO, dashed lines: IP, black lines: real system, blue lines: upper estimates, red lines: lower estimates.

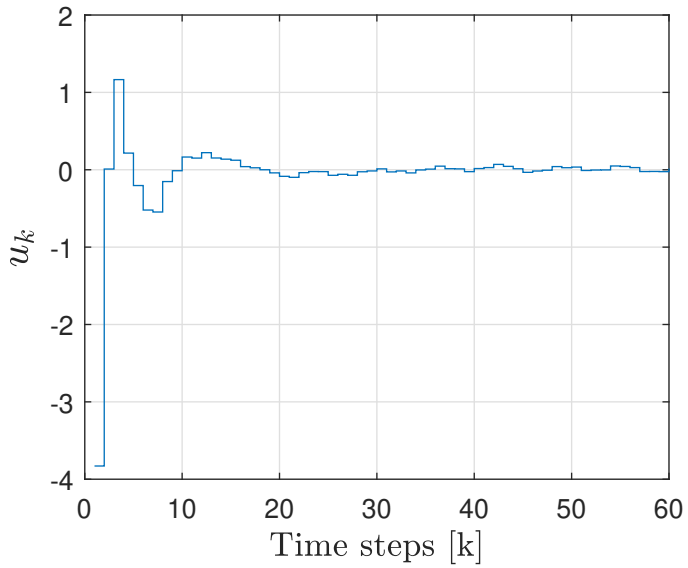

Figure 5.5: Evolution of the control input.

5.4 Design of the predictive controllers

In the previous sections, the interval estimators that will be used in the MPC design have been presented. Also, conditions for the existence of a feedback control ensuring ISS, for each one of the cases considered, was derived. To synthesize the results for the both cases presented, the interval observer and predictor routines will be abbreviated as $\mathfrak{O}(z_k, y_k, u_k)$ and $\mathfrak{P}(z_k, u_k)$, where $z_k = \text{vec}(\underline{x}_k, \overline{x}_k)$ or $z_k = \text{vec}(\underline{z}_k, \overline{z}_k)$, respectively.

Initialization

Consider the initialization of the MPC algorithm (analogously to constraint (5.5a)). As it was discussed in the previous sections, the IO uses the available measurement to update the set-membership of the states at every decision instant k, and thus can be used to initialize the predictor. However, it is worth noticing that the IO depends on the bounds of the measurement noise: if these bounds are too large, the obtained envelope of estimates can be more conservative. In this sense, the first step of the prediction can offer a more accurate estimation, as shown in Figure 5.6. Therefore, the MPC algorithm will be initialized using the following combined estimates:

$$\overline{\hat{x}}_k = \min\{\overline{x}_k, \overline{z}_{k-1,1}\}, \quad \underline{\hat{x}}_k = \max\{\underline{x}_k, \underline{z}_{k-1,1}\}.$$

The optimal control problem

Analogously to (5.4), the optimal control problem (OCP) for the IO-MPC can be formulated as follows:

$$V_N = \arg\min_{\mathcal{S}_N} V_N(z_{k,0}, \ldots, z_{k,N}, \mathcal{S}_N) \tag{5.43}$$

where $z_{k,i} \in \mathbb{R}^{2n}$ are the predicted state variables (containing both upper and lower bounds). This OCP must be solved under the following constraints:

$$z_{k,0} = \text{vec}(\underline{\hat{x}}_k, \overline{\hat{x}}_k), \tag{5.44a}$$

$$z_{k,i+1} = \mathfrak{P}(z_k, s_i), \tag{5.44b}$$

$$z_{k,i+1} \in \mathbb{X} \times \mathbb{X}, \quad s_i \in \mathbb{U}, \tag{5.44c}$$

$$z_{k,i+N} \in \mathbb{X}_f \times \mathbb{X}_f. \tag{5.44d}$$

where $\mathfrak{P}$ is the predictor used: IP (5.14) for the LTI case, and IP (5.36) for the LPV case.

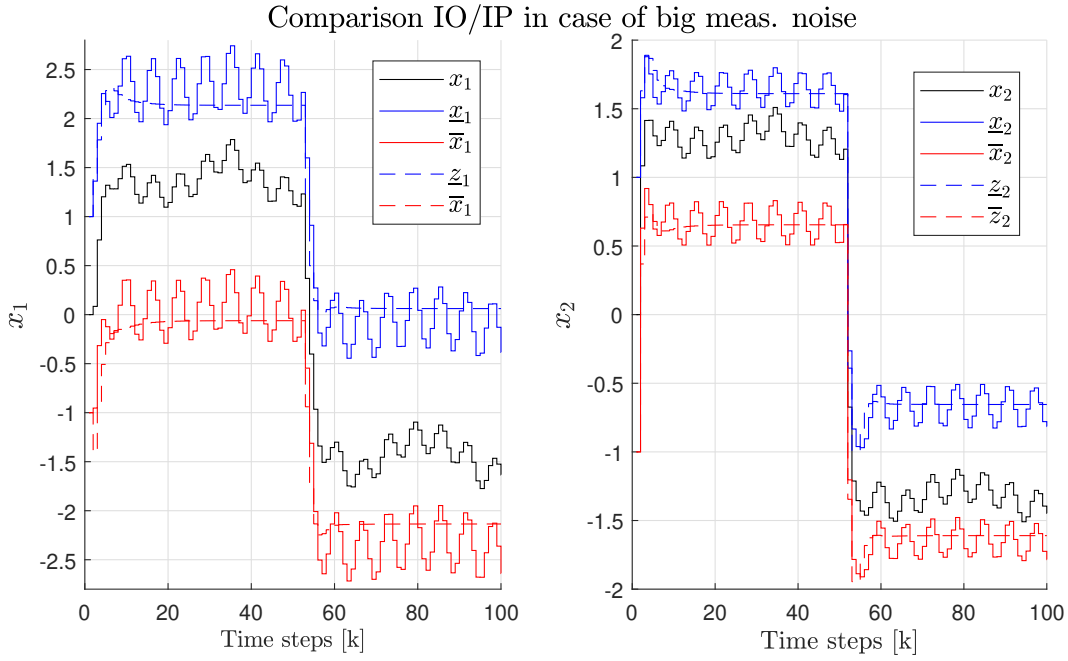

Figure 5.6: Comparison of the trajectories of the IO and IP, for model (5.42), in the case of higher measurement noises. In this simulated scenario, the state variable x_2 (left plot) is considered as available for measurement. As it can be seen in several time instants, due to this bigger measurement noise, the IP offers less conservative bounding estimates.

Remark 5.5. *Note that for the LTI case, constraint* (5.44d) *can be simplified and, instead of requiring the whole predicted interval* $z_{k,i+N}$ *to belong to* $\mathbb{X}_f \times \mathbb{X}_f$*, only that the interval center must do so, i.e.,* $z^\star_{k,i+N} \in \mathbb{X}_f$*.*

The cost function V_N is defined as

$$V_N = V_f(x_{k,N}) + \sum_{i=0}^{N-1} \left(x_{k,i+1}^\top \Psi_2 x_{k,i+1} + s_i^\top \Psi_3 s_i \right),$$

where the terminal cost V_f and the terminal set $\mathbb{X}_f$ are the stabilizing ingredients discussed, for each case, in the previous sections. The positive-definite matrices Ψ_2, Ψ_3 represent the stage costs on the state and control input, respectively. Finally, the proposed IO-MPC algorithm is described in Algorithm 1:

Algorithm 1 IO-MPC

Offline: Solve the appropriate LMIs to design the pair IO/IP and the respective controller. Estimate the terminal set $\mathbb{X}_f$ and select $\Psi_1 = P^{-1}$, $\Psi_2 \leq \frac{\alpha}{2}P^{-1}$, and $\Psi_3 \leq \frac{\alpha}{8}P^{-1}$.
Input: Initial conditions $\underline{x}_0, \overline{x}_0$, prediction horizon N.
Online:

1: **for** each decision instant $k \in \mathbb{Z}_+$ **do**
2: Measure y_k and update the IO.
3: Initialize the IP such as $z_{k,0} = \text{vec}(\underline{\hat{x}}_k, \overline{\hat{x}}_k)$.
4: Solve OCP (5.43) under constraints (5.44a)–(5.44d).
5: Assign $u_k = s_0^k$ and apply it to system (5.1).
6: **end for**

Theorem 5.7. *Let $[\underline{x}_0, \overline{x}_0] \subset \mathbb{X}$ and assumptions 5.1–5.7 be satisfied with $[\underline{w}_{k+1}, \overline{w}_{k+1}] \subseteq [\underline{w}_k, \overline{w}_k]$ for all $k \in \mathbb{Z}_+$. Then, following Algorithm 1, the closed-loop system composed by (5.1), $\mathfrak{O}(z_k, y_k, u_k)$ and $\mathfrak{P}(z_k, u_k)$ has the following features:*

1. *Recursive feasibility of reaching the terminal set in N steps;*

2. *Constraint satisfaction.*

3. *ISS of the dynamics of $\mathfrak{P}$ in $\mathbb{X}_f$ and practical ISS for system (5.1);*

Proof. Suppose that for any $[\underline{x}_0, \overline{x}_0] \subset \mathbb{X}$ a solution of OCP (5.43) exists, *i.e.*, there is a sequence of inputs $\mathcal{S}_N^0$ that leads the trajectories of $\mathfrak{P}$ to $\mathbb{X}_f$. This means that for $k = 0$, by applying $u_k = s_0^k$, we ensure that $[\underline{z}_{k+1,i}, \overline{z}_{k+1,i}] \subset \left[\underline{z}_{k,i+1}, \overline{z}_{k,i+1}\right] \subset \mathbb{X}$ at least for $i = 0$ and also $\left[\underline{z}_{k,N}, \overline{z}_{k,N}\right] \subset \mathbb{X}_f$. Then, following Algorithm 1, the procedure can be iteratively repeated for $k \in \mathbb{Z}_+$ since $[\underline{w}_{k+1}, \overline{w}_{k+1}] \subseteq [\underline{w}_k, \overline{w}_k]$. Moreover, the control sequence $\mathcal{S}_N$ that steers $\left[\underline{z}_{k,0}, \overline{z}_{k,0}\right]$ to $\mathbb{X}_f$ also steers x_k (as a consequence of (5.3)). This implies point *(1)*.

For point *(2)*, the ISS property in $\mathbb{X}_f$ follows directly by the selection of the terminal ingredients (the choice of Ψ_j, $j = \{1, 2, 3\}$, as given in Algorithm 1) which, due to the results of theorems 5.3 and 5.6 (for LTI and LPV systems, respectively), guarantees that

$$V(z_{k+1,N}) - V(z_{k,N}) \leq d_k^\top \tilde{\Gamma} d_k - \ell(z_{k,N}, s_N)$$

where d_k is the concerned disturbances depending on the case (either $w_k^\star$ or $\mathcal{W}_k$ for the LTI or LPV case, respectively). Note that the matrix $\tilde{\Gamma}$ are the same appearing in results (5.20) and (5.40). Furthermore, the practical ISS follows from the fact that

$$|x_k| \leq |z_k|, \quad |z_0| \leq |\underline{z}_0| + |\overline{z}_0| \leq |x_0| + c$$

where $c = |\underline{x}_0| + |\overline{x}_0|$.

For point *(3)*, we have that the solution of OCP (5.43) implies that $x_k \in \left[\underline{z}_{k,k+1}, \overline{z}_{k,k+1}\right] \subset \mathbb{X}$ due to relation (5.3) and $u_k = s_0^k \in \mathbb{U}$, under Assumption 5.3 (or Assumption 5.7 for the LPV case) and the discussed features of each possible set $\mathbb{X}_f$. □

5.5 Complexity and performance

The constraints imposed on the OCP (5.43) is similar for both LTI and LPV cases, and scales with $\mathcal{O}(Nn)$. Indeed, assuming that the number of hyperplanes needed to define sets $\mathbb{X}, \mathbb{U}$ and $\mathbb{X}_f$ depends linearly on n and $m = n$, the (worst-case) number of variables describing constraints (5.44a)–(5.44d) is $8Nn$ for the LTI case, and $10Nn$ for the LPV case.

It is worth noticing that, for both LTI and LPV cases, the aforementioned complexity is fixed, which is an interesting feature of the proposed methodology.

The LTI case

For the linear case, the OCP (5.43) is a quadratic programming (QP) problem, being very similar to the nominal MPC. If compared to solutions based on Tubes [Mayne et al., 2006, Mayne et al., 2009] or MHE [Chisci and Zappa, 2002], the proposed method offers many advantages: *(i)* it does not require any steady-state assumption for the observer nor any further development for compensating the initial uncertainty, since this is automatically handled by the convergence of the pair IO/IP, *(ii)* the scheme is constructive, since all gains are obtained by the solution of LMIs (it should be noted that a naive selection of observer/controller gains in approaches that uses set approximations for propagating the uncertainties might dramaticallly influence the performance of the MPC, see the discussion in [Chisci and Zappa, 2002, Sec. 5.2] and the comparison below), *(iii)* thanks to the guaranteed enclosing $x_k \in [\overline{x}_k, \underline{x}_k]$, if $[\underline{x}_0, \overline{x}_0] \in \mathbb{X}$ and if Assumption 5.3 is satisfied, the feasible region (w.r.t. $z_k^\star$) is similar to the one of the nominal MPC.

The LPV case

Approaches using zonotopic estimation often require extra procedures to limit their increasing complexity, as well as real-time knowledge on the scheduling parameter [Wang et al., 2019].

Techniques such as presented in [Ding et al., 2018] [Ding and Pan, 2016], that also assume no measurement of θ_k, are computationally more expensive. Indeed, the authors fix a prediction horizon $N = 1$ and impose a min-max optimization problem accounting for all vertexes of the polytopic system, aiming to obtain a robust prediction. This implementation requires

several relaxations for numerical tractability and the price is, obviously, an increased number of variables and conservativeness.

5.6 Numerical examples

In this section, numerical simulations are presented to illustrate the MPC algorithms proposed in this chapter. All simulations have been implemented in MATLAB 2017a, using an Intel i7-8565U processor (1.8GHz) and 16GB RAM. The toolboxes YALMIP [Löfberg, 2004], MPT3 [Herceg et al., 2013] and PnPMPC [Riverso et al., 2013] were used. The solvers employed in the optimization routines are discriminated in each case study.

5.6.1 The LTI case

To illustrate the proposed MPC algorithm, consider the CSTR model given as an example in Section 5.2.4. In this scenario, the constraints on state and control are given by $\mathbb{X} = [-2, 2] \times [-10, 5]$ and $\mathbb{U} = [-4.5, 4.5]$, respectively. The disturbance sets are assumed to be given by $\mathbb{W} = [-0.02, 0.02] \times [-0.2, 0.2]$ and $\mathbb{V} = [-0.3, 0.3]$.

The prediction horizon is selected as $N = 10$, and weighting matrices $H = 1000\mathcal{I}_2$ and $R = 0.001$. For the IO-MPC, the terminal set and the controller $K_f = [-6.99, -0.50]$ are obtained by solving the conditions given in Proposition 5.3, whereas the terminal cost is defined as its correspondent Lyapunov function.

Comparison with Tube-MPC

For comparison purposes, we have implemented the Tube-based MPC from [Mayne et al., 2009]. For this implementation, a Luenberger observer was designed by pole placement (for the pair $(A^\top, C^\top)$). The terminal set and the static controller $K_{LQ} = [5.58, 0.45]$ are obtained by computing the associated LQR with weighting matrices $Q_{LQ} = 0.1\mathcal{I}_n$ and $R_{LQ} = 0.1$.

Figure 5.7 shows the comparison of the feasible sets for both techniques. As expected, due to the constraint tightening used to guarantee robust constraint satisfaction in the Tube-MPC, the obtained feasible region for the IO-MPC is much wider (and similar to the nominal MPC). Furthermore, Figure 5.7 also illustrates the impact of a naive design of the gains for the Tube-MPC. Clearly, the obtained regions are much different depending where the closed-loop poles of the terminal controller/observer are placed, whereas our method has all gains readily obtained by conditions in the form of LMIs, which reduces the number of parameters to be tuned.

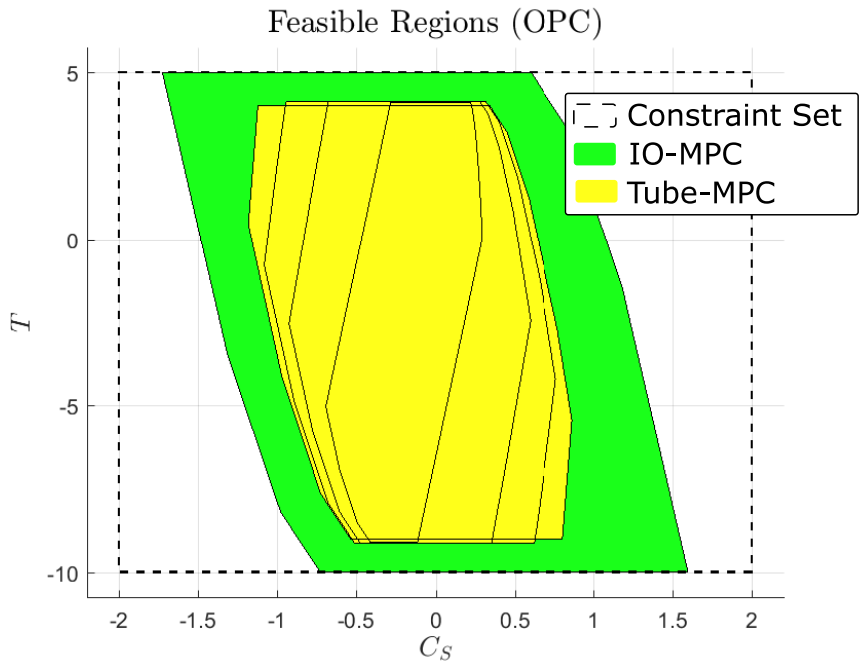

Figure 5.7: Comparison of the feasible regions (approximations obtained by ray-shooting using YALMIP [Löfberg, 2004]). For the Tube-MPC, these regions were obtained by placing different poles when designing the Luenberger observer.

For the Tube-MPC, we selected the Luenberger observer which offered the biggest feasible region (by trial-and-error), which is initialized with $\hat{x}_0 = (-0.65, -7)^\top$, while the IO is initialized with $\underline{x}_0 = (-0.8, -7.8)^\top$ and $\overline{x}_0 = (-0.5, -6)^\top$. The reactor is then simulated over a time window $T_{simu} = 60$ time steps, considering several initial conditions satisfying $x_0 \in [\underline{x}_0, \overline{x}_0]$ (note that this setup is feasible for both techniques) and several realizations of w_k and v_k. For comparison purposes, let us define a performance index $J_p = \sum_{k=0}^{T_{simu}} x_k^\top x_k + u_k^\top u_k$. Table 5.1 illustrates the average results for 25 simulation runs.

Table 5.1: Comparison between IO-MPC and Tube-MPC (time simulations)

	IO-MPC	**Tube-MPC**
Perf. index J_p	232.650	253.560
OCP sol. time	0.0265	0.0524
Final values (around origin)	$[-0.070, 0.074] \times [-0.993, 0.993]$	$[-0.047, 0.057] \times [-1.792, 1.743]$

These results show that, even for a region where both techniques are feasible, the IO-MPC shows a faster solution of the optimization problem, as well as a better performance index. This latter fact was expected, since the control constraint was not tightened, meaning that the MPC algorithm can use its full range to achieve faster stabilization. However, since the Tube-MPC is designed to control the trajectories of the observer, it stabilizes the system

closer to the origin, whereas the IO-MPC can only drive the envelope of trajectories close to it.

Simulation results

Let us initialize the IO with $\overline{x}_0 = (1.2, -8)^\top$ and $\underline{x}_0 = (1, -9)^\top$. Notice that this region is not feasible at all for the Tube-MPC presented previously. For simplicity, let $[\underline{z}_0, \overline{z}_0] = [\underline{x}_0, \overline{x}_0]$ and, again, let the reactor be simulated considering several $x_0 \in [\underline{x}_0, \overline{x}_0]$.

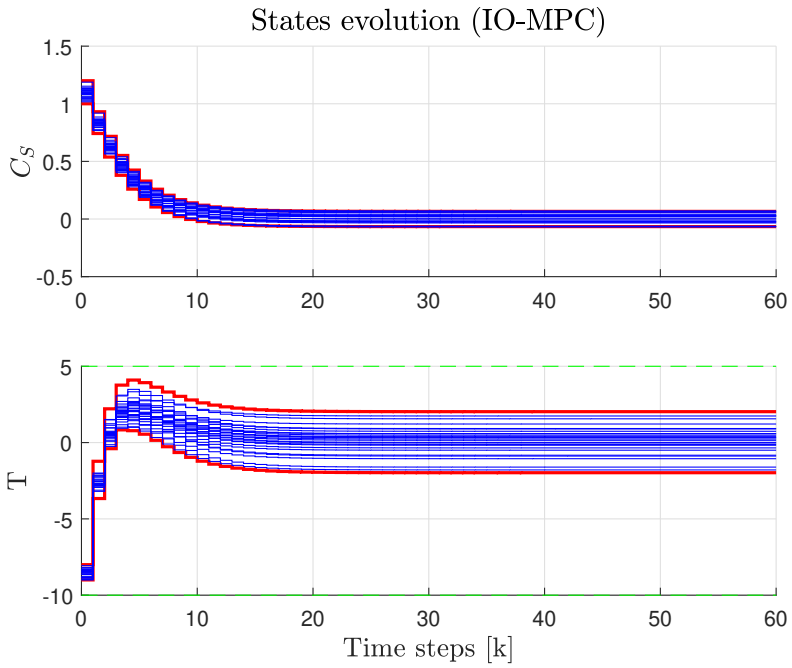

Figure 5.8: Evolution of the states under the IO-MPC.

This simulation scenario is shown in Figure 5.8, for several realizations of the perturbations v_k and w_k. As it can be seen, all trajectories of the perturbed system satisfied the constraints and were stabilized close to the origin. Furthermore, it is worth noticing that the system trajectories are able to get very close to the constraint boundaries, indicating very low conservativeness. Finally, Figure 5.9 shows the input applied to the system.

5.6.2 The LPV case

To illustrate the proposed MPC algorithm, consider the model (5.42), given in Section 5.42 with $\theta_k \in \Theta = [-0.1, 0.1]$, $w_k \in [-0.1, 0.1] \times [-0.1, 0.1]$, and $v_k \in [-0.1, 0.1]$. The constraint sets are defined as $\mathbb{X} = [3, -12] \times [3, -12]$ and $\mathbb{U} = [-2, 2]$. Clearly, this system

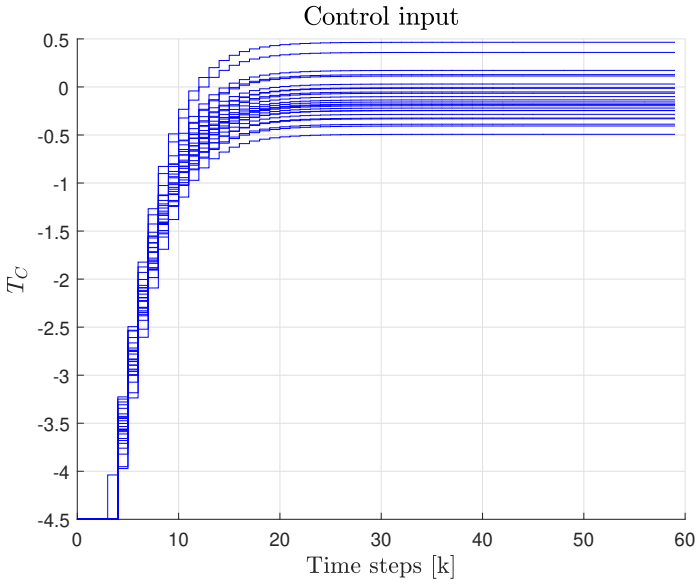

Figure 5.9: Control input under the IO-MPC

can be rewritten as (5.42) with the matrices

$$A_0 = \begin{bmatrix} 0.5 & 0.6 \\ 0 & 0.3 \end{bmatrix}, \quad A(\theta) = \begin{bmatrix} 0 & \theta \\ \theta & 0 \end{bmatrix}.$$

and interpolating functions $\lambda_1 = \frac{\theta - \underline{\theta}}{\overline{\theta} - \underline{\theta}}$ and $\lambda_2 = \frac{\overline{\theta} - \theta}{\overline{\theta} - \underline{\theta}}$. We considered initial conditions for the IP/IO as $\overline{x}_0 = \text{vec}(-7, -12)$ and $\underline{x}_0 = \text{vec}(-6, -10)$ and several initial conditions for (5.42) satisfying $x_0 \in [\underline{x}_0, \overline{x}_0]$. We ran 100 simulations of this scenario, each with a time span of $T = 20$ steps, considering several realizations of θ_k, w_k, and v_k.

The gains for the IP and the IO, obtained by solving the offline LMIs of Section III, are $L_o = [0.489,\ 0.1945]$ and $L_p = [0.232,\ 0.122]$. For the MPC algorithm, we solve the conditions of Theorem 5.6 to obtain $\alpha = 1.107$ and

$$P = \begin{bmatrix} 1.79 & \star \\ -0.285 & 1.150 \end{bmatrix}, \quad \Gamma = \begin{bmatrix} 11.57 & \star \\ -1.358 & 3.63 \end{bmatrix},$$

and thus we can estimate $\mathbb{X}_f$ and select Ψ_2. Finally, we select $N = 10$ and $\Psi_3 = 0.001$.

Fig. 5.10 illustrates the trajectories of system (5.42) and the IP (5.36), in contrast to the constraint set. It is worth noticing that all constraints were respected, including those on the unmeasured state. The IP even reaches the boundary of constraint, indicating low conservativeness.

The control input computed by solving OCP (5.43) also fulfilled the constraints, as shown in Fig. 5.11. Finally, Fig. 5.12 shows the estimated feasible regions for the initial conditions of IP (5.34). We did not observe any improvement after $N = 10$. The mean computation time

for solving OCP (5.43) was 0.22 ± 0.0313 second/step, with a maximum of 0.7725 second. An interior-point method provided by the *fmincon* solver was used to solve the optimization problem.

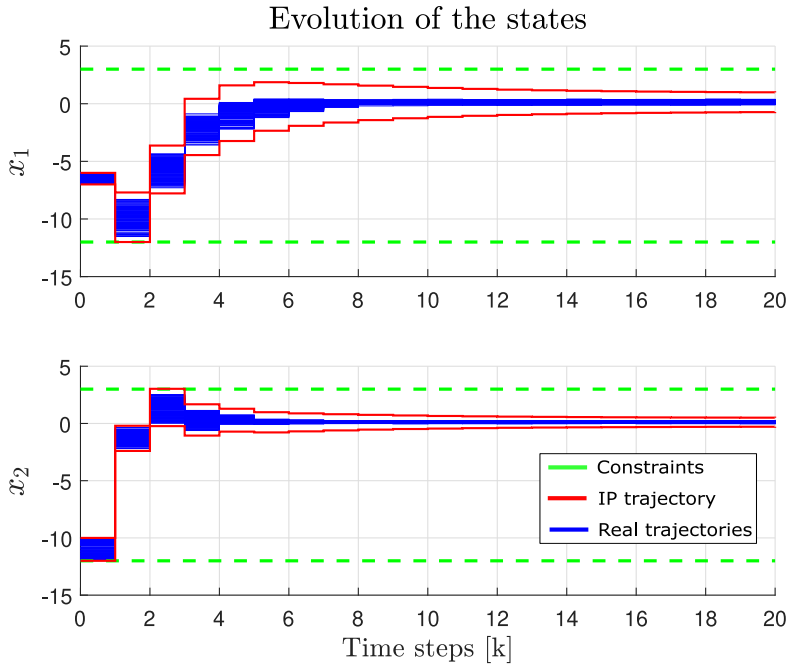

Figure 5.10: Trajectories of the system and IP in contrast to the constraint set.

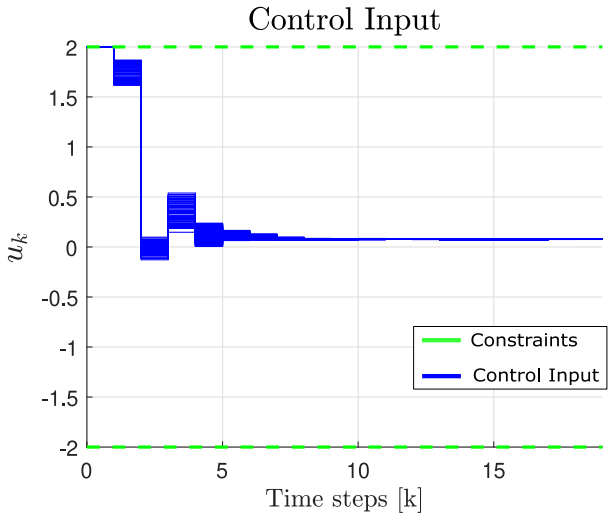

Figure 5.11: Evolution of the control inputs

5.7 Part conclusion

This part of the thesis was devoted to the robust output feedback MPC problem, applied to both LTI and LPV cases. New interval estimators (both observers and predictors) were

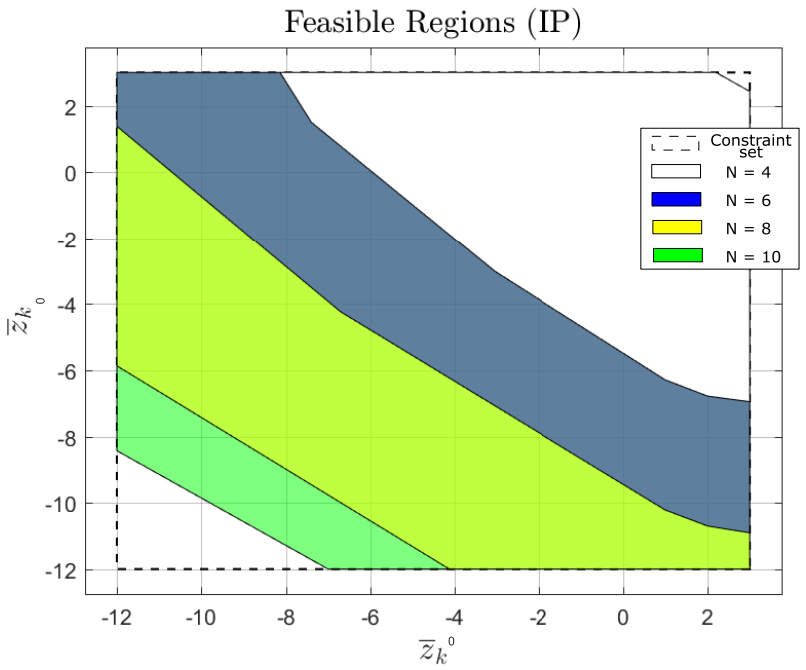

Figure 5.12: Comparison of the feasible regions for prediction horizon with different lengths ($N \in \{4, 6, 8, 10\}$). These regions were computed using YALMIP [Löfberg, 2004] and MPT [Herceg et al., 2013].

proposed, as well as their corresponding stabilizing controllers. All design conditions are formulated as offine LMIs.

These new estimators were incorporated into the classic MPC algorithm: the interval observer updates the set-membership of the states at every decision instant, and the interval predictor then casts an envelope containing all possible trajectories of the disturbed system into the prediction horizon. Using this feature, constraints on state are verified with a low computational burden.

Due to the form of these estimators, the stability analysis of the MPC algorithm is carried out following the well-known stabilizing ingredients. Numerical examples were used to illustrate both methodologies.

Part 4:

General Conclusions and Outlooks

Chapter 6

General Conclusions and Outlooks

Control and estimation of co-populations

Conclusions

In this thesis, the control and estimation problems were considered for two different models of microbial growth in continuous culture: one describing the competition of two species for a single limiting substrate, and another describing a mutualistic relationship between a producer and a cleaner strain.

These systems are structurally similar and highly complex: the dynamics of the substrates and the species are coupled by nonlinear functions of both variables, they are constrained both in states (since each state relates to a concentration, which characterizes such systems as *positive*) and control (the actuating variables take only non-negative values), and are possibly uncertain. These particularities lead to several challenges when analyzing and designing the respective state estimators and controllers, since many of the tools available are not applicable in these scenarios.

Concerning the estimation problem for such systems, the following topics have been addressed:

1. Observability analysis considering the availability of two realistic measurements (the total biomass and a fluorescent reporter). Since the first measurement is more common in real experiments, observability is also studied considering solely this measurement.

2. Design of state observers for both cases.

3. The advantage of having both measurements, in terms of the needed model parameters, is also discussed.

Indeed, if both measurements are available, it has been shown that the system is observable, whereas the case in which only the total biomass is available leads to merely detectability. The proposed state observers are based on the use of differentiators (for the first scenario), and by using nonlinear estimators with output injection (for the second scenario).

Although the observers based on output injection show better performance (as investigated through numerical experiments), they require knowledge of all parameters of the model. If

these parameters are not perfectly known, more errors will be introduced in the resulting estimation. On the other hand, the observers based on the differentiators are intrinsically sensitive to noise.

Concerning the control problem, the following topics have been tackled:

1. Robust control of the competition model (2.1), considering that all parameters are unknown but belonging to bounded interval;

2. Design of a control methodology for the COSY model (2.4), considering that all parameters are perfectly known.

For the first item above, the robust control architecture is composed of several discontinuous control laws that explicitly take into account the known bounds on the parameters. In fact, the dilution rate is actuated by a single control law, aiming to stabilize the concentration of a first species, whereas the one concerning the inflow substrate concentration is switched between to different control goals. This is due to the fact that, depending on the concentration of the substrate, the system might loose its controllability. Then, first this problem is avoided and, once a certain condition is reached, the goal then becomes the stabilization of the remain species.

For the microbial consortium described by the COSY model, however, the problem is more intricate. Indeed, the presence of acetate (excreted by the producer strain) further constrains the control. The concentration of the producer strain is regulated by state-feedback through the dilution rate, whereas the concentrations of glucose and acetate are then steered to specific levels, using the respective inflow concentration. These specific levels are selected in order to guarantee satisfaction of three constraints, which basically guarantee controllability and the permanence of the cleaner strain (*i.e.*, in a concentration higher than zero).

Perspectives

A natural continuation of the theoretical work presented in this thesis is the design of a robust control algorithm for the COSY model. Indeed, the control laws developed in Chapter 4 are highly dependent on the parameters of model (2.4). This could be done, similarly as for the competition model, by using sliding-mode controllers that explicitly take the bounds of the parameters into account. Clearly, a more intricate stability analysis would be necessary.

Another interesting directions are *(i)* developing also a control law for B_c, aiming to stabilize it at a certain level (this would reduce the consumption of glucose by this species and possibly enhance the process yield), *(ii)* developing an extra layer in the control architecture to encompass also some optimization criteria, *(iii)* couple the developed estimation algorithms to these control architectures, what would culminate in a methodology closer to the real-world.

Since the developments presented in this manuscript were theoretical, an interesting perspective is the implementation of the proposed algorithms into a real experimental set-up. This would allow, for instance, a better understanding of the levels of uncertainty present (both parametric and noise-related), as well as the variability of parameters. Also, since real controller would have to undergo discretization schemes, practical experiments would also permit the evaluation of having actual sensors and non-ideal actuators.

Robust output feedback MPC

Conclusions

The control of constrained system is a challenging problem in the control literature. This fact led MPC to be an interesting topic and several extensions were reported in the literature. In this framework, the second part of this thesis dealt with the problem of robust output feedback MPC.

Indeed, by merging the classic MPC algorithm with interval estimators (an observer and a predictor), the algorithm proposed in this thesis guarantees both robust constraint satisfaction and recursive feasibility, at a low computation complexity and ease of implementation. Two broad classes of systems are encompassed by this algorithm: linear and linear parameter varying systems (and also to the case of linear time-delayed systems, whose results were not reported in this manuscript).

For each of the cases mentioned above, several design conditions for these interval estimators, as well as for their respective feedback control, were given in the form of linear matrix inequalities. This is an interesting feature, especially if compared to other solutions available (for instance, Tube-MPC or the ones using estimation techniques such as moving-horizon or zonotopes) which rely on complex set-algebraic computations, since LMIs are widely used and easy to implement and verify.

Although the design conditions given for the interval observer are not restrictive, a drawback of this methodology concerns the design of the interval predictor: due to its structure, it may be hard to find proper gains that guarantee its stability. This fact possibly shrinks the range of possible applications.

Perspectives

The versatility of the interval estimators used in the proposed IO-MPC algorithm offers some interesting research perspectives. For instance, extra estimation techniques could be used to identify parameters and exogenous inputs and enhance the accuracy of the interval

estimation in real-time. Clearly, this would imply a reduction in conservatism and better performance.

Also, slightly out of the scope of the MPC, it would be interesting to investigate if the robust constrained control problem could be solved using solely the interval observers. Obviously, an IO would allow the computation of the interval estimates merely *one step ahead*, instead of predicting it over an entire prediction horizon of arbitrary length. Although this fact possibly reduces the feasible region, it would alleviate the drawback of the design of the interval predictor mentioned above, enlarging the possible applications.

Appendices

Appendix A

Preliminaries on input-to-state stability

Continuous-time case

Consider a general, continuous-time system given by

$$\dot{x}(t) = f(x(t), u(t)) \tag{A.1}$$

where $x(t) \in \mathbb{R}^n$ is the state, $u(t) \in \mathbb{R}^m$ is in the input, $u \in \mathcal{L}_\infty$, $f : \mathbb{R}^n \times \mathbb{R}^m \to \mathbb{R}$ is a continuously differentiable function that satisfies $f(0,0) = 0$. For each initial state $x(0) = \xi$ and each $u \in \mathcal{L}_\infty$, the trajectory of (A.1) is denoted $x(t, \xi, u)$.

Definition A.1. *[Sontag and Wang, 1995] System (A.1) is input-to-state stable if there exist a $\mathcal{KL}$ function β and a $\mathcal{K}$ function γ such that, for each input $u \in \mathcal{L}_\infty$ and each $\xi \in \mathbb{R}^n$, it holds that*

$$|x(t, \xi, u)| \leq \beta(|\xi|, t) + \gamma(|u|_\infty)$$

for each $t \geq 0$.

Definition A.2. *[Sontag and Wang, 1995] A smooth function $V : \mathbb{R}^n \to \mathbb{R}_+$ is called an ISS-Lyapunov function for system (A.1) is there exists $\mathcal{K}_\infty$-functions α_1, α_2 and $\mathcal{K}$-functions α_3 and α_4 such that*

$$\alpha_1(|\xi|) \leq V(\xi) \leq \alpha_2(|\xi|)$$

for any $\xi \in \mathbb{R}^n$ and

$$\nabla V(\xi) \cdot f(\xi, u) \leq -\alpha_3(|\xi|)$$

for any $\xi \in \mathbb{R}^n$ *and any* $u \in \mathbb{R}^m$ *so that* $|\xi| \geq \alpha_4(|u|)$.

The relation between the above definitions characterizes a Lyapunov-like criterion for ISS [Sontag and Wang, 1995].

Lemma A.1. *If system* (A.1) *admits an ISS-Lyapunov function, then it is ISS.*

Discrete-time case

Consider a general, discrete-time system given by

$$x_{k+1} = f(x_k, u_k) \tag{A.2}$$

where $x : \mathbb{Z}_+ \to \mathbb{R}^n$, $u : \mathbb{Z}_+ \to \mathbb{R}^m$ and $f(0,0) = 0$ is assumed. Let $x(\cdot, \xi, u)$ denote the trajectory of system (A.2) for a initial condition $x_0 = \xi$ and the input u. Then, the concepts of input-to-state stability (ISS) and ISS-Lyapunov function are stated as follows

Definition A.3. *[Jiang and Wang, 2001] System* (A.2) *is input-to-state stable if there exists a* $\mathcal{KL}$*- function* β *and a* $\mathcal{K}$ *function* γ *such that, for all* $\xi \in \mathbb{R}^n$ *and* $u \in \ell_\infty$*, it holds that*

$$|x(k, \xi, u)| \leq \beta(|\xi|, k) + \gamma(|u|_\infty)$$

for each $k \in \mathbb{Z}_+$.

Definition A.4. *[Jiang and Wang, 2001] A continuous function* $V : \mathbb{R}^n \to \mathbb{R}_+$ *is called an ISS-Lyapunov function for* (A.2) *if the following holds:*

1. *There exist* $\mathcal{K}_\infty$ *functions* α_1, α_2 *such that*

$$\alpha_1(|\xi|) \leq V(\xi) \leq \alpha_2(|\xi|), \quad \forall \xi \in \mathbb{R}^n.$$

2. *There exists a* $\mathcal{K}_\infty$ *function* α_3 *and a* $\mathcal{K}$ *function* σ *such that*

$$V(f(\xi, u)) - V(\xi) \leq -\alpha_3(|\xi|) + \sigma(|u|), \quad \forall \xi \in \mathbb{R}^n, \ \forall u \in \mathbb{R}^m.$$

The following result from [Jiang and Wang, 2001] establishes the relation between the definitions above:

Lemma A.2. *If system* (A.2) *admits a continuous ISS-Lyapunov function, then it is ISS.*

Appendix B

Preliminaries on sliding-mode control

Sliding-mode and sub-optimal controller

Consider the following non-linear system:

$$\dot{x}(t) = f(t, x, u, d) \tag{B.1}$$

where $x \in \mathbb{R}^n$ is the state vector, $u \in \mathbb{R}^m$ is the control input vector and $d \in \mathbb{R}^n$ is a vector containing perturbations and possibly uncertainties within the system. First, the *first-order conventional sliding mode* is discussed. Consider the following surface in the state space:

$$\mathbb{S} = \{x \in \mathbb{R}^n,\ \sigma(x) = 0\} \tag{B.2}$$

where $\sigma : \mathbb{R}^n \to \mathbb{R}$ is a continuously differentiable function called *sliding variable*.

The objective is to design $\sigma(x)$ in such a way that system (B.1), under feedback control, behaves with a prescribed performance. In this sense, if the control input is selected guaranteeing $\dot{\sigma} = -\eta \text{sign}(\sigma)$, where $\eta > 0$, one can consider a Lyapunov function as

$$V = \tfrac{1}{2}\sigma^2$$

and, computing its time derivative, we have that

$$\dot{V} = \sigma\dot{\sigma} = -\eta|\sigma| \tag{B.3}$$

which implies $\dot{V} \leq 0$, hence the origin of $\sigma(x)$ is globally stable. Moreover, it is clear that $|\sigma| = \sqrt{2}V^{0.5}$ and, consequently, it implies that

$$V^{0.5}(t) = \max\{0, V^{0.5}(0) - \sqrt{2}\eta t\}$$

meaning that the solution of (B.3) becomes zero in a finite time [Shtessel et al., 2010].

Ttwo interesting phases of this methodology can be discriminated: the *reaching phase*, which is guaranteed if condition (B.3) is satisfied, it describes the motion of the system towards the surface $\sigma(x)$, and the *sliding phase*, describing the motion of the system in the surface $\sigma(x) = 0$.

Recently, the concept of *higher-order sliding-mode control* has been widely studied. The techniques developed in this framework extend all interesting properties of standard sliding-mode control to systems with a relative degree greater than one. To introduce this concept, consider the case of relative degree 2 and assume that the dynamics of the sliding variable σ satisfies the following non-linear system:

$$\ddot{\sigma} = a(t, x(\cdot)) + b(t, x(\cdot))u(t, \sigma, \dot{\sigma}) \tag{B.4}$$

where $|a(t, x(\cdot))| \leq C$ and $0 < b_{min} \leq b(t, x(\cdot)) \leq b_{max}$, for all $x \in \mathbb{R}$. Also, constants $C \geq 0$ and $0 < b_{min} \leq b_{max}$ are supposed to be known. Many controllers have been proposed in order to steer σ and $\dot{\sigma}$ to zero in finite time, such as the twisting controller [Emelyanov et al., 1986], the suboptimal controller [Bartolini et al., 1997], quasi-continuous controllers [Levant, 2005] and others.

The properties of the suboptimal control algorithm are substantiated in the following. This algorithm is given by the control law [Bartolini et al., 1997]

$$u = -k_1 sign\left[\Delta(t)\right] \tag{B.5}$$

where $k_1, \lambda > 0$, and

$$\Delta(t) = \Delta(t, \sigma(\cdot)) := \sigma(t) - \lambda\sigma(t^*) \tag{B.6}$$

where t^* is the last instant of time in which $\dot{\sigma}(t^*) = 0$, i.e.,

$$t^* = t^*(t, \dot{\sigma}(\cdot)) := \sup_{\tau \leq t : \dot{\sigma}(\tau) = 0} \tau. \tag{B.7}$$

As one can see, control law (B.5) is a *functional*, since it requires information of its current and past trajectories of the system states. Also, it is interesting to notice that this control law does not require information on $\dot{\sigma}(t)$, but only the detection of an event where $\dot{\sigma}(t) = 0$. This clearly offers an advantage for practical implementations, since information of $\dot{\sigma}(t)$ might not be always available and its estimation might suffer from numerical complications.

Denoting $\dot{\sigma} = y$ and invoking the work presented in [Polyakov and Poznyak, 2012], a

candidate Lyapunov function for such a controller is given by

$$V_{sub}(t,\sigma(\cdot),y(\cdot)) = p\sqrt{\left|\sigma(t) - \frac{y^2(t)}{2(-C\text{sign}(\Delta(t)) - b_{\max}k_1\text{sign}(\Delta(t))}\right|} - \frac{y(t)}{-C\text{sign}(\Delta(t)) - b_{\max}k_1\text{sign}(\Delta(t))} \tag{B.8}$$

where $0 < \lambda < 1$, $\quad b_{min}k_1 > C$ and

$$\frac{\lambda}{1-\lambda} > \frac{1}{k} + k - 1, \qquad k := \frac{b_{max}k_1 + C}{b_{min}k_1 - C};$$

and, finally,

$$p := 2\sqrt{\frac{1}{b_{max}k_1 + C}\left(\frac{\lambda}{1-\lambda}k^2 + \sqrt{\left(\frac{\lambda}{1-\lambda}\right)^2 k^4 - 1}\right)} \tag{B.9}$$

Additionally, an estimate of the reaching time can be determined by

$$t_{reach} \leq t' + kp\sqrt{|\sigma(t')|} \tag{B.10}$$

where t' is the first moment in time such that $\dot{\sigma}(t) = 0$.

Corollary B.1. *Consider the suboptimal control (B.5) and dynamics (B.4). Let $\sigma(0) = 0$ and $\dot{\sigma}(0) > 0$, then the following estimates are satisfied for all $t \geq 0$:*

$$|\dot{\sigma}(t)| \leq |\dot{\sigma}(0)|$$
$$|\sigma(t)| \leq |\sigma(t')|$$

where $t' = \{\inf t \geq 0 : \dot{\sigma}(t) = 0\}$.

Proof. This proof relies on the integration of the expression of the worst-case trajectories for the closed-loop system, i.e., $\ddot{\sigma}(t) \leq C - b_{\min}k_1\text{sign}(\Delta(t))$. Initially, as $\dot{\sigma}(0) > 0$ and $\sigma(0) = 0$, we have that $\ddot{\sigma} \leq -r$, for $r = b_{\min}k_1 - C > 0$.

Considering a general time interval $[t_0, t]$ (where t_0 is a certain initial time instant), the integration of $\ddot{\sigma}(t)$ results in

$$\begin{aligned}\dot{\sigma}(t) &\leq \dot{\sigma}(t_0) - r(t - t_0)\\ \sigma(t) &\leq \sigma(t_0) + \dot{\sigma}(t_0)(t - t_0) - r\frac{(t-t_0)^2}{2}\end{aligned} \tag{B.11}$$

Evaluating (B.11) in the time interval $[0, t']$, we can conclude that

$$t' \leq \frac{\dot{\sigma}(0)}{r}, \text{ and, } \sigma(t') \leq \frac{\dot{\sigma}^2(0)}{2r}.$$

Then, it is clear that the first sign change in the control law will take place in a second instant of time $t" > t'$, in which we have (due to the form of (B.5)) that $\sigma(t") = \lambda\sigma(t')$. Consequently, the evaluation of (B.11) in the time interval $[t', t"]$ shows that

$$t" \leq \frac{\dot{\sigma}^2(0)}{r}\left(\sqrt{1-\lambda}+1\right)$$

and hence, we can finally conclude that

$$|\dot{\sigma}(t")| \leq -|\dot{\sigma}(0)|\sqrt{1-\lambda}$$

As $\sqrt{1-\lambda} < 1$ for $0 < \lambda < 1$, it is clear that $|\dot{\sigma}(t")| < |\dot{\sigma}(0)|$. Hence, as contraction and convergence properties of such a control algorithm have been proven (see [Bartolini et al., 1997] and proofs therein), we can then conclude that $|\dot{\sigma}(t)| \leq |\dot{\sigma}(0)|$ for all $t > 0$.

The proof of the remaining estimate follows by analysing the signal change of the control law. Clearly, due to the definition of the functional $\Delta(\sigma(t))$, the signal of the control law will switch every time that $\dot{\sigma}(t)$ reaches zero or when $\sigma(t) = \lambda\sigma(t^*)$ (see the definition of t^* above). This fact allows us to deduce that, as $\dot{\sigma}(t") < 0$, it is clear that $\dot{\sigma}(t) < 0$ holds for all $t > t'$. Thus $|\sigma(t)| < |\sigma(t')|$ holds for all $t > 0$, as claimed. □

Sliding-mode differentiator

As it will be discussed, the observers proposed in this thesis will require the time derivatives of the available measurements. This differentiation can be performed numerically by means, for instance, of the *robust exact differentiator*, proposed by Levant [Levant, 2003]. The *n-th* order differentiator is realized by the following observer:

$$\begin{cases} \dot{z}_0 & = -\lambda_n L^{\frac{1}{n+1}} \lceil z_0 - f(t) \rfloor^{\frac{n}{n+1}} + z_1 \\ \dot{z}_1 & = -\lambda_{n-1} L^{\frac{1}{n}} \lceil z_0 - f(t) \rfloor^{\frac{n-1}{n}} + z_2 \\ \dots & \\ \dot{z}_{n-1} & = -\lambda_1 L^{\frac{1}{2}} \lceil z_0 - f(t) \rfloor^{\frac{1}{2}} + z_n \\ \dot{z}_n & = -\lambda_0 L \text{sign}(z_0 - f(t)), \end{cases} \tag{B.12}$$

where $f(t) = f_0(t) + v(t)$ is a signal composed by an unknown base signal $f_0(t)$ with its *n-th* derivative having a known Lipschitz constant $L > 0$, and $v \in \mathcal{L}_\infty$ is the measurement noise. The constants λ_i are tuning parameters. Under (B.12), the estimation errors are bounded according to the following theorem:

Theorem B.1. *[Levant, 2003] Let the input noise satisfy $|v(t)| \leq \epsilon$ for almost all $t \geq 0$. Then the following inequalities are established in finite-time $T > 0$, for some positive constant*

ϱ_i *depending exclusively on the parameters* $\lambda_1, \ldots, \lambda_n$ *of the differentiator:*

$$|z_i(t) - f_0^{(i)}(t)| \leq \varrho_i L^{\frac{1}{n+1}} \epsilon^{\frac{n-i+1}{n+1}}, \ \forall t \geq T, \ i = 0, 1, \ldots, n. \tag{B.13}$$

According to Levant, all solutions of (B.12) are stable. Furthermore, the convergence of $z_0 \to f(t)$, $z_1 \to \frac{d}{dt} f(t)$, $\ldots$, $z_n \to \frac{d^n}{dt^n} f(t)$ is established in a finite-time in the noise-free case.

Bibliography

[Bartolini et al., 1997] Bartolini, G., Ferrara, A., and Usai, E. (1997). Output tracking control of uncertain non linear second order systems. *Automatica*, 33:2203–2212.

[Bastin and Dochain, 1986] Bastin, G. and Dochain, D. (1986). On-line estimation of microbial specific growth rates. *Automatica*, 22(6):705–709.

[Bastin and Dochain, 1990] Bastin, G. and Dochain, D. (1990). *On-line Estimation and Adaptive Control of Bioreactors*. Elsevier.

[Bayen et al., 2017] Bayen, T., Harmand, J., and Sebbah, M. (2017). Time-optimal control of concentration changes in the chemostat with one single species. *Applied Mathematical Modelling*, 50:257–278.

[Bemporad et al., 2003] Bemporad, A., Borrelli, F., and Morari, M. (2003). Min-max control of constrained uncertain discrete-time linear systems. *IEEE Transactions on Automatic Control*, 48(9):1600–1606.

[Bemporad and Garulli, 2000] Bemporad, A. and Garulli, A. (2000). Output-feedback predictive control of constrained linear systems via set-membership state estimation. *International Journal of Control*, 73(8):655–665.

[Brunner et al., 2018] Brunner, F., Muller, M., and Allgower, F. (2018). Enhancing output-feedback MPC with set-valued moving horizon estimation. *IEEE Transactions on Automatic Control*, 63(9):2976 – 2986.

[Che and Men, 2019] Che, S. and Men, Y. (2019). Synthetic microbial consortia for biosynthesis and biodegradation: promises and challenges. *J Ind Microbiol Biotechnol*.

[Chisci and Zappa, 2002] Chisci, L. and Zappa, G. (2002). Feasibility in predictive control of constrained linear systems: the output feedback case. *International Journal of Robust and Nonlinear Control*, 12:465–487.

[D'ans et al., 1971] D'ans, G., Kokotovic, P., and Gottlieb, D. (1971). Time-optimal control for a model of bacterial growth. *Journal of Optimization Theory and Applications*, 7(1).

[Davison and Stephanopoulos, 1986] Davison, B. H. and Stephanopoulos, G. (1986). Effect of ph oscillations on a competing mixed culture. *Biotechnology and Bioengineering*, 28(8):1127–1137.

[Ding, 2010] Ding, B. (2010). Constrained robust model predictive control via parameter-dependent dynamic output feedback. *Automatica*, 46(9):1517–1523.

[Ding and Pan, 2016] Ding, B. and Pan, H. (2016). Output feedback robust MPC for LPV system with polytopic model parametric uncertainty and bounded disturbance. *International Journal of Control*, 89(8):1554–1571.

[Ding et al., 2013] Ding, B., Ping, X., and Pan, H. (2013). On dynamic output feedback robust MPC for constrained quasi-LPV systems. *International Journal of Control*, 86(12):2215–2227.

[Ding et al., 2018] Ding, B., Wang, P., and Hu, J. (2018). Dynamic output feedback robust MPC with one free control move for LPV model with bounded disturbance. *Asian Journal of Control*, 20(2):755–767.

[Dochain, 2003] Dochain, D. (2003). State and parameter estimation in chemical and biochemical processes: a tutorial. *Journal of Process Control*, 13(8):801–818.

[Efimov et al., 2013] Efimov, D., Perruquetti, W., Raïssi, T., and Zolghadri, A. (2013). Interval observers for time-varying discrete-time systems. *IEEE Trans. Automatic Control*, 58(12):3218–3224.

[Efimov et al., 2013] Efimov, D., Perruquetti, W., Raïssi, T., and Zolghadri, A. (2013). On interval observer design for time-invariant discrete-time systems. In *2013 European Control Conference (ECC)*, pages 2651–2656.

[Efimov and Raïssi, 2016] Efimov, D. and Raïssi, T. (2016). Design of interval observers for uncertain dynamical systems. *Autom. Remote Control*, 77(2):191—225.

[Emelyanov et al., 1986] Emelyanov, S., Korovin, S., and Levantovskii, L. (1986). High-order sliding modes in binary control systems. *Soviet Physics Doklady*, 31.

[Farina and Rinaldi, 2000] Farina, L. and Rinaldi, S. (2000). *Positive Linear Systems: Theory and Applications*. John Wiley & Sons.

[Fiore et al., 2017] Fiore, G., Matyjaszkiewicz, A., Annunziata, F., Grierson, C., Savery, N., Marucci, L., and Di Bernardo, M. (2017). In-silico analysis and implementation of a multicellular feedback control strategy in a synthetic bacterial consortium. *AC Synthetic Biology*.

[Fridman, 2014] Fridman, E. (2014). *Introduction to Time-Delay Systems: Analysis and Control*. Systems & Control: Foundations & Applications. Birkhauser.

[Fu and Panke, 2009] Fu, P. and Panke, S. (2009). *Systems Biology and Synthetic Biology*. John Wiley & Sons, Inc.

[Gouzé et al., 2000] Gouzé, J., Rapaport, A., and Hadj-Sadok, M. (2000). Interval observers for uncertain biological systems. *Ecological Modelling*, 133(1):45–56.

[Hardy et al., 1934] Hardy, G. H., Littlewood, J. E., and Polya, G. (1934). *Inequalities*. Cambridge Mathematical Library. Cambridge University Press.

[Henson and Seborg, 1997] Henson, M. A. and Seborg, D. E., editors (1997). *Nonlinear Process Control*. Prentice-Hall, Inc., USA.

[Herceg et al., 2013] Herceg, M., Kvasnica, M., Jones, C., and Morari, M. (2013). Multi-Parametric Toolbox 3.0. In *Proc. of the European Control Conference*, pages 502–510, Zürich, Switzerland. http://control.ee.ethz.ch/~mpt.

[Hermann and Krener, 1977] Hermann, R. and Krener, A. (1977). Nonlinear controllability and observability. *IEEE Transactions on Automatic Control*, 22(5):728–740.

[Hoo and Kantor, 1986] Hoo, K. A. and Kantor, J. C. (1986). Global linearization and control of a mixed-culture bioreactor with competition and external inhibition. *Mathematical Biosciences*, 82(1):43–62.

[Hsiao et al., 2018] Hsiao, V., Swaminathan, A., and Murray, R. M. (2018). Control theory for synthetic biology: Recent advances in system characterization, control design, and controller implementation for synthetic biology. *IEEE Control Systems Magazine*, 38(3):32–62.

[Hsu et al., 1977] Hsu, S. B., Hubbell, S., and Waltman, P. (1977). A mathematical theory for single-nutrient competition in continuous cultures of micro-organisms. *SIAM Journal on Applied Mathematics*, 32(2):366–383.

[Huang et al., 2014] Huang, H., He, D.-F., and Chen, Q.-X. (2014). Quasi-min-max dynamic output feedback MPC for LPV systems. *Int. J. System Control and Information Processing*, 1(3).

[Jiang and Wang, 2001] Jiang, Z.-P. and Wang, Y. (2001). Input-to-state stability for discrete-time nonlinear systems. *Automatica*, 37(6):857–869.

[Karafyllis and Jiang, 2012] Karafyllis, I. and Jiang, Z.-P. (2012). A new small-gain theorem with an application to the stabilization of the chemostat. *Int. J. Robust. Nonlinear Control*.

[Kerner et al., 2012] Kerner, A., Park, J., Williams, A., and Lin, X. N. (2012). A programmable escherichia coli consortium via tunable symbiosis. *PLOS ONE*, 7(3):1–10.

[Kim et al., 2006] Kim, T., Park, J., and Sugie, T. (2006). Output-feedback model predictive control for LPV systems with input saturation based on quasi-min-max algorithm. In *Proceedings of the 45th IEEE Conference on Decision and Control*, pages 1454–1459.

[Kothare et al., 1996] Kothare, M., Balakrishnan, V., and M., M. (1996). Robust constrained model predictive control using linear matrix inequalities. *Automatica*, 32(10):1361–1379.

[Kravaris and Savoglidis, 2012] Kravaris, C. and Savoglidis, G. (2012). Tracking the singular arc of a continuous bioreactor using sliding-mode control. *Journal of the Franklin Institute*.

[Krieger et al., 2020] Krieger, A. G., Zhang, J., and Lin, X. N. (2020). Temperature regulation as a tool to program synthetic microbial community composition. *Biotechnology and Bioengineering*.

[Langson et al., 2004] Langson, W., Chryssochoos, I., Rakovic, S., and Mayne, D. Q. (2004). Robust model predictive control using tubes. *Automatica*.

[Lee and Park, 2007] Lee, S. M. and Park, J. H. (2007). Output feedback model predictive control for LPV systems using parameter-dependent lyapunov function. *Applied Mathematics and Computation*.

[Leenheer and Smith, 2003] Leenheer, P. and Smith, H. (2003). Feedback control for chemostat models. *Journal of Mathematical Biology*, 46:48–70.

[Levant, 2003] Levant, A. (2003). Higher-order sliding modes, differentiation and output-feedback control. *International Journal of Control*, 76(9-10):924–941.

[Levant, 2005] Levant, A. (2005). Quasi-continuous high-order sliding-mode controllers. *IEEE Transactions on Automatic Control*, 50(11):1812–1816.

[Löfberg, 2004] Löfberg, J. (2004). YALMIP: A toolbox for modeling and optimization in matlab. In *In Proceedings of the CACSD Conference*, Taipei, Taiwan.

[Mailleret et al., 2004] Mailleret, L., Bernard, O., and Steyer, J.-P. (2004). Nonlinear adaptive control for bioreactors with unknown kinetics. *Automatica*.

[Mauri et al., 2020] Mauri, M., Gouzé, J.-L., de Jong, H., and Cinquemani, E. (2020). Enhanced production of heterologous proteins by a synthetic microbial community: Conditions and trade-offs. *PLOS Computational Biology*, 16(4):1–30.

[Mayne et al., 2006] Mayne, D. Q., Ravokic, S. V., Findeisen, R., and Allgower, F. (2006). Robust output feedback model predictive control of constrained linear systems. *Automatica*, 42:1217–1222.

[Mayne et al., 2009] Mayne, D. Q., Ravokic, S. V., Findeisen, R., and Allgower, F. (2009). Robust output feedback model predictive control of constrained linear systems: time-varying case. *Automatica*, 45:2082–2087.

[Mayne et al., 2000] Mayne, D. Q., Rawlings, J. B., Rao, C. V., and Scokaert, P. O. M. (2000). Constrained model predictive control: stability and optimality. *Automatica*, 36:789–814.

[Mazenc and Bernard, 2011] Mazenc, F. and Bernard, O. (2011). Interval observers for linear time-invariant systems with disturbances. *Automatica*, 47(1):140–147.

[Mazenc et al., 2017] Mazenc, F., Harmand, J., and Malisoff, M. (2017). Stabilization in a chemostat with sampled and delayed measurements and uncertain growth functions. *Automatica*, 78:241–249.

[McCarty and Ledesma-Amaro, 2019] McCarty, N. S. and Ledesma-Amaro, R. (2019). Synthetic biology tools to engineer microbial communities forbiotechnology. *Trends in Biotechnology*.

[Milias-Argeitis et al., 2016] Milias-Argeitis, A., Rullan, M., Aoki, S. K., Buchmann, P., and Khammash, M. (2016). Automated optogenetic feedback control for precise and robust regulation of gene expression and cell growth. *Nature Communitications*, 7.

[Mohd Ali et al., 2015] Mohd Ali, J., Ha Hoang, N., Hussain, M., and Dochain, D. (2015). Review and classification of recent observers applied in chemical process systems. *Computers & Chemical Engineering*, 76:27–41.

[Nijenhuis, 1974] Nijenhuis, A. (1974). Strong derivatives and inverse mappings. *The American Mathematical Monthly*, 81(9):969–980.

[Peng et al., 2016] Peng, X., Gilmore, S. P., and O'Malley, M. A. (2016). Microbial communities for bioprocessing: lessons learned from nature. *Current Opinion in Chemical Engineering*.

[Ping et al., 2020] Ping, X., Yang, S., Wang, P., and Li, Z. (2020). An observer-based output feedback robust MPC approach for constrained LPV systems with bounded disturbance and noise. *International Journal of Robust and Nonlinear Control*, 30(4):1512–1533.

[Polyakov and Poznyak, 2012] Polyakov, A. and Poznyak, A. (2012). Unified lyapunov function for a finite-time stability analysis of relay second order sliding mode control systems. *IMA Journal of Mathematical Control and Information*, pages 529–550.

[Postiglione et al., 2018] Postiglione, L., Napolitano, S., Pedone, E., Rocca, D. L., Aulicino, F., Santorelli, M., Tumaini, B., Marucci, L., and di Bernardo, D. (2018). Regulation of gene expression and signaling pathway activity in mammalian cells by automated microfluidics feedback control. *ACS Synthetic Biology*.

[Raimondo et al., 2009] Raimondo, D. M., Limón, D., Lazar, M., Magni, L., and Camacho, E. F. (2009). Min-max model predictive control of nonlinear systems: A unifying overview on stability. *Eur. J. Control*, 15:5–21.

[Riverso et al., 2013] Riverso, S., Battocchio, A., and Ferrari-Trecate, G. (2013). Pnpmpc toolbox.

[Robledo, 2006] Robledo, G. (2006). *Control of the chemostat: Some Results*. PhD thesis, Université Nice Sophia Antipolis.

[Rodrigues and Odloak, 2000] Rodrigues, M. and Odloak, D. (2000). Output feedback MPC with guaranteed robust stability. *Journal of Process Control*, 10(6):557 – 572.

[Rosero-Chasoy et al., 2021] Rosero-Chasoy, G., Rodríguez-Jasso, R. M., Aguilar, C. N., Buitrón, G., Chairez, I., and Ruiz, H. A. (2021). Microbial co-culturing strategies for the production high value compounds, a reliable framework towards sustainable biorefinery implementation – an overview. *Bioresource Technology*, 321:124458.

[Said and Or, 2017] Said, S. B. and Or, D. (2017). Synthetic microbial ecology: Engineering habitats for modular consortia. *Frontiers in Microbiology*, 8:1125.

[Schlembach et al., 2021] Schlembach, I., Grünberger, A., Rosenbaum, M. A., and Regestein, L. (2021). Measurement techniques to resolve and control population dynamics of mixed-culture processes. *Trends in Biotechnology*.

[Schmidt, 2012] Schmidt, M., editor (2012). *Synthetic Biology*. Industrial and Environmental Applications. Wiley-Blackwell.

[Scott et al., 2019] Scott, T. D., Sweeney, K., and McClean, M. N. (2019). Biological signal generators: integrating synthetic biology tools and in silico control. *Current Opinion in Systems Biology*.

[Shtessel et al., 2010] Shtessel, Y., Edwards, C., Fridman, L., and Levant, A. (2010). *Sliding Mode Control and Observation*. Control Engineering. Birkhauser.

[Smith, 1981] Smith, H. L. (1981). Competitive coexistence in an oscillating chemostat. *SIAM Journal on Applied Mathematics*, 40(3):498–522.

[Smith and Waltman, 1995] Smith, H. L. and Waltman, P. (1995). *The theory of the Chemostat*. Cambridge University Press.

[Sontag, 1998] Sontag, E. (1998). *Mathematical Control Theory: Deterministic Finite-Dimensional Systems*. Springer, 2nd ed. edition. DOI: 10.1007/978-1-4612-0577-7.

[Sontag and Wang, 1995] Sontag, E. D. and Wang, Y. (1995). On characterizations of the input-to-state stability property. *Systems & Control Letters*, 24(5):351–359.

[Souza et al., 2020] Souza, A. R., Efimov, D., Polyakov, A., and Gouzé, J.-L. (2020). Robust stabilization of competing species in the chemostat. *Journal of Process Control*, 87:138–146. doi:doi.org/10.1016/j.jprocont.2020.01.010.

[Souza et al., 2021a] Souza, A. R., Efimov, D., Polyakov, A., Gouzé, J.-L., and Cinquemani, E. (2021a). State observation in microbial consortia: a case study on a synthetic producer-cleaner consortium. *Submitted to the International Journal on Robust and Nonlinear Control*.

[Souza et al., 2021b] Souza, A. R., Efimov, D., and Raïssi, T. (2021b). Robust output feedback mpc for lpv systems using interval observers. *Accepted in the IEEE Transactions on Automatic Control*.

[Souza et al., 2021c] Souza, A. R., Efimov, D., and Raïssi, T. (2021c). Robust output feedback mpc of time-delayed systems using interval observers. *Submitted to the International Journal on Robust and Nonlinear Control*.

[Souza et al., 2021d] Souza, A. R., Efimov, D., Raïssi, T., and Ping, X. (2021d). Robust output feedback model predictive control for constrained linear systems via interval observers. *Accepted on Automatica*.

[Toettcher et al., 2011] Toettcher, J., Gong, D., Lim, W. A., and Weiner, O. D. (2011). Light-based feedback for controlling intracellular signaling dynamics. *Nature Methods*, 8.

[Treloar et al., 2020] Treloar, N. J., Fedorec, A. J. H., Ingalls, B., and Barnes, C. P. (2020). Deep reinforcement learning for the control of microbial co-cultures in bioreactors. *PLOS Computational Biology*, 16(4):1–18.

[Utkin, 1992] Utkin, V. I. (1992). *Sliding Modes in Control and Optimization*. Communications and Control Engineering. Springer.

[Wang et al., 2019] Wang, Y., Wang, Z., Puig, V., and Cembrano, G. (2019). Zonotopic set-membership state estimation for discrete-time descriptor lpv systems. *IEEE Transactions on Automatic Control*, 64(5):2092–2099.

[Wolkowicz and Lu, 1992] Wolkowicz, G. S. K. and Lu, Z. (1992). Global dynamics of a mathematical model of competition in the chemostat: General response functions and differential death rates. *SIAM Journal on Applied Mathematics*, 52(1):222–233.

[Yang et al., 2016] Yang, W., Gao, J., Feng, G., and Zhang, T. (2016). An optimal approach to output-feedback robust model predictive control of LPV systems with disturbances. *International Journal of Robust and Nonlinear Control*, 26(15):3253–3273.

[Yang et al., 2019] Yang, Y., Ding, B., Xu, Z., and Zhao, J. (2019). Tube-based output feedback model predictive control of polytopic uncertain system with bounded disturbances. *Journal of the Franklin Institute*, 356(15):7990–8011.